Ref. Ares(2015)5347928 - 25/11/2015

LEXNET
Low EMF Exposure Future Networks

Deliverable D6.2:
Report on validation, Part-A

Contractual delivery date: M36
Actual delivery date: M36

Document Information

Version	V1.0	**Dissemination level**	PU
Editor	Y. Corre (Siradel)		
Other authors	S. Bories, A. Clemente, F. Fezai, D. Dassonville (CEA) M. Wilson, Y. Fang (FLE) G. Vermeeren (Iminds) P. Zimmermann (Orange) M. Lalam (Sagemcom) S.M. Anwar, M. Le Henaff, Y. Toutain (Satimo) J. Stéphan, M. Brau, G. Gougeon, Y. Lostanlen (Siradel) Y. Fernández, A. Sánchez (TTI) P. Chambers, T. Brown (UniS)		

PROPRIETARY RIGHTS STATEMENT
This document contains information, which is proprietary to the LEXNET Consortium. Neither this document nor the information contained herein shall be used, duplicated or communicated by any means to any third party, in whole or in parts, except with prior written consent of the LEXNET consortium.

	L. Díez, L. Rodríguez de Lope, R. Agüero (UC) M. Popović, J. Milinković, S. Nikšić, M. Koprivica, A. Nešković (TKS)
Abstract	This deliverable presents the validations and proofs of concept of methodologies and technical solutions elaborated in the LEXNET project. Part-A details the developed EMF measurement tools and their characterization. Different methods for the Exposure Index (EI) assessment are implemented and demonstrated in various environments. In Part-B, a set of promising low EMF components and techniques are evaluated from both QoS and EMF metrics, either through laboratory tests, large-scale real cellular testbeds, or system-level simulations.
Key words	EI assessment validation, testbed, low EMF solutions, demonstration

Project Information

Grant Agreement n°	318273
Dates	1st November 2012 – 31th October 2015

Document approval

Name	Position in project	Organisation	Date	Visa
Joe Wiart	Coordinator	Orange	19/11/2015	OK

Document history

Version	Date	Modifications	Authors
V1.0	18/11/2015		All

Table of contents

1 INTRODUCTION 8

2 OVERVIEW ON EI ASSESSMENT DEMONSTRATIONS 10

3 EVALUATION SCENARIOS 13

3.1 MULTI-RAT SANTANDER SCENARIO 13
3.2 LTE PARIS SCENARIO 14
3.3 LEXNET URBAN REFERENCE SCENARIO 15
3.4 GSM AND UMTS BELGRADE SCENARIO 16

4 RESULTS IN A NUTSHELL 18

5 EMF MEASUREMENT TOOLS 21

5.1 LOW-COST DOSIMETER 21
5.1.1 Dosimeter 21
5.1.2 Repeater 25
5.2 WEARABLE DOSIMETER 26
5.2.1 Characterization methodology 28
5.2.2 Characterization results of the dosimeter with tunable filter 30
5.2.3 Characterization results of the dosimeter with fixed filters 32
5.2.4 Real-time dosimeter measurements with GPS data 35
5.3 TX/RX PLATFORM 37

6 EI IMPLEMENTATION AND ASSESSMENT 38

6.1 IN-FIELD MEASUREMENTS (DEMONSTRATION IN SANTANDER) 38
6.1.1 EI assessment from the wearable dosimeter measurements 39
6.1.2 EI assessment from the Tx/Rx platform measurements 42
6.1.3 EI assessment from the Trace mobile measurements 44
6.2 SMART SANTANDER PLATFORM 47
6.2.1 Deployment procedure 47
6.2.2 EI assessment method 49
6.2.3 Results 50
6.3 CELLULAR NETWORK MEASUREMENTS 56
6.3.1 Sources of data 56
6.3.2 EI implementation challenges 58
6.3.3 EI assessment method 60
6.3.4 Results 68
6.4 CELLULAR NETWORK SIMULATIONS 70
6.4.1 EI assessment method 70
6.4.2 Results 73
6.5 IN-BUILDING SIMULATIONS 78
6.5.1 EI assessment method 79
6.5.2 Results 81
6.6 LEXNET EI VALIDATION PLATFORM (LEI-VP) 81
6.6.1 EI assessment method 82
6.6.2 Results 83

7 CONCLUSIONS 85

8 REFERENCES 88

APPENDIX A1: INTERNAL REVIEW 90

APPENDIX A2: SANTANDER MEASUREMENTS 91

A2.1. METHODOLOGY AND ENVIRONMENT OF THE MEASUREMENT CAMPAIGN 91
A2.2. DL E-FIELD MEASUREMENTS FROM THE MOBILE DOSIMETER 96
A2.3. EXTRAPOLATION FROM MONO-AXIAL MEASUREMENTS TO ISOTROPIC E-FIELD 99
A2.4. EXTRAPOLATION FACTOR FOR FIXED DOSIMETERS 102

A2.5. TX/RX PLATFORM RESULTS 104
A2.6. TRACE MOBILE MEASUREMENTS 105
A2.7. COMPARISON BETWEEN TX/RX PLATFORM VS PROFESSIONAL DRIVE-TEST EQUIPMENT 112
A2.8. SCANNER LTE RSSI MEASUREMENTS 114

APPENDIX A3: COMPARISON BETWEEN LEXNET DOSIMETER AND STATE OF THE ART EMESPY200 DOSIMETER 116

APPENDIX A4: PLANNING THE LOW-COST DOSIMETER DEPLOYMENT 118

A4.2 PLANNING THE LOW-COST DOSIMETER DEPLOYMENT 118
A4.2 MEASUREMENT-BASED SEQUENTIAL EMF SENSOR NETWORK DEPLOYMENT 122

Executive Summary

This deliverable presents the validations and proofs of concept of solutions developed in the framework of the LEXNET project. Following the organisation of the project itself, the document distinguishes two main parts.

The first part (Part-A) focuses on the Exposure Index (EI) assessment validation. This concerns how the global metric defined in the framework of the project can be practically implemented to provide the full picture of a population Electromagnetic Field (EMF) exposure from all the wireless standards considered in LEXNET. The characteristics and validation of the three EMF measurement tools developed in LEXNET are detailed (or reminded when already described in the first WP6 deliverable): the low cost dosimeters deployed in the city of Santander; the selective wearable dosimeter version integrated from individual WP3 sub-components; and a connected measurement device (i.e. with an active wireless communication) that capture downlink (DL) and uplink (UL) key parameters. Part-A also presents the implementation and demonstration of EI assessment methodologies based on dosimeters, network monitoring tools, drive-test equipment, multi-source database, or simulations, and finally how and by whom they could be exploited to evaluate the LEXNET global metric. In particular, the demonstrations include two real-life measurement campaigns leading to the EI assessment in large-scale cellular networks: in the cities of Santander (involving drive test, dosimeter measurements, simulations and a smart city infrastructure) and Belgrade (involving network monitoring and drive test).

Compared to Part-A that aims to provide absolute values of EI, the second part of the deliverable (Part-B) re-uses the EI metric but for relative exposure reduction evaluation applied to a set of low EMF techniques. Some of the components and radio link techniques studied in WP4 have been selected for such demonstration. The LTE superdirective antenna combined with a low noise receiver are integrated into a demonstrator; characterization, laboratory radio-link tests and simulations show how this solution can fulfil dense deployment of low EMF small-cell base stations. Besides, the smart beamforming test bench demonstrates how to reduce the Specific Absorbtion Rate (SAR) for mobile or laptop usages.
Part-A also illustrates how a change in a cellular network topology, i.e. adding a macro-cell or micro-cell, affects the user QoS and EMF exposure. We understand from those use cases how the installation of new antennas can reduce the population exposure. The analysis on topologies is broadened with system-level simulations on dense urban small-cell deployments, in addition to the macro co-channel layer, and considering the contribution from the wireless NLOS small-cell backhaul.
WiFi offloading is also evaluated, showing how the offloading policy and the WiFi AP deployment influence the network performance and exposure.
Finally, exposure reduction in WLAN-managed networks is addressed thanks to an optimized AP deployment design, and gateways that propagate scheduled on/off commands to APs.

List of acronyms

Abbreviation	Meaning
3GPP	Third generation partnership project.
ADC	Analog to Digital Converter
ADC	Automatic Device Configuration
ANDSF	Access Network Discovery and Selection Function
AP	Access point
BS	Base Station
BTS	Base Transceiver Station
CDF	Cumulative Distribution Function
CL	Cell Load
DAS	Distributed Antenna System
DL	DownLink
EMF	Electromagnetic field
E-Field	Electric Field
eNB	Evolved Node B
FBS	Femtocell Base Station
FTP	File Transfer Protocol
GPS	Global System Positioning
GSM	Global System for Mobile communications
HetNet	Heterogeneous Network
HSPA	High Speed Packet Access
ICT	Information and Communications Technologies
IoT	Internet of Things
IP	Internet Protocol
ISM	Industrial, Scientific and Medical
KPI	Key Performance Indicator
LNA	Low Noise Amplifier
LOLA	LOcal Linear Approximation
LTE	Long Term Evolution
MC	Macro Cell
MeNB	Macro eNB
MIMO	Multiple Inputs Multiple Outputs
NF	Noise figure
NLOS	None Line Of Sight
PCB	Printed Circuit Board
PRB	Physical Resource Block
QoS	Quality of service

RAT	Radio Access Technology
RF	Radio Frequency
RRC	Radio Resource Control
RSRP	Reference Signal Received Power
RSRQ	Reference Signal Receiver Quality
RSSI	Reference Signal Strength Indication
RSS	Receive Signal Strength
RS	Rest Period
Rx	Receiver
SAR	Specific Absorption Rate
SC	Small Cell
SCeNB	Small Cell eNB
SINR	Signal to Interference plus Noise Ratio
SNR	Signal to Noise Ratio
SWT	Standard Working Time
Tx	Transmitter
UE	User Equipment
UL	UpLink
USB	Universal Serial Bus
UMTS	Universal Mobile Telecommunications System
VoIP	Voice over IP
VoLTE	Voice over LTE
WLAN	Wide Local Area Network
WSN	Wireless Sensor Network

1 INTRODUCTION

The LEXNET project aims to assess the human exposure to EMF originating from existing and future radio communication devices. The ground-breaking approach of LEXNET has been to propose a global EMF exposure metric: the Exposure Index (EI). The concept consists of evaluating simultaneously all the different telecom EM sources that can impact the daily exposure of a population scaled over a considered area. Thus, both the user equipment and network infrastructure exposure are considered for different radio access technologies. Some large scale bottom-up synthesis can be reached, leading to the EI by merging the Information and Communications Technologies (ICT) usages, population life segmentation with telecommunication networks and wireless technologies engineering. All of this relies on several aspects, such as statistics, modelling, measurements and simulations, as discussed in [D2.8].

One objective of LEXNET is to face its real feasibility, considering its complexity and finite available inputs to assess the EI. Thus, several activities have been dedicated to EMF measurement tools and processing in order to practically implement the EI assessment. For instance, EI assessment is possible based on measurements, by recording the UL (e.g., trace mobile) and DL exposure (e.g. dosimeter) of a representative set of people in the considered area.

Last but not least, another key goal of LEXNET is to introduce innovative low EMF components, techniques and network solutions and demonstrate their quantitative impacts both on the exposure reduction and on the Quality of Service (QoS). The EI metric has been defined to provide a fair and global comparison network solution, either based on absolute EI values or relative differences on EMF proxies.

Deliverable D6.2 is dedicated to the validation of the LEXNET solutions and thus directly addresses both of the aforementioned objectives. Descriptions of the methodologies, implementation, test beds in progress and observed metrics to derive EI reduction are laid down in the deliverable.

The purpose of the LEXNET approach has been to never opposed modelling (statistic or deterministic) and measurements. Both activities are used to complement each other in order to refine their results, compensate missing data, or take into account dynamic or evolving aspects.

LEXNET deliverable D6.2 is organised in two separated parts. Part-A addresses the EI assessment validation. The developed dosimeters and tools to measure EMF are described and characterized. The implementations of absolute evaluation of the LEXNET metric are presented for various scenarios, including urban and in-office environments; measurements from drive test, dosimeters, or network monitoring; EI assessment from multi-source database; and a hybrid measurement plus simulations approach.
Part-B introduces the demonstrations of the low EMF solutions on components, radio link techniques, or network topology solutions.

Part-A is organized as follows.

Section 2 gives an overview of the EI assessment demonstrations; and specifically discusses the application of the demonstrated methodologies over real network deployments.
Section 3 introduces some scenarios that have been used in several evaluations (in Part-A and Part-B):

- The Santander scenario is composed of a traditional multi-operator multi-RAT macro cellular network. Santander downtown was used as a major LEXNET testbed, thanks to the presence of the original SmartSantander infrastructure in which a fixed dosimeter network has been integrated.
- A LTE modeled macro deployment in Paris downtown is used as the basis for several simulation studies.
- A LEXNET scenario built from population and network data statistics reported in [D2.8] serves as a reference to calculate the EI.
- The Belgrade 2G and 3G network is used as the testbed for network monitoring evaluation and micro-cell measurements.

The main absolute EI values that have resulted from the demonstrations are summarized in section 4.
Section 5 presents the hardware prototypes developed and validated for exposure measurements: the low cost dosimeters deployed in the city of Santander; the selective wearable dosimeter version integrated from individual WP3 sub-components; and a connected measurement device (i.e. with an active wireless communication) that capture downlink (DL) and uplink (UL) key parameters.
The implementation and methodologies for the EI assessment are detailed in section 6:

- In-field measurements in Santander downtown, with the involvement of trace mobile and wearable dosimeter equipment.
- Downlink exposure measure from the SmartSantander solution.
- Cellular network measurements by the operator, by the exploitation of monitoring data and drive tests.
- Cellular network simulations, taking advantage from the Santander measurements for a preliminary calibration step.
- In-building EI simulations in a scenario composed of a two-tier macro and femto-cell deployment.
- EI computation from a devoted platform that combines multi-source inputs into a unique database.

The main conclusions on EI implementation and evaluations are drawn finally in section 6.6.

2 OVERVIEW ON EI ASSESSMENT DEMONSTRATIONS

The demonstration scenarios are distributed into four main classes illustrated in Figure 1: Traditional 3GPP outdoor cellular network; Smart city with traditional 3GPP outdoor cellular networks and sensing capabilities; Managed WLAN, mainly in large environments; and Small-cell offloading in heterogeneous networks (including 3GPP small-cells and WiFi access points).

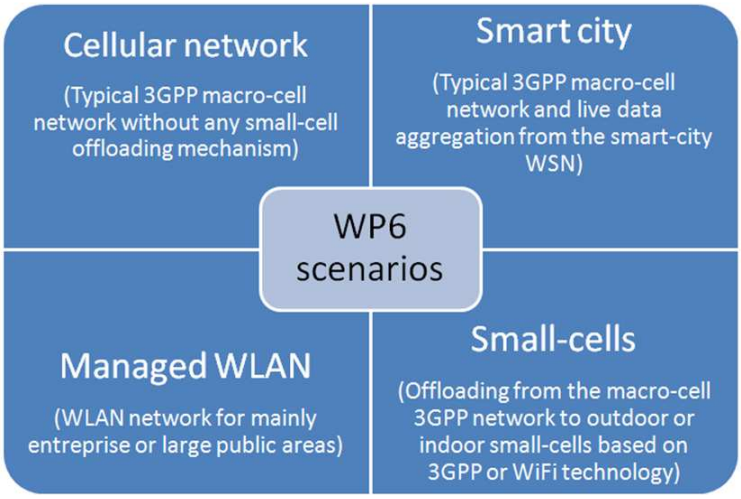

Figure 1: Four main evaluation scenario classes.

Figure 2 shows all individual demonstration scenarios, each being part of one specific class.

EI assessments by means of radio-planning techniques (i.e. based on coverage simulations) are implemented and tested for traditional cellular networks, heterogeneous networks and WLAN. This kind of tools is already widely employed by cellular network operators to pre-design the network deployment (e.g. selection of antenna locations, sectorization, selection of the frequency, tilt adjustment) and to optimize some parameters (after analyzing live network measurements); it can also be used by engineers in charge of WLAN optimization in large complex environments, e.g. airport, commercial mall, university, etc. The integration of EMF metrics, and EI in particular, in those radio-planning tools is essential to demonstrate how the LEXNET concept can be introduced and considered at the earliest stage of new wireless network deployment planning process (if operators were required to do it).
Some public regulatory authorities are also using simulation tools (or do request the network operators to use such tools) in order to control the peak DL EMF exposure levels, verifying that they do not exceed the maximum allowed field strength. The new LEXNET view on EMF would require the regulatory authorities to rely on more advanced simulations able to consider real cell loads and predict the UL transmit power and throughput, i.e. simulations that are very similar to radio-planning.

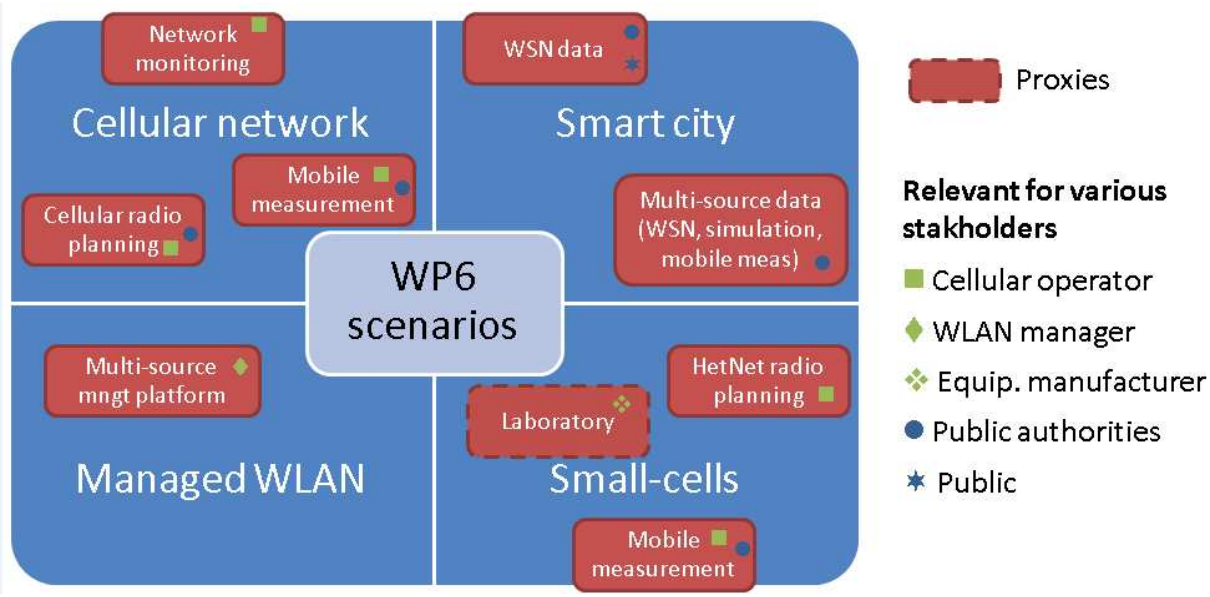

Figure 2: Scenarios for EI assessment demonstration.

EI assessment from network monitoring is demonstrated in real cellular networks (TKS operating networks). Such approach is complex, in particular in case of cellular networks, as the EI calculation requires collecting and crossing a large amount of data that comes from heterogeneous sources. But it is also very powerful as it provides live and continuous data from real network operations. The monitored exposure may have two main applications: first, to measure the EI and observe its variation in time (relevant for the network operator); second, to feed some optimization algorithms (implemented by network manufacturers) that automatically adapt the resource management policy, the power allocation, and so on, according to the user and network performances. This second objective does not necessarily need for a complete EI calculation.

On-field measurement is another important approach, both for network operators and public authorities like regulatory entities or municipalities concerned by EMF exposure. In the case of the network operators, on-field measurements can be a complement or an alternative to the network monitoring approach, especially when the exposure must be characterized for a specific area or usage.
Besides, the public authorities will be interested in assessing the exposure level from all radio sources (not only the ones specific to a given operator) and possibly in an independent way.
Mobile on-field measurements have been demonstrated at the scale of a city (Santander). A combination of different tools was involved: in particular the wearable dosimeter for DL field strength measurements and Trace mobile for measurement of the UL throughput and UL transmit power in 3GPP networks.

The Santander environment enables the implementation of another innovative measurement procedure, where the smart-city platforms aggregates, processes and publishes live data collected by probes distributed throughout the city. This kind of platform, which should be developed in next decades to speed up and optimize various diagnostics and decision procedures in the cities, can offer the municipalities and general public an easy access (e.g. through web applications) to the DL EMF levels captured by fixed dosimeters.

The joint usage of measurements and simulations has also been demonstrated in the Santander environment. Dosimeter and TRACE measurements provide the reference material for the simulation model calibration, while the simulation results are exploited to get extrapolation rules to be applied on dosimeter levels. The combination of both data leads to realistic DL+UL exposure maps and EI assessment.

The platform called LEI-VP demonstrates how EI can be calculated and analysed into a user-friendly application, based on multi-source data (measurements, simulations) imported into a unique database.

Finally, the LEXNET demonstration includes a laboratory testbed capable of measuring the SAR (Specific Absorption Rate) induced by a wireless communication link. Such testbed is not able to evaluate the EI by itself, since it embraces the wireless activity in several links. But it is very relevant to capture the impact of adaptive antennas on both the DL and UL exposure generated by a real wireless link. This laboratory testbed is not described here, but in Part-B.

3 EVALUATION SCENARIOS

This section gives a description of the main evaluation scenarios employed in the EI assessment and LEXNET technology demonstrations. The description is not exhaustive, but includes all scenarios involved in at least two different studies.
The remaining ones are introduced in the section that reports on the specific study carried out over them.

3.1 Multi-RAT Santander scenario

The Santander city, in Spain, has been chosen for several LEXNET experimentations, essentially for characterization of the exposure into a live large-scale multi-RAT cellular network. At the time of the measurement campaigns conducted in Santander (in 2014 and 2015), the cellular network was composed of 2G/3G/4 technologies that operated in 900/1800/2100 MHz frequency bands. Table 1 gives the detailed frequency usage per operator. It is worth highlighting that two operators are devoting the 1800 MHz band to 2G communications, while two other ones are providing 4G in this same frequency band.

Table 1: Frequency usage in Santander.

900 MHz Band - 2G

Block	Uplink	Downlink	Operator
2x10 MHz	880,1-890,1 MHz	925,1-935,1 MHz	Orange
2x10 MHz	890,1-900,1 MHz	935,1-945,1 MHz	Movistar
2x4,8 MHz	900,1-904,9 MHz	945,1-949,9 MHz	Movistar
2x10 MHz	904,9-914,9 MHz	949,9-959,9 MHz	Vodafone

1800 MHz Band - 2G and 4G

Block	Uplink	Downlink	Operator	
2x20 MHz	1710,1-1730,1 MHz	1805,1-1825,1 MHz	Movistar	
2x20 MHz	1730,1-1750,1 MHz	1825,1-1845,1 MHz	Vodafone	4G
2x5 MHz	1750,1-1755,1 MHz	1845,1-1850,1 MHz	Yoigo	
2x5 MHz	1755,1-1760,1 MHz	1850,1-1855,1 MHz	Yoigo	
2x4,8 MHz	1760,1-1764,9 MHz	1855,1-1859,9 MHz	Yoigo	
2x20 MHz	1764,9-1784,9 MHz	1859,9-1879,9 MHz	Orange	4G

2100 MHz Band - 3G

Block	Uplink	Downlink	Operator
2x15 MHz	1920-1935 MHz	2110-2125 MHz	Yoigo
2x15 MHz	1935-1950 MHz	2125-2140 MHz	Orange
2x15 MHz	1950-1965 MHz	2140-2155 MHz	Vodafone
2x15 MHz	1965-1980 MHz	2155-2170 MHz	Movistar

Most of the measurement campaigns have been conducted in the downtown area included in the blue rectangle of Figure 3. This area (of about 1km²) is composed of dense building blocks of similar height.

The reason why many measurements and simulations have been realized in this area is twofold: 1) the building density, architecture and height are similar to those of many dense urban centers in Europe; and 2) the deployment of low-complexity dosimeters in SmartSantander platform [D6.1] offers a unique infrastructure for the EI assessment methodology.

(a) Main area of interest in Santander.

(b) Digital geographical map data.

Figure 3: Santander environment.

The city of Santander has also been the support for simulations, for demonstrating the possible measurements and simulation complementarities; in this sense, the simulations illustrate how the EMF exposure varies when changing an existing network topology.

3.2 LTE Paris scenario

This scenario is used for simulation only. It is composed of a modeled yet realistic LTE macro deployment with base station antennas located on dominant building rooftops, as illustrated in Figure 4.

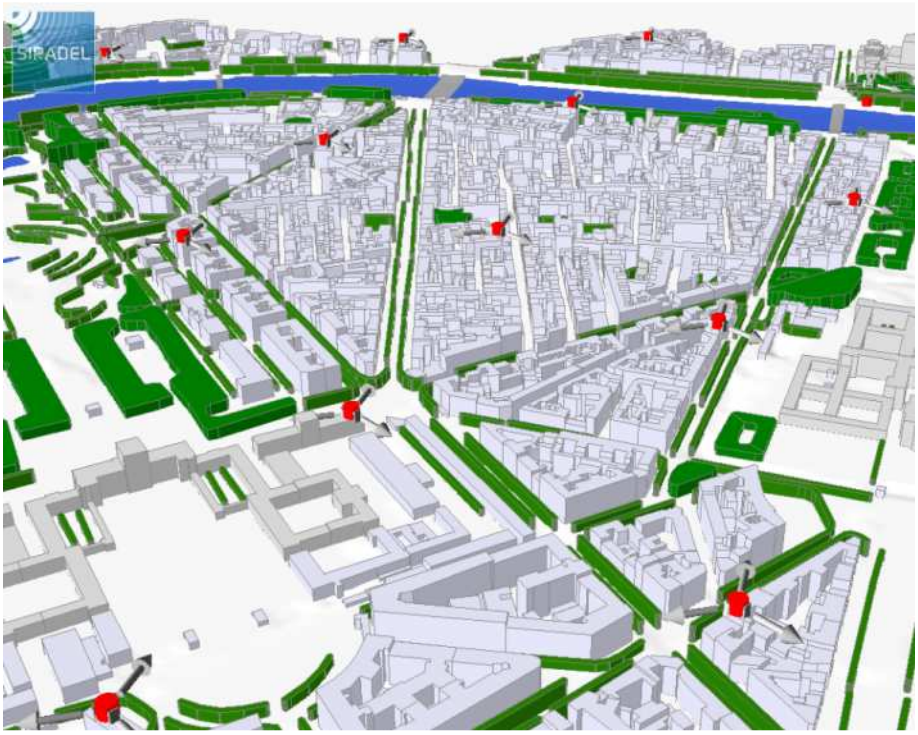

Figure 4: Paris LTE deployment.

The details regarding the deployment and LTE parameters are summarized in Table 2.

Table 2: Deployment and system parameters in the Paris LTE scenario.

System	LTE FDD 2x10 MHz. Central frequency: 2.6 GHz. UL/DL MIMO configuration: 2 x 2 (tx diversity). UL path-loss compensation factor: 1. UL SINR Target: 20.8 dB (when UL ICIC is disabled).
Macro-cell layout	Hexagonal site deployment: two rings around the central site, i.e. 19 sites corresponding to 57 cells (see Fig. 1). Inter-site distance (ISD): 450 m. ICIC FFR scheme: 5% of total radio resources being allocated to each sub-band, re-use factor of 3. Average antenna height: 32 m above ground. Maximum total transmit power: 40 W. Antenna: directional, 14 dBi, 6° electric down-tilt, 32 m above ground. UL noise figure: 2.5 dB
User equipment	UL total transmit power: from -40 dBm to +23 dBm. Antenna: omni-directional, 0 dBi, 1.5 m above ground. Number of antennas: 2. DL noise figure: 9 dB.

The LTE Paris scenario is involved in several studies, including WiFi offloading (Part-B, section 5.1), small-cell densification (Part-B, section 3.3), and small-cell beamforming (Part-B, section 4.3). The specific network deployment, system parameters, user distribution and user traffic assumptions that have been employed in those studies are detailed in the corresponding sections.

3.3 LEXNET urban reference scenario

It was not possible in all evaluation scenarios to capture all inputs needed in the EI calculation. Therefore a reference scenario was built from data given in [D2.8], in order to provide a common baseline for the EI evaluations conducted in urban environments.

The information related to the population and network users comes from a statistical analysis in Lyon downtown [D2.8, section 4]. First, the population is segmented in four categories: “children”, “young people”, “adults” and “seniors”, according to [D2.8, Table 29]. Furthermore, it considers a population distribution between outdoor and indoor users, and day and night periods; detailed information can be found in [D2.8, Table 30].

This network data has been estimated from recent measurements in the French Orange network. The average voice call duration and data volume is given by [D2.8, Table 32] for 3G “light”, “medium” and “heavy” users, while the percentage of voice and data users in the population is given by [D2.8, Table 31] and the repartition between “light”, “medium” and “heavy” users come from [D28, Table 33].

The 4G network usage is limited to data applications, as it is assumed that neither VoIP or VoLTE is deployed. The repartition between “light”, “medium” and “heavy” users, as well as the amount of data traffic per user category, are extrapolated from the 3G values with the correction factors of [D2.8, section 3.2.5.3]. The number of

devices connected to 4G is assumed to be 10 times lower than the number of 3G devices, based on 2013 figures [D2.8, section 3.2.2].

Finally, the reference SAR values are extracted from [D2.8, section 3.3], assuming that “adult” SAR values are relevant for “young people”, “adults” and “seniors” population categories. People being outdoors are supposed to be standing, while people being indoors are supposed to be seated.

3.4 GSM and UMTS Belgrade scenario

The scenarios for testing topology changes versus exposure reduction in a live network involve GSM and UMTS micro cells with overlaid macro layer, in the urban environment in Belgrade. These scenarios are intended to show the exposure reduction with the introduction of the micro layer, as well as to demonstrate EI calculation using measurements and data extracted from the network. The environment is shown in Figure 5, where the cells of the micro layer are denoted as “Mirijevo pijaca” (Mirijevo market).

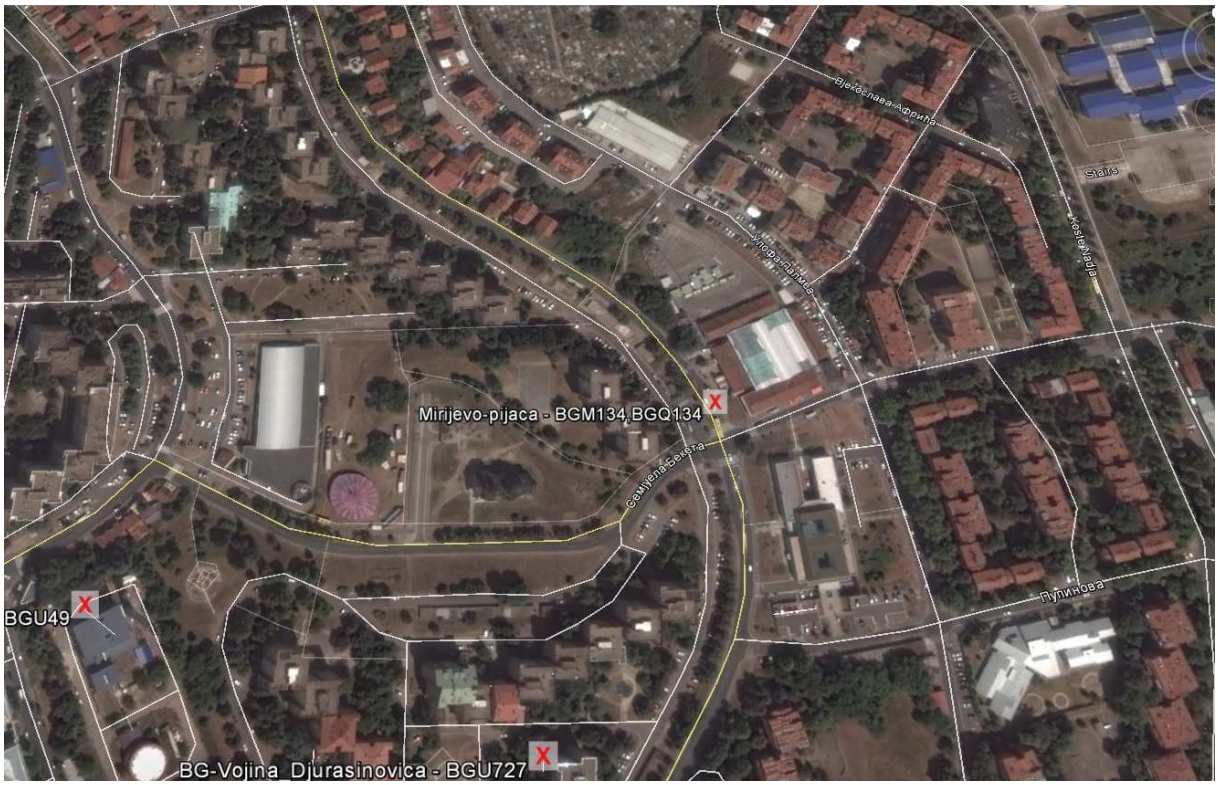

Figure 5: Belgrade environment.

The micro layer consists of one GSM cell and two UMTS cells, for two carriers used. The dominant site of the overlaid macro layer is at the location denoted as BG49 and it has two sectors targeting the area. GSM macro layer thus consists of two GSM cells, while the UMTS macro layer consists of 6 cells: two sectors with three carriers each.

The EI is calculated and compared for two scenarios, with micro layer turned on and off, and for two areas: macro area that represents the coverage of the two sectors of

macro base stations, and micro area that considers the coverage of micro base stations. The EI is calculated for the daytime and it represents the contribution of Telekom Srbija, as one of three mobile operators in the area, in the overall daytime EI. The methodology is presented in section 6.3, and illustrated with the results obtained during previous measurement campaign, partially presented in [D5.2]. The measurement results for the evaluation scenarios are presented in Part-B, section 3.2.

Data used for user segmentation and user profiles are statistical data and information obtained from various network resources for the urban cells in Belgrade, presented in [D2.8, 2015]. Fractions of users per technology layers are determined based on signalization data in the network during the observed period. Fractions of non-users are determined based on statistical data and data on market share per active users.

For the uplink calculation, data from network reports for the cells of interest is used, as well as data from cell statistics for the observed period. Power samples recorded in network reports for GSM technology are voice-only, so the calculation for GSM uplink concerns only voice service. For the downlink calculation, data from network reports for the cells of interest is used along with results of electric field measurements performed in the area. The coverage areas have been determined based on network planning tools and verified with drive-test measurements conducted in the area. DL measurements include the impact of surrounding base stations.

4 RESULTS IN A NUTSHELL

The EI assessment realizations are summarized in Table 3 (scenarios) and Table 4 (results). The template in Table 4 explains how the results have been organized, i.e. providing for each evaluated RAT the outdoor DL-EI, indoor DL-EI, total DL-EI, outdoor UL-EI, indoor UL-EI, total UL-EI and finally the total EI. As the investigated evaluation methodologies are not all able to capture all EI components, Table 4 does not give the same list of results for each scenario. All details can be found below in section 6.

Table 3: Summary on EI assessment scenarios.

Scenario	Section	Environment	Assessment methodology	Life segmentation	User traffic
1) Santander	6.1.1	Dense urban Macro-cells Multi-RAT	DL measurements from wearable dosimeter	Reference	-
2) Santander	6.1.2	Dense urban Macro-cells LTE	DL+UL measurements from a LEXNET connected device (so-called Tx/Rx platform)	Reference	Reference
3) Santander	6.1.3	Dense urban Macro-cells Multi-RAT	DL+UL measurements from a professional Trace mobile	Reference	Reference
4) Santander	6.2	Dense urban Macro-cells Multi-RAT	DL measurements from fixed dosimeters (sensor network)	Reference	-
5) Santander	6.4	Dense urban Macro-cells UMTS + LTE	DL+UL simulations (after calibration)	Reference	Reference
6) Belgrade	6.3	Dense urban Macro+Micro-cells GSM + UMTS	DL+UL network measurements	Belgrade	TKS network
7) Macro + Femtos	6.5	Urban outdoor + Office indoor Macro+femto-cells UMTS	DL+UL data	Specific	Specific

Table 4: Summary in EI assessment results.

TEMPLATE		
DL-Out	UL-Out	Out
DL-In	UL-In	In
DL	UL	**Total**

Scenario	Environment	EI calculation
1) Santander	Dense urban Macro-cells Multi-RAT	2G 900MHz: 6.49E-8 2G + 4G 1800MHz: 6.35E-8 3G 2100MHz: 2.85E-8 Wi-Fi 2400MHz: 1.83E-9
2) Santander	Dense urban Macro-cells LTE	4G 1800MHz: 1.02E-9, 2.78E-11, 1.05E-9
3) Santander	Dense urban Macro-cells Multi-RAT	2G 900MHz: 7.54E-11, 7.08E-7, 7.08E-7; 8.32E-11, 7.62E-6, 7.62E-6; 1.59E-10, 8.33E-6, **8.33E-6** 3G 2100MHz: 2.01E-9, 7.25E-10, 2.73E-9; 5.03E-9, 3.12E-8, 3.63E-8; 7.04E-9, 3.19E-8, **3.90E-8** 4G 1800MHz: 1.82E-9, 1.86E-8, 2.04E-8; 2.98E-10, 2.21E-8, 2.24E-8; 2.12E-9, 4.07E-8, **4.29E-8**
4) Santander	Dense urban Macro-cells Multi-RAT	2G 900MHz: 7.75E-8; 2.18E-8; 9.94E-8 2G 1800MHz: 2.78E-8; 7.85E-9; 3.57E-8 3G 2100MHz: 8.29E-9; 2.40E-9; 1.07E-8 Wi-Fi 2400MHz: 5.05E-9; 1.50E-9; 6.55E-9 4G 1800MHz: 5.05E-9; 1.50E-9; 6.55E-9
5) Santander	Dense urban Macro-cells LTE	4G 1800MHz: 1.48E-9, 2.42E-10, 1.72E-9; 3.82E-10, 4.04E-8, 4.08E-8; 1.86E-9, 4.06E-8, **4.25E-8** 3G 1800MHz: 3.14E-8; 7.07E-8; 1.02E-7
6) Belgrade	Dense urban Macro+Micro-cells GSM + UMTS	2G + 3G: 2.80E-06, 5.30E-06, **2.80E-06**
7) Macro + femtos	Urban Macro+femto-cells UMTS	3G 2100MHz: 2.24E-9, 2.02E-11, 2.26E-9; 9.68E-9, 1.44E-12, 9.69E-9; 1.19E-8, 2.16E-11, **1.19E-8**

Table 4 provides, in a nutshell, the main results that have been derived from the LEXNET EI assessment demonstrations. We cannot easily compare the values from the Santander, Belgrade and Macro+femto testbeds, but we can still draw some conclusions from all the figures gathered in the table:

- 2G networks generate the networks that generate the highest exposure level: **2 orders of magnitude higher** compared to other RATs.

- 4G DL exposure in Santander is particularly low, partly due to the small number of 4G networks and the limited cell load when the measurements were carried out.

- Having femto-cells in office buildings may significantly reduce the exposure level.

- Similar evaluations carried out with different assessment methodologies in the Santander testbed show that EI results suffer from significant uncertainty.
  This is quite relevant for the outdoor DL-EI of the Santander 3G network, which is measured in five different scenarios (1 to 5) and where variations over an order of magnitude have been seen.
  The reason is that the EI is sensible to the accuracy of many input parameters, and thus different methodologies, each of them having its own sources of uncertainty, were very unlikely provide similar results in the first large-scale trial. There is obviously some room for optimisation of the assessment methodologies. But this also stresses how important will be the characterization of uncertainty sources, protocols and equipment performance if absolute values of EI must be introduced into industrial or regulatory processes.

The EI values given above are one important LEXNET output, but the main interest of the validation work relies on the practical implementation, demonstrations and acquired know-how. The next sections of this document report with more details on those experimentations.

5 EMF MEASUREMENT TOOLS

This section describes the implementation and characterization of new measurement tools developed in the framework of LEXNET, which are involved in some of the EI assessment methodologies.
Three EMF measurement instruments have been developed by LEXNET partners: the first two are dosimeters (sections 5.1 and 5.2); the last one is a low-cost version of a Trace mobile, the so-called Tx/Rx platform (section 5.3).

5.1 Low-cost dosimeter

In order to perform a reliable evaluation of the EI, one of the challenges faced by the LEXNET project is the assessment of EMF over real networks. This evaluation requires on-field measurements over large scenarios and extended periods of time that need the development of new measurement methodologies.

With this purpose, a number of low-complexity dosimeters have been deployed within the city of Santander (Spain). They have been integrated as Internet of Things (IoT) devices within the SmartSantander [SMA] testbed. The low-complexity dosimeters therefore act as regular IoT nodes, so as to facilitate the process of gathering the produced data. In a few words, the sensor network, resulting of the dosimeters deployment, can be seen as a *macro* tool which will be able to fulfil the aforementioned requirements: ability to cover large-scale scenarios; and availability of continuous measurements during extended time periods.

The measurements obtained by the sensor network may provide useful information to calibrate the network simulations and E-field heat maps over a given area. Also the real time measurement data during a given period of time can be used to obtain statistical models of the E-field variations with time and population usage.

In the following, the integration of the dosimeters into the testbed is detailed. More information about the preliminary and calibration tests, as well as dosimeter design can be found in [D6.1].

5.1.1 Dosimeter

The low-complexity dosimeter, thoroughly described in [D6.1], is developed with the main requirement of undertaking a large scale deployment for EMF data collection over a given area. Against more capable dosimeters, like the wearable one [D3.2], the low-complexity dosimeter design is focused on its cost reduction, while ensuring an appropriate operation and accuracy of its measures.

In brief, the device is externally powered (by means of a cable provided with the dosimeter) and controlled. It provides a voltage level as output, which can be converted to the corresponding Electric field (E-field) value (in V/m) by means of lookup tables; the conversions have been studied after analysing the Antenna Factor (AF) and RF chain parameters (gain and losses). A vertical polarized printed monopole antenna has been chosen as the dosimeter probe, due to its good omnidirectional characteristics and low-cost integration. Table 5 shows the electrical and mechanical specifications of the dosimeter.

Parameter	Value
Dimensions	189 × 80 × 57 (mm)
Frequency standards covered	GSM DL, DCS DL, UMTS DL, WiFi 2.4 GHz
Dynamic range	60 dB
Sensitivity	5 mV/m
Polarization	Vertical
Power supply	3.3 V / 300 mA
Power supply type	External
Output type	DC Voltage level

Table 5: Low-complexity dosimeter main characteristics.

The dosimeter has been designed to monitor the downlink of the most widespread bands, as indicated in Table 6. The cellular standards are the source for most of the outdoor exposure, while WiFi 2.4 GHz band has been included to estimate the exposure from outdoor WiFi hot-spots, together with the indoor WiFi sources.

Application	3GPP band number	Frequency band (MHz)
GSM 900 DL	8	925 – 960
DCS / GSM 1800 DL	3	1805 – 1880
UMTS DL	1	2110 – 2170
WiFi 2.4 GHz	--	2400 – 2483.5

Table 6: Low-complexity dosimeter frequency band coverage.

It is worth highlighting that the cellular bands indicated in Table 6 are the only ones used in Santander at the time of the measurement campaigns. Furthermore, due to “spectrum refarming” techniques that are being exploited by the operators, bands that were initially devoted to a specific technology may accommodate a different one (for instance, the use of traditional 2G bands for LTE deployment). Despite being able to measure the E-Field in the aforementioned bands, the low-complexity dosimeter cannot distinguish between the contributions of different technologies in the same frequency band.

The block diagram of the low-complexity dosimeter is presented in Figure 6 below.

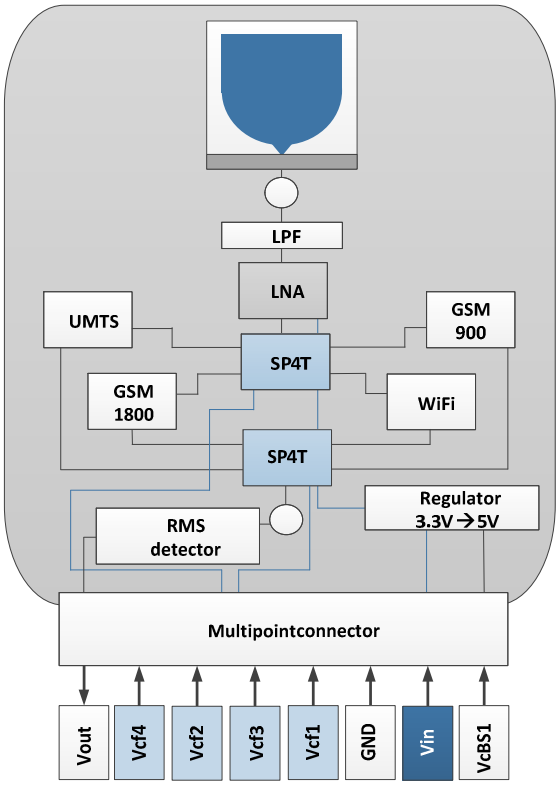

Figure 6: Functional block diagram of the low-complexity dosimeter and final product.

The control signals coming from the IoT node are able to switch between different frequency bands (marked as Vcf1 to Vcf4) and to enable/disable the dosimeter supply (marked as VcBS1), thus ensuring that the dosimeter consumes energy only when it is measuring. Section 5.1.2 provides more detailed information regarding the dosimeter control.

A total of 50 fixed dosimeters have been delivered for deployment in the Santander testbed. A separate calibration file has been provided for each dosimeter, after calibration measurements in controlled environment, which took into account the variations due to different tolerances (RF board fabrication, RF components, etc.). Thus each calibrated dosimeter provides the same value when subjected to a particular level of E-field (Figure 7a).

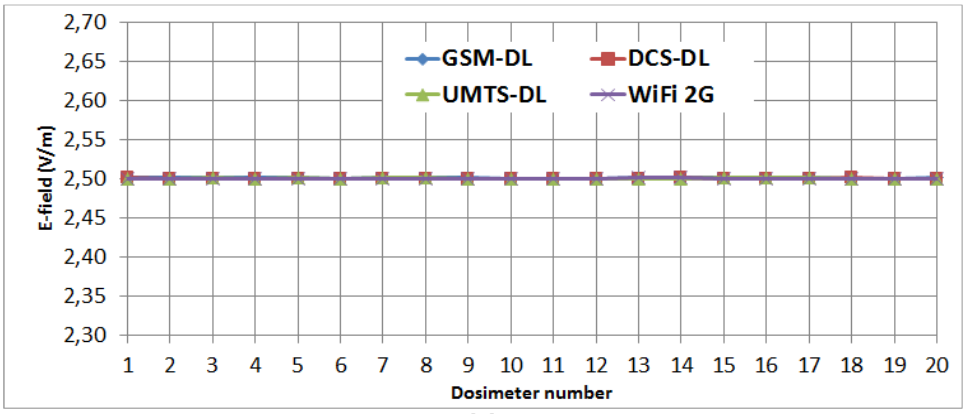

(a)

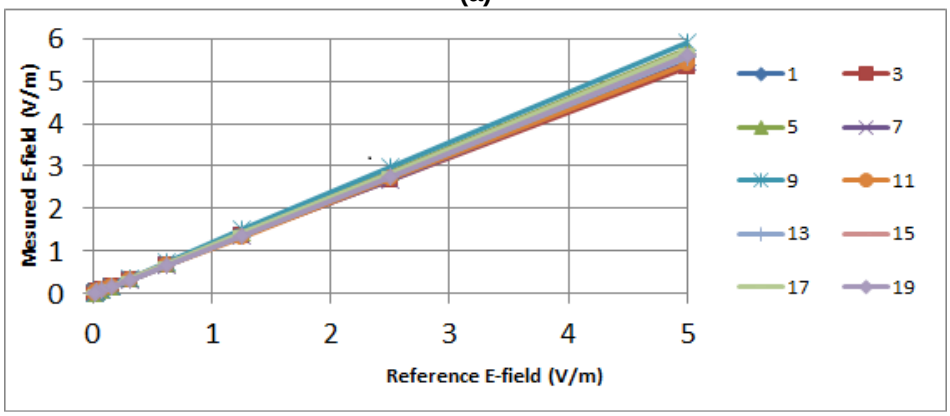

(b)

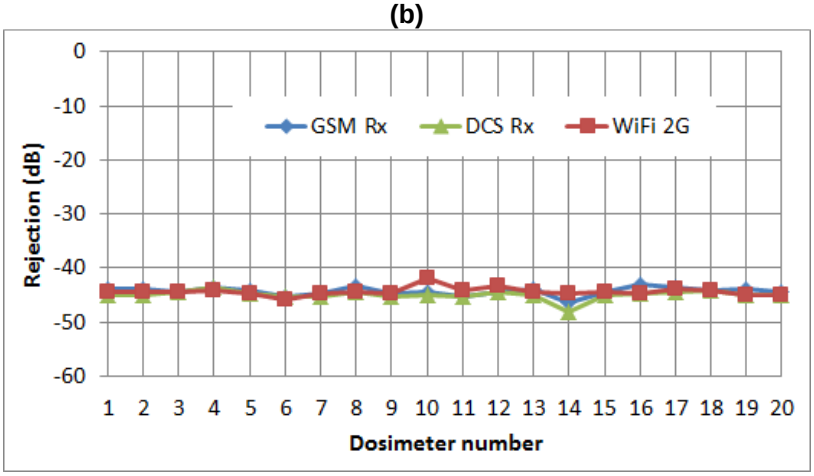

(c)

Figure 7: (a) Response of 20 dosimeters to a 2.5 V/m E-field in an anechoic chamber for the four frequency bands, (b) Linearity curve for the 10 dosimeters for UMTS-DL signal from measurements in an anechoic chamber, (c) Rejection between UMTS-DL and other bands for the 20 dosimeters.

The linearity curves for the dosimeters are shown in Figure 7b for a UMTS-DL signal as an example. We can see very good linearity characteristics for all the dosimeters. Only the measurements points at 5V/m shows somedeviation from the linear curve. This is attributed to the non-linearities generated by the instrumentation (signal generator and amplifiers working near the saturation levels). The rejection between UMTS-DL and the other three bands is shown in Figure 7c. A minimum rejection level of 40 dB is maintained.

5.1.2 Repeater

From the SmartSantander perspective the low-complexity dosimeters are deployed as IoT nodes, which are connected to repeaters. After considering different alternatives for the repeaters, the TSmoTe, provided by TST (see Figure 8) has been selected.

This solution ensures compatibility with the already deployed infrastructure in SmartSantander testbed since it uses the same protocols and communication hardware (namely, native 802.15.4 and Digimesh modification over Digi modules).

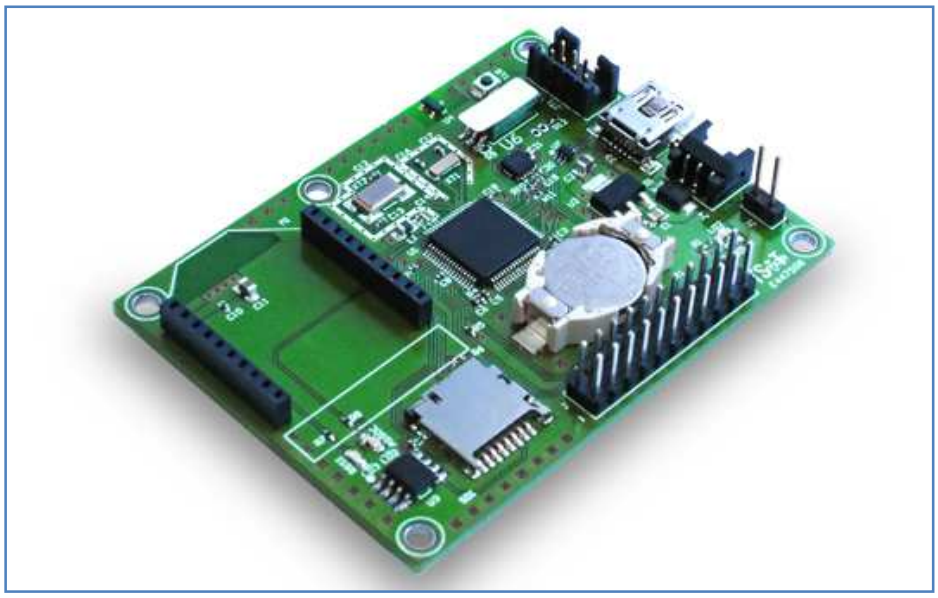

Figure 8: TsmoTe.

Since the repeater has to be connected to a power supply that allows recharging, it has been installed on lamp-posts, or on walls with nearby power source, so that they can be supplied, at least during the night, from the street lights. This solution allows battery recharging during the night and also the installation of the equipment at a certain height, to avoid vandalism.

The interaction between the dosimeter and the repeater is performed through an interface composed by 8 signals, as shown in Figure 6. These signals are controlled by a software routine installed in the repeater as briefly outlined below.

After a thorough phase of dosimeter calibration, the routine that takes the measurements is composed of the 5 steps described below:

1. *Power supply:* by controlling the VcBS1 signal, the dosimeter supply (Vin) is enabled and later regulated from 3.3 V to 5 V. Some experiments have shown that it is advisable to wait, at least, 1 ms after VcBS1 is enabled before starting the measurements.

2. *Frequency band selection:* this step consists of controlling the Vcf1-Vcf4 signals to switch on the desired frequency band.

3. *Vout voltage sampling:* once the dosimeter is switched on the desired band, the sampling of the Vout voltage can begin. According to the results obtained in the calibration process, the number of samples depends on the time required to sample each frequency band (see Table 7), and on the speed of the Analog to Digital Converter (ADC) of the hardware controller.

4. *Samples treatment:* once the list of values of each band has been acquired, these samples are treated in order to obtain a single voltage value; either the maximum of the median is used, depending on the particular band, as specified inTable 7.

5. *Field calculation:* finally, the voltage values are converted to EMF values (mV/m). This conversion is done by means of a lookup table that contains 3301 values, corresponding to each possible sample that the ADC can return (in the range 0 - 3300 mV). The field value is given in mV/m within the range 5- 5001 where the value of 5001 mV/m indicates that the measured field is higher than 5 V/m.

Table 7: Sample time for each frequency band.

Frequency band	Minimum sample time	Sample time used	Sample treatment
GSM	4.616 ms	6.3 ms	Median
DCS			
UMTS	6 ms		
WiFi	100 ms	200 ms	Maximum

5.2 Wearable dosimeter

The fixed dosimeter provides E-field measurements for limited standards and cannot distinguish between different operators. In order to obtain detailed E-field exposure data from different service providers and standards, an advanced dosimeter with a flexible architecture has also been developed. This device, when carried by a user over a day (for example), would reveal the exposure variations according to the different environments (work, school, home, transit, indoors activities, outdoor activities, etc.) and time (working hours, resting period, etc.). During the project, the dosimeter has been used for drive-test measurements (section 6.1.1). The state of the art dosimeters are presented in [D3.2]. They have two major limitations.

- The hardware of the existing dosimeters is not flexible. In order to modify the frequency bands (or to add new ones), all the hardware would need to be modified. LEXNET dosimeter addresses this problem by proposing a flexible architecture capable of including new bands and modifying the existing ones without the need to make any hardware changes. This will be a huge cost saving factor in the long term development plan, where the frequency spectrum is updated every 5 years, and also in terms of proposing a single solution for different geographical areas that employ different frequencies for the same technologies.
- The impact of the user body on the dosimeter measurements is not taken into account in the existing dosimeters. During the LEXNET project, an exhaustive

study has been carried out in order to evaluate this impact, and several correction schemes have been proposed [D3.2, 2014].

The block diagram of the wearable dosimeter and the final prototype is recalled in Figure 9. The wearable dosimeter characteristics, individual component characterisation, validation, and integration scheme have been presented in details in [D3.2]. The main characteristics are also discussed in Table 8.

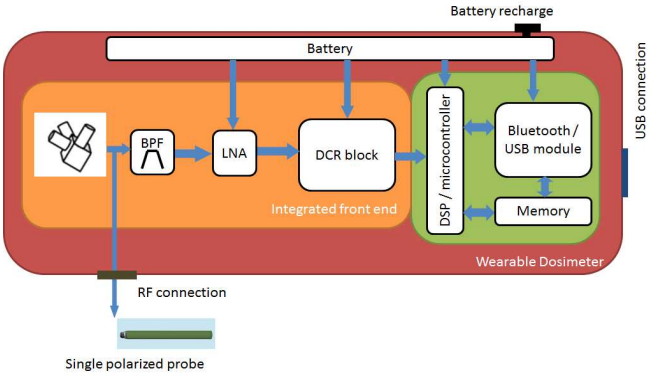

(a)

(b)

Figure 9: (a) Block diagram for the LEXNET wearable dosimeter, (b) final prototype compared to the state of the art dosimeter and a smartphone.

Table 8: Main specifications of the wearable dosimeter.

Frequency standards covered	All bands from 400 MHz up to 6 GHz
Frequency band resolution	From 7 MHz up to 100 MHz
Polarization	Three axes - isotropic
Dynamic range	60 dB
Sensitivity	5mV/m
Power supply	Flat battery 3.7 volts / 3700 mAh
Power supply type	Integrated battery
Output type	E-field in real time with dedicated Android app, or E-field stored in the memory on-board the device
Dimensions (mm)	166 x 70 x 42.5
Weight	360 g
Certification	IP55 (vertical position)

5.2.1 Characterization methodology

There are two modes of operation of the dosimeter. One is the standard mode, used to measure the E-field from different RATs. The second one is the operator measurement mode, where all frequency bands from different operators can be measured (with a minimum resolution of 7 MHz). The frequency bands supported by the two modes are summarized in Table 9.

The standard mode frequencies are the ones deployed generally over Europe, while the operator frequencies are the ones used in France. This choice was simply made because the operator frequency map was easily available in France. For future usage, the dosimeter can be programmed according to the user requirements in any country / area. The dosimeter can measure both UL exposure (from user's terminal) and DL exposure (from Base stations, access points, and other UE active around the user). Due to body masking effects, and the uncertainty of the position of the dosimeter with regards to the UE, the UL exposure data is not used for the evaluation of the EI. However, the dosimeter can be used to accurately assess the exposure due to other user's devices by measuring the UL bands.

Table 9: Frequency bands for the LEXNET wearable dosimeter in standard and operator modes of measurement.

Standard Mode 14 bands (UL & DL)	Operator Mode (DL only) 24 bands
LTE B20 DL (791 MHz – 821 MHz)	LTE B20 Bouygues (791 MHz – 801 MHz)
	LTE B20 SFR (801 MHz – 811 MHz)
	LTE B20 Orange (811 MHz – 821 MHz)
LTE B20 UL (832 MHz – 862 MHz)	
GSM 900 UL (880 MHz – 915 MHz)	
GSM 900 DL (925 MHz – 960 MHz)	GSM 900 Bouygues (925 MHz – 935 MHz)
	GSM 900 SFR (950 MHz – 960 MHz)
	GSM 900 Orange (935 MHz –945 MHz)
	GSM 900 Free (945 MHz – 950 MHz)
DCS 1800 / LTE B3 UL (1710 MHz – 1785 MHz)	
DCS 1800 / LTE B3 DL (1805 MHz – 1880 MHz)	DCS 1800 / LTE B3 Bouygues (1853 MHz – 1880 MHz)
	DCS 1800 / LTE B3 SFR1 (1805 MHz – 1808 MHz)
	DCS 1800 / LTE B3 SFR2 (1832 MHz – 1853 MHz)
	DCS 1800 / LTE B3 Orange (1808 MHz – 1832 MHz)
DECT (1880 MHz – 1900 MHz)	DECT (1880 MHz – 1900 MHz)
UMTS / LTE B1 UL (1920 MHz – 1980 MHz)	
UMTS / LTE B1 DL (2110 MHz – 2170 MHz)	UMTS / LTE B1 Bouygues (2125 MHz – 2140 MHz)
	UMTS / LTE B1 SFR 1 (2110 MHz – 2125 MHz)
	UMTS / LTE B1 SFR 2 (2150 MHz – 2155 MHz)
	UMTS / LTE B1 Orange 1 (2140 MHz – 2145 MHz)
	UMTS / LTE B1 Orange 2 (2155 MHz – 2170 MHz)
	UMTS / LTE B1 Free (2145 MHz – 2150 MHz)
Wi-Fi 2GHz (2400 MHz – 2483.5 MHz)	Wi-Fi 2GHz (2400 MHz – 2483.5 MHz)
LTE B7 UL (2500 MHz – 2570 MHz)	
LTE B7 DL (2620 MHz – 2690 MHz)	LTE B7 Bouygues (2655 MHz – 2670 MHz)
	LTE B7 SFR (2620 MHz – 2635 MHz)
	LTE B7 Orange (2635 MHz – 2655 MHz)
	LTE B7 Free (2670 MHz – 2690 MHz)
WiMax (3300 MHz – 3900 MHz)	
Wi-Fi 5GHz (5150 MHz – 5850 MHz)	Wi-Fi 5GHz (5150 MHz – 5850 MHz)

To characterize this dosimeter, a two-step approach is followed. First, the dosimeter RF board is tested alone, connected to a signal generator. A dedicated software is used to control the dosimeter and the signal input from the generator. The output from the dosimeter is recorded for all frequency bands, together with the variation in the power levels. The objective of this test is to determine the dynamic range of the dosimeter and to adjust the RF chain gain in order to achieve the required sensitivity levels.

Once these tests are finalized, the next step entails a measurement campaign in the anechoic chamber. The dosimeter is placed inside the chamber on a revolving platform in front of an antenna source. The chamber is calibrated, and a known E-field level is generated at the position of the dosimeter, using a wide band probe and a spectrum analyser. Then a measurement cycle is carried out over all the frequency bands at a fixed E-field level. The output of the dosimeter is then calibrated using the on-table tests (from the first step); as a result, the sensitivity levels and the complete dynamic range of the dosimeter are evaluated. In addition to these calibration tests, several other experiments are also carried out during the qualification phase. They include:

i- Rejection testing by injecting known signals in out-of-band frequency range and evaluating their impact on the system. The rejection curves are generated and analysed.
ii- Two-tone signals injected in order to evaluate their impact on the system,
iii- At fixed frequencies, a ramp of power is generated and the linearity of the dosimeter is evaluated by comparison to the measurements from a reference wide-band probe.

Several operational tests are carried out in parallel, including the correct transfer of data to memories or to external devices using the Bluetooth chip or the USB.

5.2.2 Characterization results of the dosimeter with tunable filter

Two technologies have been evaluated for the RF Bandpass filter: fixed filter and tunable filter. Fixed filters are SAW or ceramic filters covering an entire cellular band. Instead, the tunable filters can be adjusted to a specific frequency. The tunable filter design has been exposed in detail in [D3.2]. Since then, a PCB has been designed to integrate 2 tunable filters and 2 fixed filters (Figure 10). The measured results of this prototype are shown in Figure 11. In Table 10, the tuning states for the filter are recalled.

Table 10: Tunable Filter State for each target frequency band.

	Start	Center	Stop	BW	Tuning State
LTE 20 - Uplink	791	806	821	30	F1 (23)
LTE 20 - Downlink	832	847	862	30	F1(20)
GSM 900 - Uplink	880	897.5	915	35	F1(16)
GSM 900 - Downlink	925	942.5	960	35	F1(14)
DCS1800 - Uplink	1710	1747.5	1785	75	F2(23)
DCS 1800 - Downlink	1805	1842.5	1880	75	F2(20)
DECT	1880	1890	1900	20	F2(18)
UMTS - Uplink	1920	1950	1980	60	F2(16)
UMTS Downlink	2110	2140	2170	60	F2(12)
Wifi	2400	2441.75	2483.5	83.5	F2(8)
LTE band VII - Uplink	2500	2535	2570	70	F2(6)
LTE band VII - Downlink	2620	2655	2690	70	F2(5)

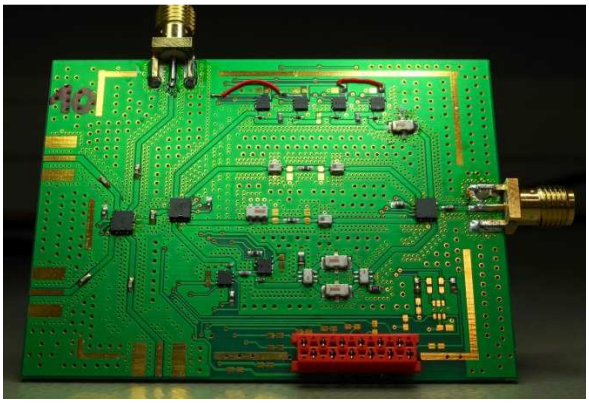

Figure 10: Prototype of Tunable filter PCB.

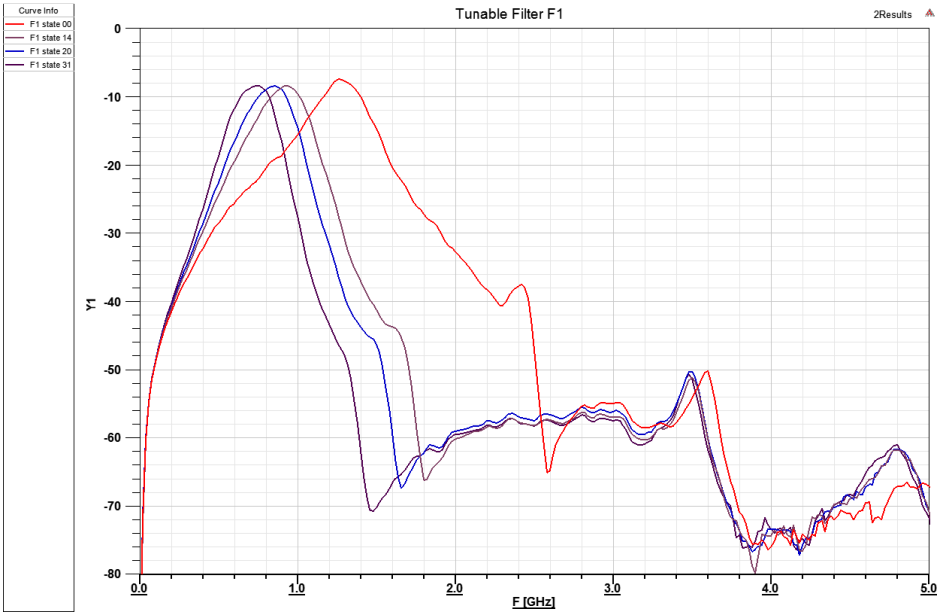

Figure 11: Results for Tunable Filter Prototype.

A dosimeter has been designed with the tunable filter solution, altogether on a single board with the LNA, detector and digital circuitry. Unfortunately, the integration of the tunable filter has not been successful because of the lack of ground vias, that are essential to the correct functioning of the filter (Figure 12). As a result, the frequency response of the filters show severe distortion and loss of performance (Figure 13). However, a proper implementation of the tunable filters would still be possible in a single PCB dosimeter, allowing for increased flexibility in the dosimeter design.

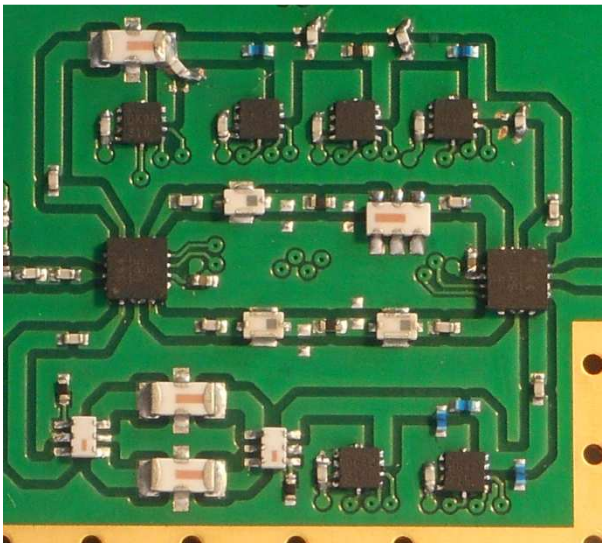

Figure 12: Tunable filter implemented on dosimeter.

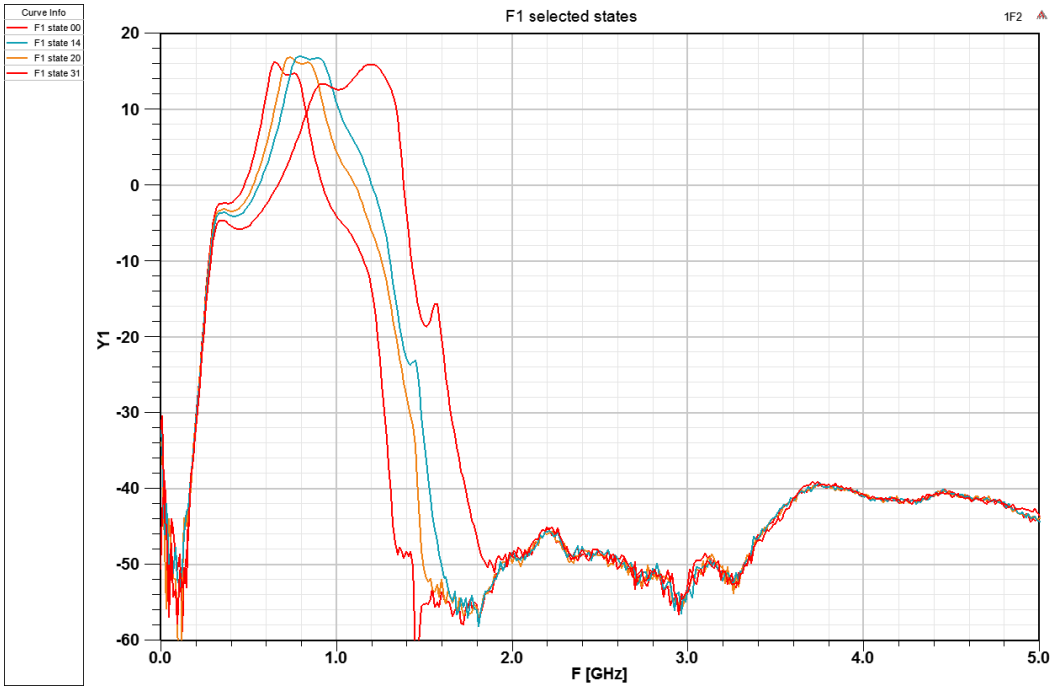

Figure 13: Results for single PCB implementation.

5.2.3 Characterization results of the dosimeter with fixed filters

The results of the on-table tests for both modes of operation are shown in Figure 14 for some of the frequency bands.

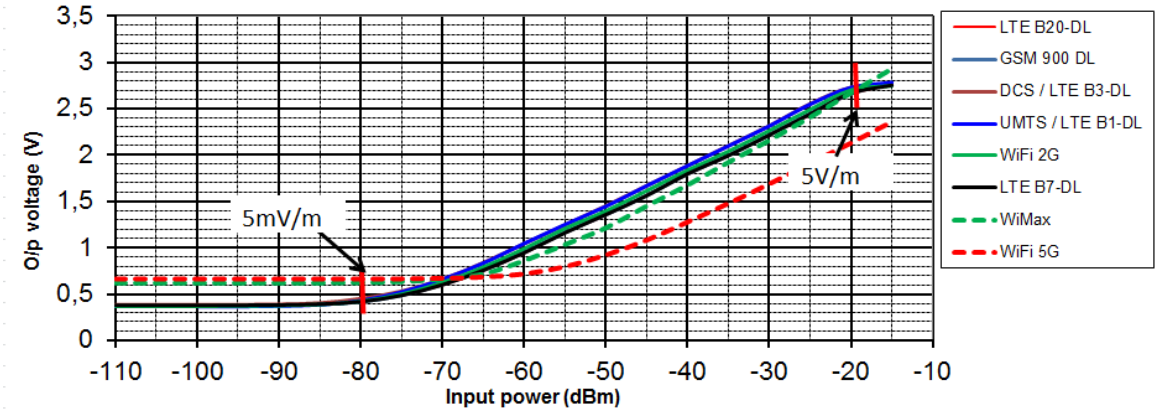

(a)

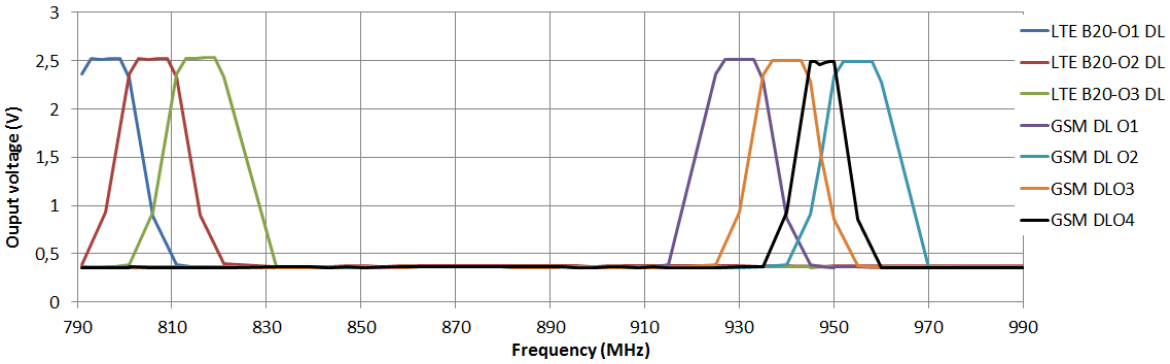

(b)

Figure 14: LEXNET wearable dosimeter on-table measurement results (a) standard mode output voltage vs. input power, (b) operator mode rejection curves between different frequency bands.

The curves in Figure 14a represent the output from the dosimeter for all bands with the variation of input power (from the signal generator). We can observe stable response of all bands up to LTE B7-DL, representing more than 60 dB of dynamic range (5mV/m up to 5V/m). For the Wimax and WiFi 5G frequency bands, the RF chain gain is not enough to achieve the 5mV/m sensitivity level, as both the amplification chain and the losses increase with frequency.

The curves in Figure 14b represent the rejection curves for a fixed power level with variation in the frequency. We can observe the excellent rejection between the operator frequencies. The legend “LTEB20-O1 DL” represents the first operator of the LTE band 20 for DL frequencies and so on. The natural overlap due to the baseband filter taper is caused by the contribution of the other operators while measuring a specific band. This overlap error can be calibrated using post-processing of the results with a simple mathematical operation.

After the on-table testing, the next step is to characterize the complete dosimeter in radiation mode, because the three-axial probes are not taken into account during the on-table tests. This characterization takes place in the anechoic chamber as explained in the previous sub-section. The measurement setup is presented in Figure 15.

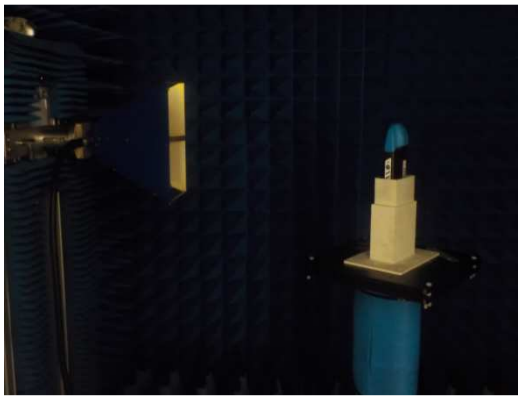

Figure 15: LEXNET wearable dosimeter characterization in anechoic chamber.

The dosimeter is rotated around itself and a known field is generated at the dosimeter position. Hence, the isotropy in the azimuth plane is evaluated for all frequency bands. The isotropy patterns at some of the frequencies are presented in Figure 16. The isotropy is evaluated for both vertical and horizontal incident polarizations.

Vertical polarization incidence

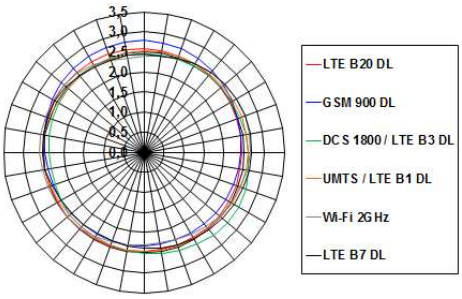

Horizontal polarization incidence

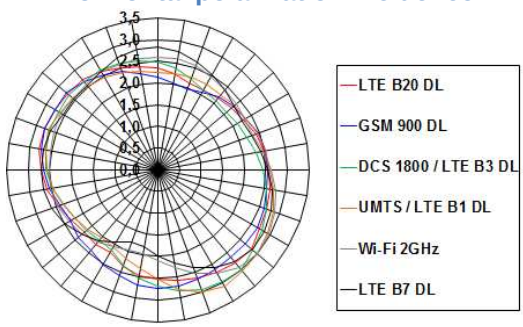

(a)

Frequency bandes	Isotropy VP ± dB	Isotropy HP ± dB
LTE B20 DL (791 MHz – 821 MHz)	0,29	1,29
LTE B20 UL (832 MHz – 862 MHz)	0,47	1,19
GSM 900 UL (880 MHz – 915 MHz)	0,71	1,37
GSM 900 DL (925 MHz – 960 MHz)	0,78	1,48
DCS 1800 / LTE B3 UL (1710 MHz – 1785 MHz)	0,68	1,32
DCS 1800 / LTE B3 DL (1805 MHz – 1880 MHz)	0,66	1,60
DECT (1880 MHz – 1900 MHz)	0,72	1,32
UMTS / LTE B1 UL (1920 MHz – 1980 MHz)	1,19	1,35
UMTS / LTE B1 DL (2110 MHz – 2170 MHz)	0,30	1.80
Wi-Fi 2GHz (2400 MHz – 2483.5 MHz)	0,66	1,85
LTE B7 UL (2500 MHz – 2570 MHz)	0,66	2,04
LTE B7 DL (2620 MHz – 2690 MHz)	0,65	2,04
WiMax (3300 MHz – 3900 MHz)	1,06	1,49
Wi-Fi 5GHz (5150 MHz – 5850 MHz)	3,98	3,97

(b)

Figure 16: LEXNET wearable dosimeter probe isotropy radiation patterns in the azimuth plane at (a) for vertical polarization incidence, (b) for horizontal polarization incidence, (c) Table with isotropy values for all frequency bands.

The linearity of the dosimeter is measured by applying a calibrated E-field level at the dosimeter position from 5mV/m up to 5V/m in the anechoic chamber, comparing it with the values measured by the dosimeter. The results are shown in Figure 17. It can be concluded that excellent linearity results are observed for all the measured frequency bands, i.e. from 1700 MHz up to 2700 MHz.

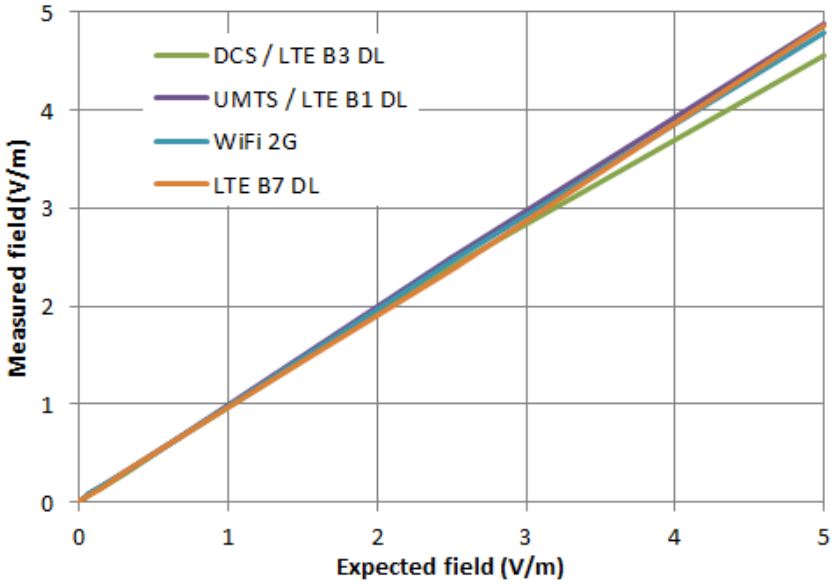

Figure 17: Linearity measurement results for the LEXNET wearable dosimeter.

5.2.4 Real-time dosimeter measurements with GPS data

After the proper calibration and qualification of the dosimeter, the final step is to test it with real time measurements. For this, a dedicated Android app has been developed at Satimo industries. The measurement setup and screen capture of the app is presented in Figure 18. The dosimeter and the Android phone are hand-held and the user walks within an outdoor light urban environment. The dosimeter measurements are transferred in real time to the Android phone and are coupled with the time stamp and the GPS location. The E-field for both modes (standard and operator mode) is displayed as shown in Figure 18b and Figure 18c. The user can scroll the screen to see the different bands. The results are automatically saved on the mobile phone memory for later use and post-processing.

Figure 18: LEXNET wearable dosimeter real time measurement android app, (a) measurement setup, (b) display in standard mode for RATs, (c) display in operator measurement mode.

To conclude, the LEXNET dosimeter provides a flexible and robust measurement solution as compared to the state of the art. The ability to differentiate the E-field exposure from different service providers, its smart and low-cost design, and its wearable capability make it an interesting candidate for large-scale E-field measurements compared to legacy dosimeter solutions, as well as to high-end devices (e.g. spectrum analysers). The easy-to-use Android app brings the ability to carry out real-time measurements with GPS locations and is suitable for general public use, as well as for professional end-users.

5.3 Tx/Rx platform

Trace mobiles are far from being part of traditional EMF measurement tools. However, the LEXNET exposure index combines both DL and UL contributions, the later one being related to the UL transmit power that may be measured only from devices connected to the network. That is why Trace mobiles are proposed as part of the measurement tool portfolio in LEXNET methodologies.

Common trace mobile solutions are dedicated to professional use and are expensive. During the LEXNET project, an alternative solution was envisaged to provide a low-cost alternative to the high end solutions. A dedicated prototype was developed and tested during the project. The design details, working principles and main characteristics have been reported in [D6.1, section 3.4.4]. This equipment has been used during the Santander measurement campaign which is presented in section 6.1 of this document. A comparison is made with professional drive test tools in appendix-2.5.

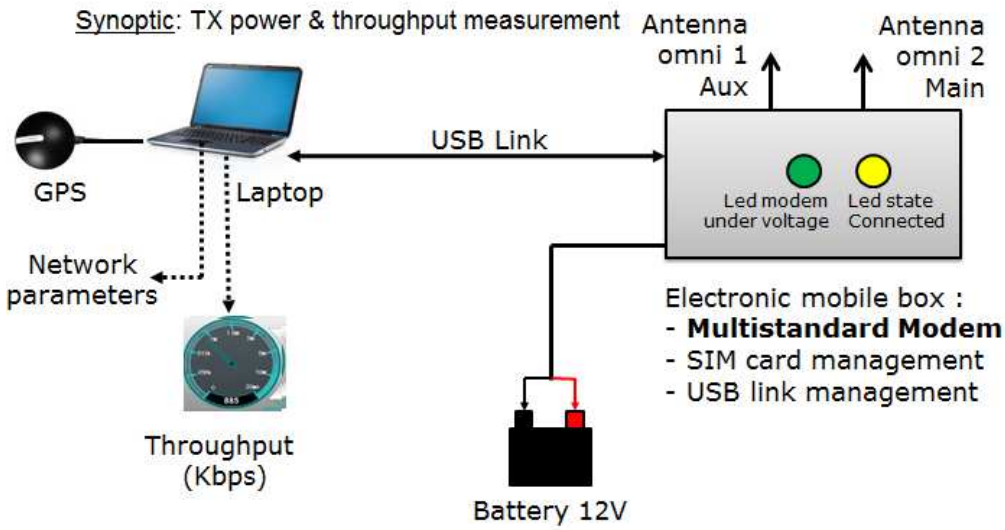

Figure 19: Tx/Rx platform schematic.

The network parameters available for different RATs from this platform are summarized in Table 11.

Table 11: List of network parameters available from Tx/Rx platform.

	CELL ID	RSSI (dBm)	RSCP (dBm)	Ec/No (dB)	RSRP (dBm)	RSRQ (dB)	SINR (dB)	TX Power (dBm)	DL Throughput (Mbps)
2G	*yes*	*yes*	*yes*	*yes*					
3G	*yes*	*yes*	*yes*	*yes*					*Yes*
4G	*yes*	*yes*			*yes*	*yes*	*yes*	*yes*	*Yes*

6 EI IMPLEMENTATION AND ASSESSMENT

6.1 In-field measurements (Demonstration in Santander)

Santander downtown is the place chosen by the LEXNET partners to simultaneously test several large-scale EI assessment methodologies and protocols for a real cellular network. Those protocols are illustrated in Figure 20.

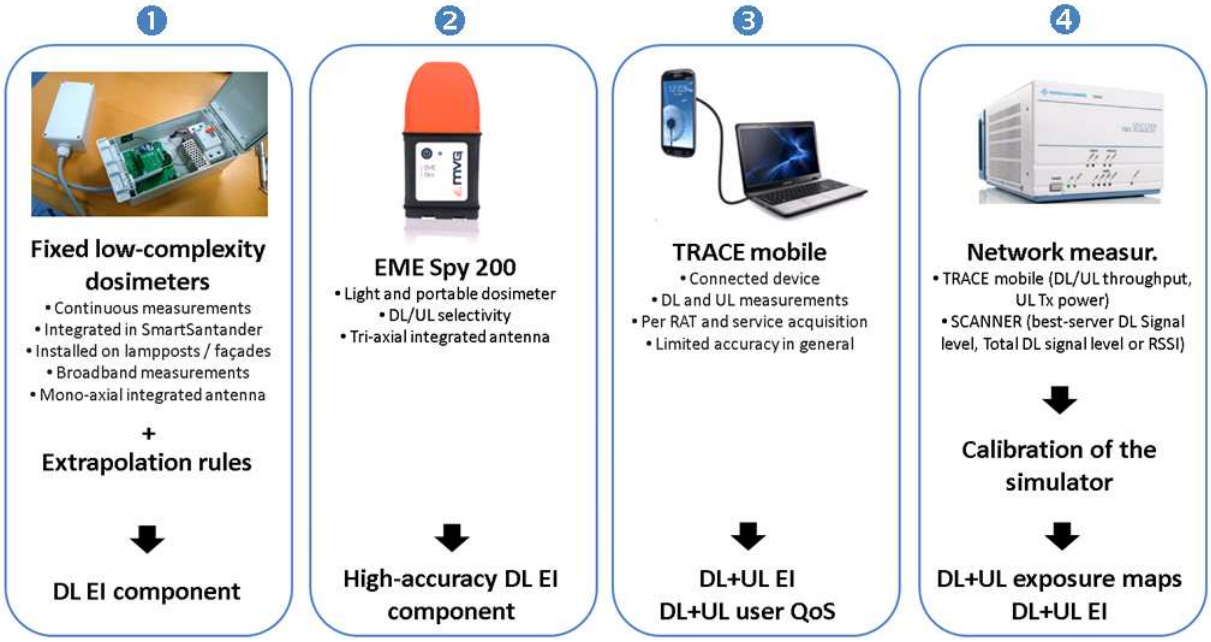

Figure 20: EI assessment protocols experienced in Santander downtown.

Protocol ❶ relies on the low-complexity dosimeters described in section 5.1, and deployed in the SmartSantander platform

The three other protocols involve in-field measurements collected from drive-test (i.e. into a vehicle) or pedestrian campaigns.
The wearable dosimeter EME Spy 200 in Protocol ❷ is a professional device [EME] close to the LEXNET dosimeter presented in section 5.2, although having only one measurement per frequency band (i.e. no distinction between operators). This equipment provides a very accurate measurement of the field strength, thanks to the integrated and fully-characterized three-axis antenna, and dedicated in-lab calibration.
Protocol ❸ has been experienced with two different Trace mobile equipments: a professional one with a Samsung mobile phone and the XCal Accuver software; this latter alternative is the low-cost version developed in LEXNET and described in section 5.3.

Finally, in Protocol ❹, the measurements of network metrics (related to exposure or QoS) are exploited for the adjustment of a simulator. The involved Scanner equipment is the multi-band network scanner from Rohde & Schwarz that provides simultaneous and passive DL measurements of GSM, HSPA and LTE networks. It is used with an external antenna (installed on the vehicle roof) for which we have a precise and accurate characterization of the radiation pattern.

The drive-test measurements of the Protocols ❷-❹ have been simultaneously conducted along a measurement path that covers the whole Santander downtown area, matching that where low-cost dosimeters have been deployed.
The measurements were repeated at several time periods in a day, in order to observe potential significant daily variation in the exposure.
Furthermore, an assessment of the outdoor/indoor differences has been realized from measurements in and around two covered market places.
The reader might refer to Appendix A2.1 for additional details on this measurement campaign.

The EI evaluation in SmartSantander is extensively reported in section 6.2, while the calibration of the simulation tool is discussed in section 6.4. The EI calculation from the EME Spy 200 and the Trace mobile equipment are given in the sub-sections below.

Drive-test measurements and simulations have been exploited to assess the performance of some of the protocols proposed in [D3.3], but also to refine the protocols themselves:

- Correction from mono-axial antenna measurement to isotropic field strength: see Appendix A2.2.
- Correction factor for low-cost dosimeter measurements: see Appendix A2.3.
- Extrapolation from outdoor to indoor field strength: see below in sections 6.1 and 6.4.
- Characterization of the low-cost Trace mobile equipment: see Appendix A2.4.

6.1.1 EI assessment from the wearable dosimeter measurements

The results from the passive dosimeter measurements following Protocol ❷ are divided into two categories.

1. Outdoor DL E-field exposure results – See section 6.1.1.1;
2. Indoor DL E-field exposure results – See section 6.1.1.2.

A characterization of a correction factor to be applied from outdoor to indoor is furthermore described in Section 6.1.1.3.

6.1.1.1 Outdoor DL E-field exposure results

The distribution for the four main frequency bands (i.e. GSM 900 DL, GSM 1800 and LTE B3 DL, UMTS 2100 DL, and Wi-Fi 2GHz) over the five different time periods are detailed in Appendix A2.

The average and standard deviation values for the above mentioned curves are summarized in Table 12.

Table 12: Average 'μ' and standard deviation 'σ' for the outdoor dosimeter measurements (V/m).

	GSM 900 DL		GSM1800 / LTE B3 DL		UMTS 2100 DL		Wi-Fi 2GHz	
	μ	σ	μ	σ	μ	σ	μ	σ
Wed-SWT-AM	0.182	0.176	0.253	0.267	0.124	0.149	0.047	0.030
Wed-RP1-PM	0.195	0.186	0.2	0.221	0.137	0.148	0.035	0.028
Wed-SWT-PM	0.197	0.208	0.23	0.236	0.125	0.131	0.043	0.023
Wed-RP2-PM	0.229	0.302	0.153	0.267	0.134	0.129	0.018	0.020
Fri-SWT-AM	0.200	0.227	0.205	0.330	0.174	0.206	0.045	0.047

The slight variations between the different measurements from the above table indicate the differences in usage and time (working hours or rest period).
From the above measurements we can easily calculate the DL component of the EI, using the reference usage data from section 3.3. The results are presented in Table 13.

Table 13: DL Exposure index results from outdoor mobile dosimeter measurements (W/Kg).

	GSM 900 DL	GSM1800 / LTE B3 DL	UMTS 2100 DL	Wi-Fi 2GHz
Wed-SWT-AM	5.31e-8	9.14e-8	2.23e-8	0.29e-8
Wed-RP1-PM	6.10e-8	5.71e-8	2.73e-8	0.16e-8
Wed-SWT-PM	6.23e-8	7.55e-8	2.27e-8	0.24e-8
Wed-RP2-PM	8.41e-8	3.34e-8	2.61e-8	0.04e-8
Fri-SWT-AM	6.42e-8	6.00e-8	4.4e-8	0.27e-8
Mean	**6.49e-08**	**6.35e-08**	**2.85e-08**	**1.83e-09**
Std deviation	**1.15e-08**	**2.17e-08**	**8.94e-09**	**1.09e-09**

The obtained results yield that the highest DL EI is observed for the two GSM bands. The lowest is for the Wi-Fi 2GHz band, which is scarcely deployed outside; the corresponding EI is basically due to the exposure to Wi-Fi access points used in the smart city platform and some indoor access points. Looking at the variation with respect to the time period, we see that the EI values are generally higher early in the morning and later in the day, which corresponds to an office (working hours) area. Looking at the UMTS values, which mostly account for data usage, we see fairly constant values during the whole day of Wednesday while for Friday morning the values are twice as large. This probably shows the increase in data traffic due to user demand at the weekend but it is difficult to conclude based on a single set of measurements.
These results would help in comparison with the results from the fixed dosimeters deployed in Santander.

6.1.1.2 Indoor DL E-field exposure results

The indoor DL E-field measurements were carried out inside two market place buildings as indicated in Appendix A2.1. All indoor measurements were carried out during Thursday. The time line for different indoor measurements is shown in Table 14.

Table 14: Dosimeter measurement cycles for indoor measurements.

	Market 1	Market 2
Market name	Mercado Del Este	Mercado la Esperanza
Cycle 1	SWT-AM	RP-PM
Cycle 2	RP-PM	SWT-PM
Cycle 3		SWT-PM

The average and standard deviation values for the different cases above are summarized in Table 15. The distribution curves can be found in Appendix A2 to get a higher level of detail.

Table 15: Average 'μ' and standard deviation 'σ' for the indoor dosimeter measurements (V/m).

	GSM 900 DL		GSM1800 / LTE B3 DL		UMTS 2100 DL		Wi-Fi 2GHz	
	μ	σ	μ	σ	M	σ	μ	σ
Market1 (SWT-AM)	0.025	0.010	0.045	0.020	0.060	0.021	0.010	0.005
Market1 (RP-PM)	0.027	0.015	0.044	0.017	0.064	0.037	0.012	0.007
Market2 (RP-PM)	0.092	0.028	0.048	0.010	0.053	0.011	0.009	0.004
Market2 (SWT-PM)	0.082	0.022	0.045	0.008	0.051	0.011	0.009	0.005
Market2 (SWT-PM)	0.082	0.021	0.044	0.009	0.056	0.011	0.009	0.007

These results can be then used to extract the extrapolation between indoor and outdoor E-field exposure.

6.1.1.3 Extrapolation factor for outdoor to indoor E-field

In order to have an idea of the mean difference between the E-field exposures indoors and outdoors, specific pedestrian measurements were carried out in and around a market place. These consist of collecting dosimeter measurements along two itineraries: one inside and the other one just outside the market 1. The two itineraries are shown in Figure 44 in Appendix A2.1 (red for the indoor and green for the outdoor.

The average and standard deviation values are summarized in Table 16. An average extrapolation factor "α" between indoor and outdoor DL E-field measurements is evaluated for each band, as shown in the table below. Here α is the ratio of the average value of E-field measured inside the market hall, to the average value of the E-field measured outside the market hall.

It should be noted that these results are based on a single measurement campaign in a specific scenario (with light indoor structure) at a given time. To have a more

reliable extrapolation factor, more measurement data sets, obtained over different scenarios, are required.

Table 16: Average 'μ' and standard deviation 'σ' for the indoor and outdoor dosimeter measurements and the extrapolation factor.

	GSM 900 DL		GSM1800 / LTE B3 DL		UMTS 2100 DL		Wi-Fi 2GHz	
	μ	σ	μ	σ	μ	σ	μ	σ
Inside (V/m) (Market1-SWT-AM)	0.025	0.01	0.045	0.02	0.06	0.021	0.01	0.005
Outside (V/m) (Market1-SWT-PM)	0.053	0.018	0.092	0.029	0.105	0.039	0.012	0.005
Extrapolation factor (μ_{in} / μ_{out})	0.472		0.489		0.571		0.833	
Extrapolation factor (dB)	-6.527		-6.212		-4.861		-1.584	

6.1.2 EI assessment from the Tx/Rx platform measurements

This section reports on the EI assessment from the Tx/Rx platform, which is one particular implementation of Protocol ❸. Only LTE measurements are reported here, including both DL and UL.

In Appendix A2.5, the main parameters concerning QoS and EMF exposure are presented. The UL measurements, in particular, depend on the running application. Hence, several measurements have been collected for different applications. For FTP upload measurements a file of 600 Mb was uploaded to a server. For LTE browsing measurements, web browsing of Google, Flickr, and Getty images was carried out, emulating a heavy user scenario. For LTE streaming measurements, a HD YouTube video was retrieved. For all the above mentioned measurements, the Iperf protocol was used to calculate the throughput (approximately every 8 seconds). The rest of the network parameters were recorded every 4 seconds.

The average and standard deviation values are summarized in Table 17 below. The distribution curves for each case are detailed in Appendix A2.5.

Table 17: Average 'μ' and standard deviation 'σ' for the outdoor drive tests (LTE only) using the dongle.

	RSSI (dBm)		RSRP (dBm)		RSRQ (dB)		SINR (dB)		Tx power (dBm)		UL Throughput (Mbps)	
	μ	σ	μ	σ	μ	σ	μ	σ	μ	σ	μ	σ
Iperf only (Monday SWT-PM)	-61.6	10.6	-89.3	9.7	-9.3	3.1	9.7	8.3	8.6	11.3	12.9	4.2
FTP Upload (Monday SWT-PM)	-64.6	10.9	-88.9	9.9	-5.9	2.0	10.6	8.1	16.1	8.4	8.5	2.8
Browsing (Wednesday SWT-AM)	-60.0	8.9	-84.2	9.2	-6.0	1.2	11.9	8.0	12.7	12.0	14.4	3.9
Streaming (Wednesday SWT-AM)	-58.7	9.8	-84.0	9.8	-5.6	1.9	12.0	8.8	10.8	12.5	13.4	3.3
Browsing (Wednesday SWT-PM)	-59.4	10.4	-84.1	10.3	-5.5	1.8	11.6	7.9	14.5	10.3	12.4	3.2
Streaming (Wednesday SWT-PM)	-58.8	9.8	-83.7	10.2	-5.7	2.4	12.4	8.5	12.0	11.8	13.5	3.6

It can be observed that DL parameters (RSSI, RSRP) are quite stable throughout the different time periods. On the other hand, UL and QoS parameters (RSRQ, SINR, Tx power, and throughput) show a dependency on the usage at the time of measurement (browsing, streaming, etc.) and the measurement conditions in general (network traffic, load, environment, time period etc.).
From the above measurement data, the EI can be calculated for the UL and DL components. The EI for UL is the weighted sum for each service according to the traffic distribution from [CIS, Table 13]:

- FTP upload: 1%;
- Voice: 8%;
- Data & browsing: 36%;
- Streaming: 55%.

The DL component of the EI is the average all the measurements per service. The results are presented in Table 18.

Table 18 EI (W/Kg) from the Tx/ Rx platform measurement results for the LTE B3 in outdoor environment.

	DL-EI	UL-EI	Total EI
Exposure index (W/kg)	1.02e-9	2.78e-11	1.05e-9

We see from the above results that the DL component of the EI is dominant. This actually was expected from outdoor-only measurements:

1- DL exposure dominates in outdoor environment case due to better propagation conditions for the UE (and hence low uplink power emissions).
2- The number of LTE users is limited and hence the representative UL exposure for LTE case scenario is quite small.

6.1.3 EI assessment from the Trace mobile measurements

This section reports on the EI assessment based on the commercial Trace mobile measurements, following Protocol ❸.
The test protocols consist of performing drive and static measurements for different Radio Access Technologies, services and time periods, as described in Appendix A2.1. Then the measurement statistics related to QoS or EMF are processed. The details are given in Appendix A2.4.
The EI is computed according to those statistical results. It is done for each RAT following the guidelines provided in [D2.8], and taking into account the user and population distribution of the reference LEXNET scenario (section 3.3) .

6.1.3.1 EI assessment for LTE 1800

Table 19 to Table 20 summarize all exposure-related measurements from different services.

Table 19: Measurements from LTE FTP Downlink.

FTP-DL	Outdoor drive	Indoor
Mean Downlink Field Strength (W/m²)	1.70E-06	2.41E-07
Mean Uplink active transmit power (W)	2.48E-02	1.07E-01
Mean Uplink throughput (kB/s)	22.5	20.8

Table 20: Measurements from LTE FTP Uplink.

FTP-UL	Outdoor drive	Indoor
Mean Downlink Field Strength (W/m²)	8.22E-07	1.70E-07
Mean Uplink active transmit power (W)	1.12E-01	1.67E-01
Mean Uplink throughput (kB/s)	1662	1835

Table 21: Measurements from LTE Video Streaming.

Video Streaming	Outdoor drive	Indoor
Mean Downlink Field Strength (W/m²)	1.59E-06	3.50E-07
Mean Uplink active transmit power (W)	2.27E-02	8.86E-02
Mean Uplink throughput (kB/s)	13.7	7.9

Table 22: Measurements from LTE Web browsing.

Web browsing	Outdoor drive
Mean Downlink Field Strength (W/m²)	6.75E-08
Mean Uplink active transmit power (W)	1.15E-01
Mean Uplink throughput (kB/s)	7.5

Some comments can be drawn from these results:

- DL field strength is quite similar for all services as expected. There is one exception with web browsing, where EI is lower by a factor 4-8 times, and

which we do not have any obvious explanation. Additional test would have been required to identify the source of this variation.

- Mean DL field strength is 5.5 times lower in indoor than outdoors. Of course, as the indoor measurements were collected from only two different locations, we actually expect some uncertainty.
- The UL transmit power efficiency (ratio between throughput and transmit power) is in average 4.3 times higher in outdoor than indoors.

In Table 23, the measurements per service are combined to provide a global EI contribution.

Table 23: EI for LTE 1800.

	Outdoor	Indoor	Total
EI-DL contribution (W/m²)	1.82E-09	2.98E-10	2.12E-09
EI-UL contribution (W/m²)	1.86E-08	2.21E-08	4.07E-08
Global EI (W/m²)	2.04E-08	2.24E-08	**4.29E-08**

These final results show that:

- Outdoor and indoor EI are of similar order.
- EI-UL contribution is about 19 times higher than EI-DL.
- Main EI-DL contribution is coming from the outdoor environment, while the uplink components are similar for outdoor and indoor.
- The global EI is very close to the one obtained by simulation, presented in section 6.4.

6.1.3.2 EI assessment for 3G 2100

For 3G measurements, voice service has also been considered. DL and UL measurement results are presented in Table 24 and Table 25 for data and speech respectively.

Table 24: Mean DL field strength for 3G data and voice.

Mean DL field strength (W/m²)	Data	Voice
Outdoor	3.74E-07	5.45E-07
Indoor	1.18E-07	1.36E-07

Table 25: Mean UL transmit power for 3G and voice.

Mean Uplink transmit power (W)	Data DL	Data UL	Voice
Outdoor	1.07E-04	1.19E-03	1.02E-04
Indoor	9.63E-03	5.39E-02	1.03E-03

As expected, the DL mean field strength is quite similar for both data and voice. The mean UL transmit power is significantly higher (x10 in outdoor and x5.6 in indoor) for UL data transfer.

Table 26 presents the EI assessment results for 3G 2100 MHz.

Table 26: EI for 3G 2100.

	Outdoor	Indoor	Total
EI-DL contribution (W/m²)	2.01E-09	5.03E-09	7.04E-09
EI-UL contribution (W/m²)	7.25E-10	3.12E-08	3.19E-08
Global EI contribution	2.73E-09	3.63E-08	**3.90E-08**

These results show that EI indoor contribution is about 13x higher than EI outdoors. And EI-UL contribution is about 4.5x higher than EI-DL.

The global EI contribution for 3G is equivalent to LTE in this measurement test campaign.

6.1.3.3 EI assessment for 2G 1800

Only voice service has been measured in 2G. The results are presented in Table 27 and Table 28 for DL and UL respectively.

Table 27: Mean DL field strength for 2G voice.

Mean DL field strength (W/m²)	Voice
Outdoor	3.12E-08
Indoor	3.91E-09

Table 28: Mean UL transmit power for 2G voice.

Mean Uplink transmit power (W)	Voice
Outdoor	9.00E-02
Indoor	4.17E-01

Table 29 summarizes the EI contribution for 2G voice..

Table 29: EI for 2G 1800.

	Outdoor	Indoor	Total
EI-DL contribution (W/m²)	7.54E-11	8.32E-11	1.59E-10
EI-UL contribution (W/m²)	7.08E-07	7.62E-06	8.33E-06
Global EI contribution	7.08E-07	7.62E-06	**8.33E-06**

Uplink is obviously the main EI contribution in 2G. And it is 10x higher in indoor than in outdoor.

Finally, when comparing all radio technologies, it appears that 2G UL indoor speech usage provides the highest EI contribution, far ahead of other technologies and services.

6.2 Smart Santander platform

This section describes the EI assessment carried out over the sensor network that is built with the low-complexity dosimeters. As mentioned before, the resulting deployment gives rise to a distributed macro tool able to take on-field measurements over a large area and during extended time periods.

This section is structured as follows. First, subsections 6.2.1 and 6.2.2 depict the methodology applied for the dosimeter deployment. Then, subsection 6.2.3 details the main results obtained from the sensor network, both temporal statistics of the E-field throughout the city and the implementation of the downlink component of the EI, based on the previous statistics and using the appropriate methodology.

6.2.1 Deployment procedure

This section discusses the techniques used in the design of the sensor network deployment. They are used to estimate the expected EMF measurement accuracy from the on-field deployment and optimize the location of dosimeters.

The deployment methodology first aims at characterizing the RF-EMF on the target area. To this end, it shall produce a good approximation of the statistical distribution of the E-field over the whole area, and, furthermore, it must provide an interpolation model with a reasonable accuracy. Since the deployment is tuned to improve the EI characterization, it can be referred to as part of the EI implementation.

This first objective is addressed by estimating the required density of dosimeters over the area. Simulation mimics the measurements from different sensor deployments in a dense urban area in the HSPA frequency band. The setup is made according to the Santander scenario, such that the comparison of different sensor densities or deployment rules becomes more relevant. The same simulations are exploited to derive a basic model that transforms outdoor lamppost-height measurements to in-street and in-building estimations.

The second goal, the deployment optimization, is fulfilled by an efficient procedure that establishes the location of the dosimeters based on the iterative method. This method defines the location of a set of dosimeters based on the measurements provided by those already deployed.

The overall procedure is briefly described below in a step-wise manner, while more information can be found in [DIE]:

1. Initial simulations are performed using detailed information about the target area. This provides valuable data (model based) that will be considered during the whole deployment process.

2. Partial deployment. In an initial phase there are not real measurements to guide the deployment, and a preliminary simulation study is used. In the subsequent steps, the sequential algorithm provides insights about the best possible locations.

3. After a certain period of time, the dosimeter measurements are analysed, spatially and temporally, a more detailed description can be found in A4.2. This information is then used by the algorithm to estimate the best locations for the new batch of dosimeters.

4. Steps (2) and (3) are repeated until all dosimeters are distributed.

5. Once the whole deployment is completed, the obtained measurements are used to calibrate simulation tools and models.

The information necessary to trigger the deployment is obtained by means of simulation tools as follows:

- First, the EMF metric is predicted over a map (or pixel grid) that covers the whole study area; this map is considered as a realistic EMF realization; it is afterwards used as a reference for the creation and evaluation of sensor measurements;
- Then, the EMF sensor measurements are emulated by selecting sample values in the reference map, at given fixed locations.
- Finally, the EMF statistics computed from the whole map are compared to the EMF statistics from the sensor measurements, in order to evaluate the performance of the sensor network.

The simulation is carried out following a deterministic approach, as thoroughly described in Appendix A4.1. The main conclusions are summarized in Table 30 for the 3G network at 2.1 GHz, where the absolute mean error and the RMSE from the WSN estimation is given as a function of the dosimeters deployed in Santander downtown. Increasing the number of dosimeters from 10 to 25 significantly reduces the estimation error; however additional dosimeters do only have a limited impact.

Table 30: Error statistics on the sensor network estimation.

Sensor network with	50 probes		25 probes		10 probes	
	Mean |bias| (dB)	RMSE (dB)	Mean |bias| (dB)	RMSE (dB)	Mean |bias| (dB)	RMSE (dB)
Single HSPA network	1.17	3.06	1.03	3.48	2.38	5.19
All HSPA networks	1.38	2.52	1.40	2.63	1.71	3.87

Appendix A4.1 also reports on additional simulation studies on the indoor penetration loss and height extrapolation factor that may be used in the conversion procedure from the dosimeter measurements to the population DL exposure.

The technique for sequential EMF sensor deployment optimization, which is applied in the steps following this initial deployment analysis, is still under test. It has not yet been fully demonstrated; however the main principles can be found in Appendix A4.2.

The overall procedure has not been completed at the time of writing this document. In this sense, one iteration of the above mentioned methodology has been performed resulting in the deployment of 20 devices. Due to limitations, inherited from a

deployment over a real scenario, the locations of the rest of devices will be determined by the availability of positions.

6.2.2 EI assessment method

While the deployment of the sensor network allows large scale (temporal and spatial) E-field measurements, it also has some limitations in the accuracy of the measurements.

In this sense, the low-complexity dosimeter performs wide-band measurements and it is not able to distinguish the E-field induced by different operators. Furthermore, the device is single-polarized, so that the values gathered by the whole platform must be appropriately processed to correct this effect. Considering the above mentioned limitations, the data collection follows the diagram described in [D3.3], Figure 2.b.
Besides, the installation also produces a distortion of the E-field values measured by the dosimeter, which should be also taken into account when calculating the EI.

The calculation of the EI from the sensor network follows the steps described in Figure 21. Once the dosimeters are deployed according to the methodology previously discussed, the wide-band E-field values are measured and tagged both temporally and spatially. Then different correction factors are applied in order to improve the accuracy of the measurements.

First, the extrapolation from mono-axial to isotropic factor is applied to the values for each frequency band as described in Appendix A2.3. Once the samples' accuracy is comparable to a 3-axis device, we consider the effect that both the installation and the environment may have on the measurements. For that, the correction factors obtained during the measurements, and presented in Appendix A2.4, are applied. Since the variation of the correction factors for different periods of the day is not relevant, the average value during the whole day is used for each frequency band.

Once the samples have been processed to overcome the simplifications of the dosimeter and the distortion caused by the installation, the values from bands with more than one technology are divided, according to the estimated weight of each technology. This step is needed to apply appropriate ICT statistics corresponding to different technologies. At this point, E-field values corresponding to each technology are finally obtained; from these, the downlink component of the EI can be estimated. Regarding the uplink component of the EI, a clear mapping between the wideband downlink E-field and the transmission power of the user device does not exist yet.

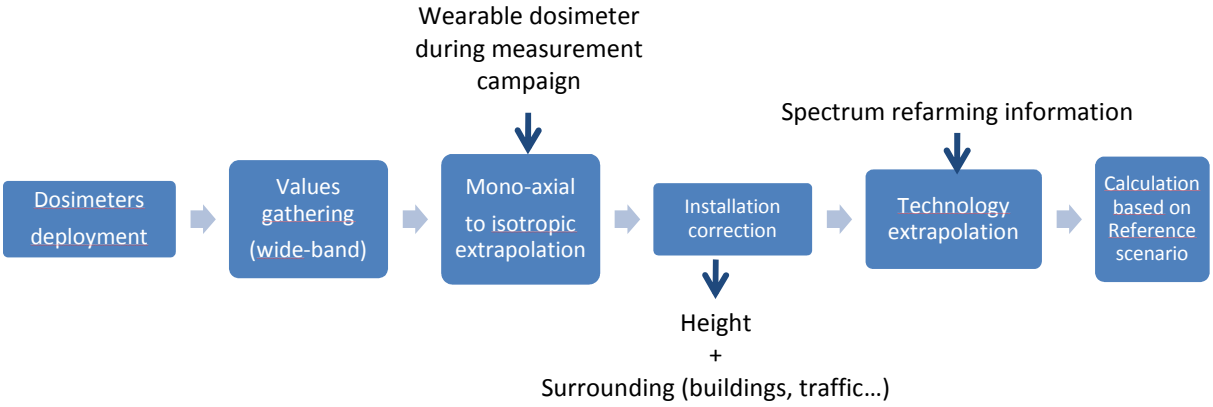

Figure 21: EI calculation for the SmartSantander testbed.

In this sense, the sensor network is able to provide continuous evaluation of the EI based on on-field measurements, and the EI evolution over the given area can be studied. From a measurement point of view, the main innovation is that the resulting macro tool continuously takes measurements over a larger area. Besides, unlike other solutions, this approach can be implemented without much information about the network deployments within the area.
On the other hand, as has been previously explained, there exist some intrinsic limitations to the approach, which are enumerated below along with the solution adopted for each of them for the EI calculation:

- Impact of the installation: this might be better corrected by characterizing each single installation point with a more suitable measurement device, such as a wearable dosimeter. In cases where the number of points is large, this solution might be infeasible. Besides, due to the fact that the EI is averaged over one day, an average correction factor might be otherwise appropriate.
- The wide band measurement: the fact that all the E-field values of the same band are measured together might be overcome with more information about the particular deployment in the area.
- EI uplink extrapolation: to overcome this limitation, statistical values can be used to extrapolate the transmission power of the user terminal from the measured E-field. For instance [GAT] proposes a statistical mapping between downlink and uplink transmission for different technologies.

To conclude, this approach can be a good solution for monitoring the population exposure in a continuous manner without requiring too much precise information about the deployment.

6.2.3 Results

This section presents the main results obtained from the sensor network tool. As discussed in the previous section, the *macro* tool consisting on the low-complexity dosimeters can be used to provide statistical data on the E-field exposure over a given area and also to calibrate network simulations, which, in turn, can be used to

generate exposure heat-maps and calculate the EI. A statistical evaluation carried out from the values obtained during the last months is presented in section 6.2.3.1.

Besides, the values gathered can be directly used to estimate the downlink component of the EI based on typical ICT data. This is presented in section 6.2.3.2.

6.2.3.1 Statistical evaluation of the E-field

Firstly, the temporal variation of the E-field measurements has been analysed to study the large variation of the E-field over the area. Figure 22 shows the temporal variation of the average value of the measurements during a four-month period and for the different bands. It is worth pointing out that the raw measurements have been scaled by using the extrapolation factor from mono-axial to isotropic and by applying the correction factor to consider the impact of the deployment. In both cases, the factors applied are band-specific.

As can be seen in Figure 22, the E-field values remain quite stable along the measurement period. Nevertheless, there is a noticeable decrease on the 900 MHz band in August, which might coincide with the most common holiday period in Spain. As that band entails only GSM technology (mainly used for voice service), we can conclude that the number of voice calls is reduced during the summer break.

On the other hand, while the band of 1800 MHz is also used for the GSM technology, operators are using “re-farming”, and LTE is partially deployed within such band. This might explain some of the differences with the 900 MHz band.

Concerning the 2100 MHz band, which is used for 3G technology, does not experiment a remarkable variation along the time; this is mostly due to the intrinsic characteristics of the CDMA access methodology used by 3G.

Finally, it is observed a slightly increase on the E-field on the 2400MHz band. It can be due to the deployment of WiFi hot-spots that some operators are carrying out in the city downtown. Anyway, the values obtained in the band are much lower than those due to cellular technologies.

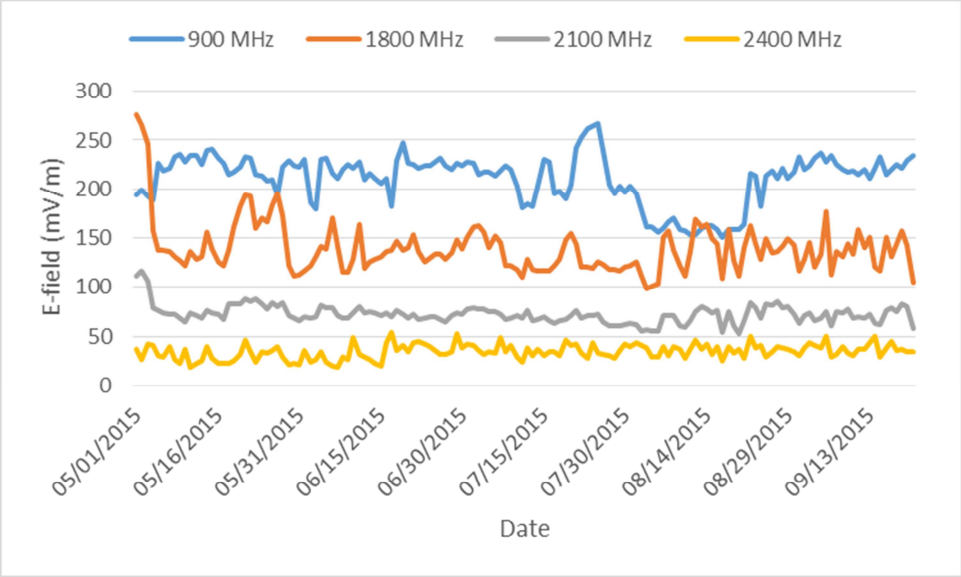

Figure 22: Temporal variation of E-field for the different frequency bands.

It is worth highlighting that this type of macro-analysis cannot be carried out with other traditional tools.

After studying the temporal variation of the E-field, the statistical variation of the E-field during different periods of the day was also analysed.

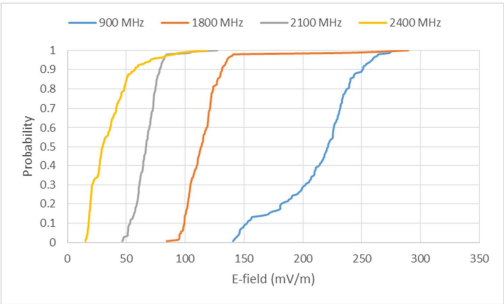

a. SWT1: from 9:00 to 13:00

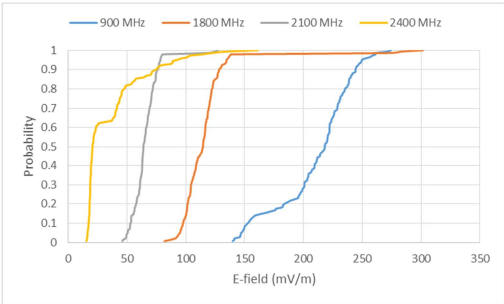

b. RP1: from 14:30 to 16:00

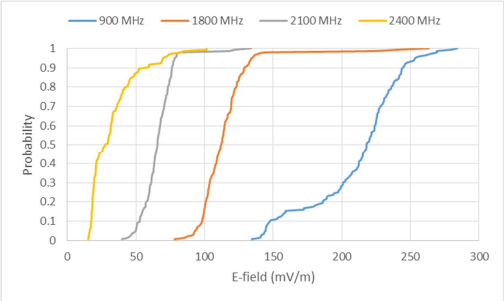

c. SWT2: from 16:00 to 19:00

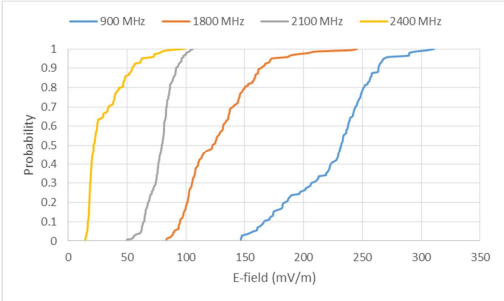

d. RP2: from 19:00 to 22:00

Figure 23: CDF of the E-field for different frequency bands and during different periods of time. SWT holds for "Standard Working Time" and RP for "Rest Period".

In this sense, Figure 23 shows the corresponding CDFs for the E-field obtained during aforementioned 4 month period. The CDF graphs are shown for the different frequency bands and the values have been averaged during periods of the day that correspond to both the working hours and those with less expected activity. As can

be observed, the variation corresponding to the period of the day is much lower than the one due to the different frequency bands.

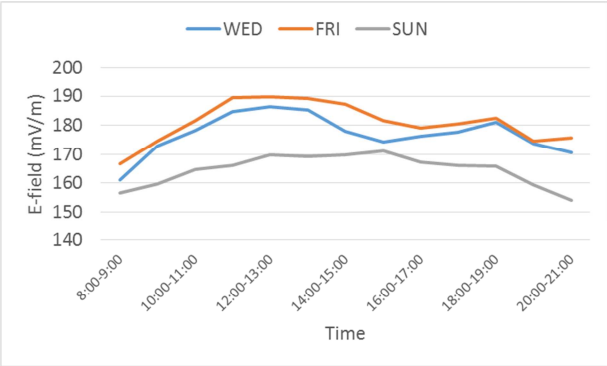

a. **Band of 900 MHz**

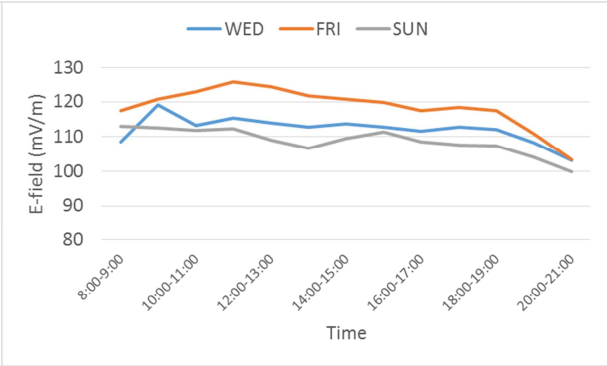

b. **Band of 1800 MHz**

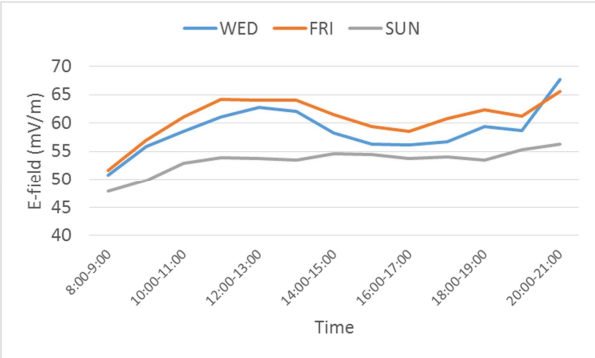

c. **Band of 2100 MHz**

Figure 24 E-field temporal evolution in different days of the week: WED holds for Wednesday, FRI for Friday and SUN for Sunday

Finally, the variation corresponding to the different days of the week has been investigated. In this case, only the cellular technologies have been illustrated, since the results corresponding to WiFi (2400MHz band) are rather low and unpredictable. Figure 24 illustrates the temporal evolution of the electric field during different of the days. As can be observed, there is not a remarkable temporal variation during the day, but there exist a different tendency depending on the band. While the E-field in the 2100MHz band tends to increase at the end of the temporal frame, the other cellular bands present the opposite trend. There are also some differences regarding the day of the week. It is observed a difference between a day in the middle of the week (Wednesday), close to the weekend (Friday) and Sunday. For all the bands, Sunday presents the lower values all the time. On the other hand, the values on Friday are almost always above the other days; it might be due to different job timetables applied on Friday.

6.2.3.2 EI computation

This section presents the EI calculation using the data provided by the sensor network. The results have been obtained following the procedure described in Figure 21.

Regarding the presence of different technologies in a particular band (for instance, 1800 MHz band), based on the on-field measurements presented in A2.8, we consider the E-field due to GSM to be 4.5 times greater than the one corresponding to LTE. Hence, weights of 0.18 and 0.81 have been used for GSM and LTE, respectively.

First, Figure 25 shows the temporal evolution of the downlink component of the EI. It shows that the main contribution comes from GSM at 900 MHz, and illustrates the tendency of the total downlink exposure in time. It can be indeed observed that the impact of the E-field reduction at 900 MHz on the total downlink exposure is predominant.

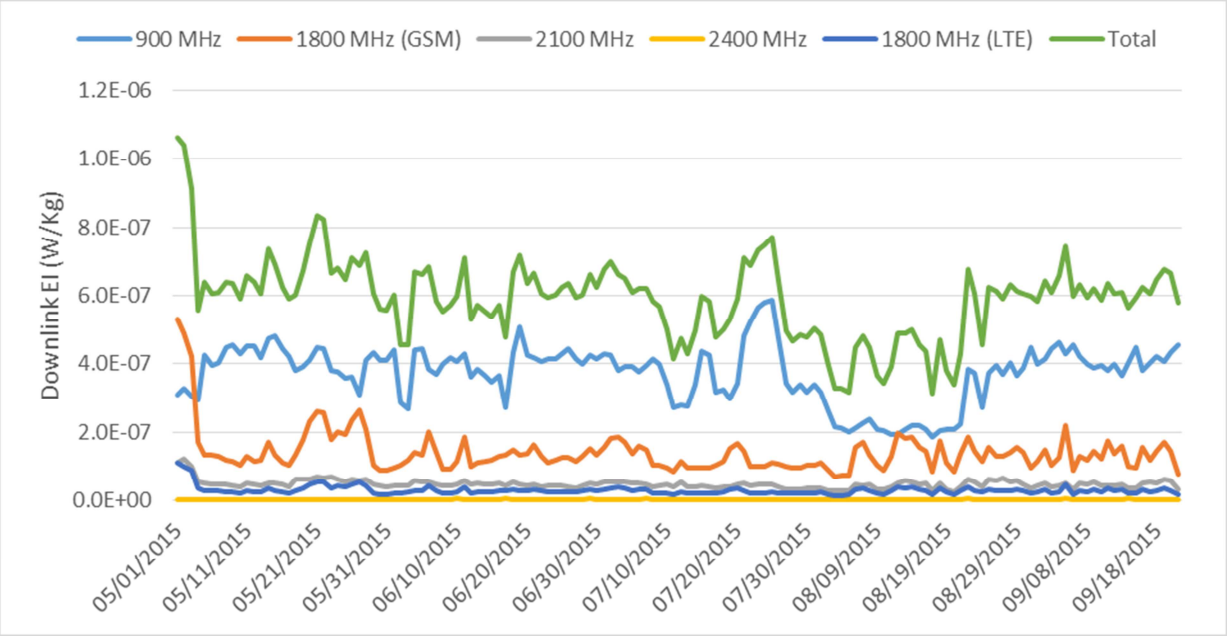

Figure 25: Temporal evolution of the downlink component of the EI in Santander.

In Table 20, the average values of the EI downlink component are shown for each technology. Expected indoor values, which have been calculated assuming a typical attenuation of 15dB, are also shown. The values due to WiFi technology (2.4GHz) are not presented as the indoor extrapolation from outdoor measurements would not be representative of the real exposure, since the most important exposure sources for this band are indoor.

Table 31: Average values of the downlink component of the EI for each technology.

DL EI (W/Kg)	Outdoor	Indoor	Total
900 MHz	2.75E-07	2.18E-08	2.97E-07
1800 MHz (GSM)	2.78E-08	7.85E-09	3.57E-08
1800 MHz (LTE)	5.05E-09	1.50E-09	6.55E-09
2100 MHz	8.29E-09	2.40E-09	1.07E-08

Since the results obtained from the sensor network can be used to feed other tools (such as simulators) or for data analysis, a web page has been developed to allow

open and easy access of the E-field values. Figure 26 shows some illustrative snapshots of the web page. A user might visualize the current deployment of the dosimeters, as well as the locations of base stations of different technologies in the area, see Figure 26a. Afterwards, the measurements can be downloaded after selection of a specific area (the final deployment will be present in different areas), the duration of the measurements (one week or month) and the period of the day. Furthermore, it also includes the possibility of selecting individual dosimeters, to download the E-field measured by such device; this might be of outer relevance for indoor deployed dosimeters.

a. **Network information**

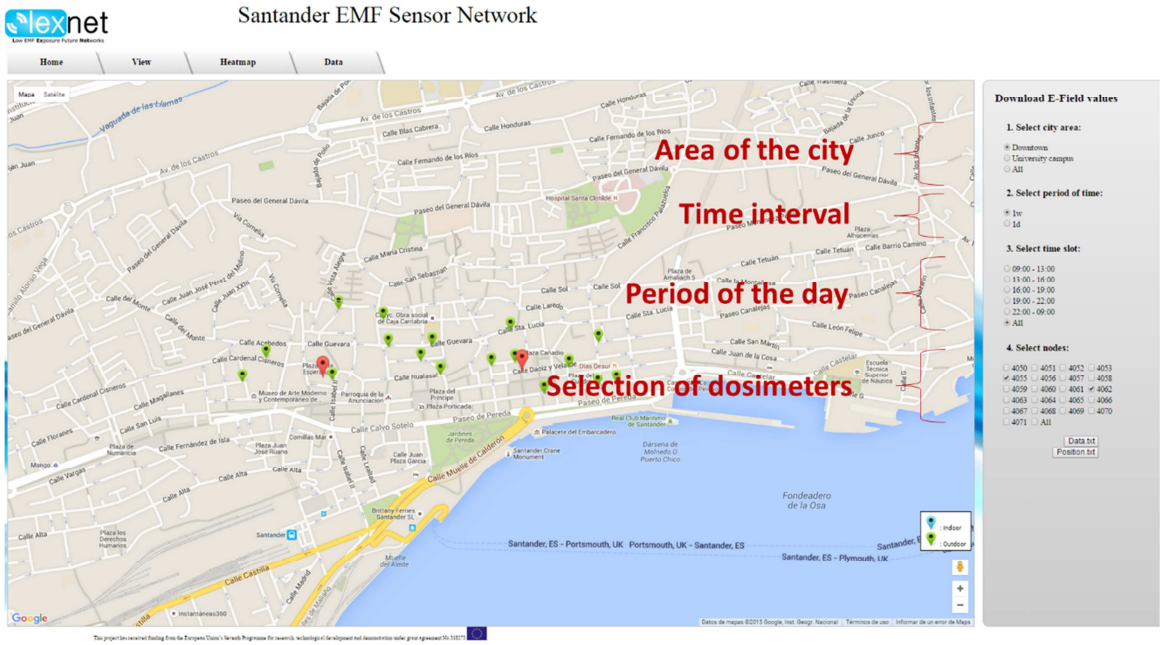

b. **Interface to access the gathered data**

Figure 26: Web interface to provide network information and to ease the access to the E-field measurements.

6.3 Cellular network measurements

The EI assessment based on cellular network measurements is targeted for future EMF exposure monitoring. The aim is to use as much data available in the live network as possible, together with external data or measurements when necessary. The aim is also to identify which data could be collected in future networks in order to facilitate the near-real-time EI assessment.
The methodology is described and illustrated in this section, based on the scenario given in section 3.4. It is further exploited in Part-B, section 3.2, for evaluating the impact of micro-cells on EMF exposure.

6.3.1 Sources of data

Currently available data in most networks are:

- UL/DL power measurements contained in triggered network reports, on either per-cell or per-user basis; per-cell data is based on a sample of users,
- Cell statistics (data volume, throughputs…),
- Data on applications used from probes on network interfaces,
- User profiles for registered users, with usage data in minutes of talk, average throughputs, data volume, UE type.

The sources of data for EI assessment based on measurements in a live network can be divided as follows:

- Network resources:
  - Network Management Systems,
  - Various databases and platforms (call data records, customer analytics systems, etc.),
  - Systems for additional analysis of network data (probes on network interfaces, optimization tools with geolocation etc.),
  - Drive-test measurements (per-user basis),
- Non-network, but available resources: field measurements, statistical data on population,
- External resources: SAR measurements.

The available sources of data in Telekom Srbija (TKS) network, where the implementation of the EI assessment methodology has been investigated, are summarized in Table 32.

Table 32: Sources of data for live-network EI calculation.

Source	Data	Purpose
Cell statistics	♦ network KPIs: traffic load, voice and data usage duration, traffic volume, throughput	♦ assessing the traffic load per type of cells, high/low traffic hours, classes of services used (voice, data, interactive) etc. ♦ extracting average voice and data call durations for the period of interest, average data volumes and throughputs
Network reports	♦ measurements of UE Tx/Rx power per user, per cell	♦ statistical data on power profile, for an area ♦ time-averaging in terms of EI requires scaling the recorded samples based on duty factor for technology and services used [D5.1]
Drive-test measurements	♦ per-user measurements of UE Tx/Rx powers	♦ per-user data, thus intended for single-user exposure assessment based on UE type, applications used, time of day (traffic load), type of cell etc.
Call data records	♦ users (MSISDNs, IMEIs) that made an active call in a period in a cell	♦ data on users who made an active call, as an input for other systems ♦ no data on connected users in a cell who did not make a call
Customer analytics system (SAS)	♦ per MSISDNs, usage data (avg. call duration, avg. No. of calls, avg. session duration, avg. data volume, profile data	♦ user profiles and typical behaviour ♦ with CDR data on active calls in a cell: typical usage profile for a specific area
Automatic Device Configuration (ADC) Platform	♦ mapping IMEI to UE type and model	♦ UE type segmentation: phone, laptop ♦ presumption on posture, position of the UE relative to the body based on the type of UE and service (voice/data)
Probes on network interfaces	♦ exchanged messages in the core network	♦ data on the usage of specific applications ♦ Location Update messages for determining distribution of users in observed cells for the observed period
Field measurements	♦ duty factor measurements (per applications, technologies, radio conditions)	♦ time averaging of UL power samples recorded in network reports/drive-test measurements
	♦ overall DL field intensity per operator bands	♦ assessment of the DL exposure
Census	♦ population segmentation	♦ distribution of population per age
ICT surveys	♦ usage of mobile telephony	♦ mobile telephony overall penetration
Regulator reports	♦ operator's market share per active users	♦ the share of users and non-users per operator
Laboratories	♦ normalized SAR values for UL and DL	

Currently, there is no optimization tool with geolocation available in TKS network. Such software tools could be a valuable source of data. They collect Layer 3 messages from various Network management systems, extract position using

patented algorithms, analyze call and network data, giving meaningful information for a customer-based optimization.

6.3.2 EI implementation challenges

EI implementation in a live network involves dealing with many uncertainties and uncorrelated data, but with real measurement results.
The main challenge in the EI calculation in a live network is mapping user plane data with radio measurements. Cell measurements give a power profile of a cell [3GPP], based on a statistical sample of users, and there is no connection between power samples and applications used, that directly affects the time-averaging of power. Power samples are taken when the transmitter is actually transmitting (both in network reports and using the drive test tool), and the silent periods in between need to be determined statistically, with field measurements, for each type of application, technology, network load (high/low), radio conditions (strong/weak signal). The activity on the radio interface, or the duty factor, takes into account both the application activity brought down to the radio interface (includes lower-layer processing, i.e. headers, coding...) and the specific properties of the radio interface (in GSM, 1 TS used for voice and 1-3 for most UE types for data; UMTS Radio Resource Control (RRC) state transition for data). The activity (duty) factor determined with field measurement equipment serves for scaling the network-measured samples, which corresponds to time-averaging.

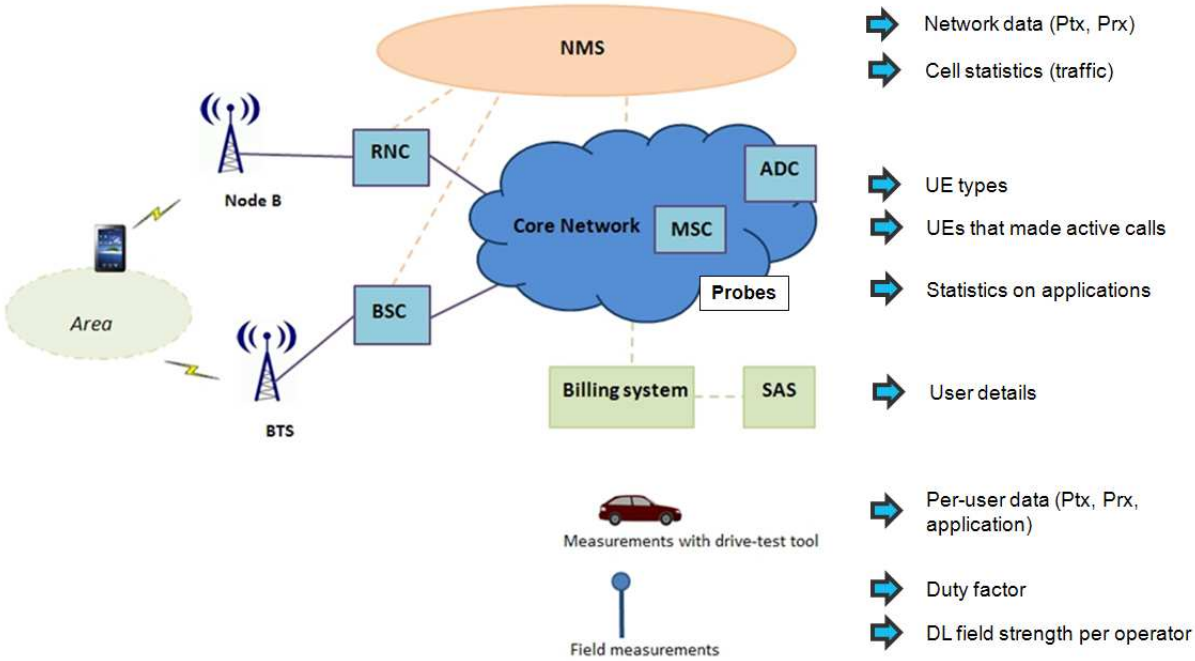

Figure 27: Sources of network and external measurements and data.

Key challenges for EI evaluation using available network monitoring tools and other network data, shown in Figure 27, are:

- **The notion of an area**
  The "area" unit for a network is a cell. Cell borderlines change with ever-changing radio and load conditions. Co-located cells of different technologies have different coverage. Thus, it is hard to define a rigid geographical area and evaluate the EI.

The other way would be on per-user basis, for all users in a geographical area, but this would require geolocation tools and advanced data processing.

- **Duty factor – activity on the radio interface**
  Currently, external measurements performed using field measurement equipment are needed, as the power samples in network reports are taken when the transmitter is actually transmitting and no data is available on non-emitting periods in between. Duty factor is different for different applications, technologies, radio and load conditions. It can be measured externally for a set of typical conditions and then applied to network-measured power levels in order to average them over time.

- **Linking radio and core data**
  In order to perform the averaging of recorded UL power levels over time, i.e. to apply the right duty factor, recorded power levels should be mapped with the application used. Without an agent on the phone, or advanced software tools that would link radio data with data from probes on network interfaces in the core, these can be combined only on pure mean-value basis, over the whole area. Without this mapping, there is no notion whether higher UE Tx power samples recorded are due to demanding data upload close to the base station or because the user was far from the base station. Further, per-cell measurements are not taken for all users in a cell, only for a sample. Mapping data on UE Tx and Rx power levels would be possible only on per-user basis, and without advanced tools we cannot get this data (on per-user basis) for all users in a cell. As well, per-cell measurements are not possible for GSM data service.

- **Extracting data on customers**
  Customer data is available for registered customers only. Further, the distribution of child and adult users, in order to apply the right SAR value, can only be assumed based on external sources (census), as the registered user can only be an adult. Data on posture may be assumed according to the type of the mobile device (laptop, tablet, phone).

- **"Background" exposure** – everything else but own UL and DL exposure, i.e. exposure from other operators' base stations and exposure from all surrounding users.
  Exposure from other operators can only be assessed statistically based on field measurements in an area, as well as exposure from other customers.

The introduction of software tools that combine radio and core data (geolocation, probes in the core) would eliminate part of uncertainties in EI evaluation. Further, introducing agents on phones, that would send correlated data on radio parameters and applications used, or even some customer data, would also decrease the uncertainties.

Another practical challenge for implementing the EI is related to DL exposure for the population in an area, i.e. combining data from several operators, which is described in detail in section 6.3.3.2. An operator could monitor its network and assess the EI contribution that is induced from their own equipment and customers. If all the operators would monitor the network for exposure evaluation and perform actions to

decrease it (topology changes, network management techniques) [POP1], the exposure of the population originating from cellular networks in an area could be minimized.

However, this has not been yet experimented. Simulations and live network measurements could be used together to calibrate models, and provide a powerful tool for future EMF-aware network planning.

6.3.3 EI assessment method

To illustrate the EI assessment methodology, it is calculated over an urban area with GSM and UMTS micro and overlaid macro cells. Based on the base station density, we can consider the borders of coverage for GSM and UMTS to be alike.

The following network measurements are used:

- UE Tx and Rx power distribution taken from per-cell network reports, for 2G voice service, for both micro and macro cells;
- UE Tx and Rx power distribution taken from per-cell network reports, for 3G voice and data service, for both micro and macro cells;
- Electric field strength taken with field measurement equipment in a number of locations within the area of interest.

Due to the limitations described in the previous section, the single valuable data extracted from these power profiles is the mean UE transmit power. It should be noted that UE Tx power samples for GSM are taken only for voice service.

Fraction of users per GSM macro/micro and UMTS macro/micro can be obtained in two ways:

- From customer analytics system, based on customers who made an active connection during a month (Table 33): in this way, all users normally active in the area are taken into account (on average), and data processing cannot be done on a near-real-time basis;
- From signalling i.e. Location Update messages in the core network: these data provide information on users who were actually connected to the observed cells in the observed period (some time is needed to process).

Table 33: Fractions of users per technology layers.

Fractions of users per technologies and layers	
UMTS macro	56,39%
UMTS micro	15,86%
GSM macro	21,54%
GSM micro	6,22%

The process of EI calculation is depicted in Figure 28. The EI is calculated as the index of exposure originated from Telekom Srbija equipment and users connected to this network. In order to estimate the EI for the population, the UL component needs to be scaled with respect to the share of Telekom Srbija users in the population.

The UL component is dependent on the usage of voice and data service, per RAT and layer (micro/macro), while the DL component is dependent on postures. In the considered scenario the exposure from close users is neglected.

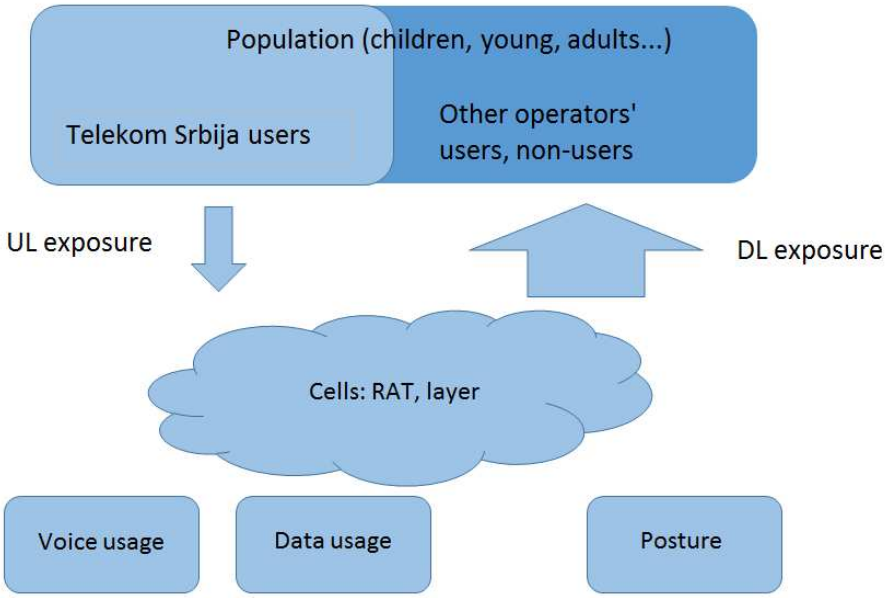

Figure 28: Components of the EI: UL component of users depending on usage of voice and data service, and the DL component for the population depending on posture.

For the uplink component of the EI, in order to get the $\bar{P}_{TX}$ value in the EI equation [D2.8], the duty factor needs to be applied. As the samples are taken when the transmitter is actually transmitting, duty factor needs to be applied to account for „silent“ periods in between, when using voice or different data applications.

Duty factor is measured for different applications and RATs, for the UL, in good, medium and bad radio conditions, and shown in [D5.2].

Based on UE Rx power samples, the statistical distribution of users in good, medium and bad radio conditions may be assessed, for each cell (technology, layer). This is a basis for statistical averaging of the duty factor per technology, and good/bad/medium radio conditions. In case of UMTS, recorded samples refer to both voice and data usage, so the statistical averaging of the duty factor must aditionally take into account:

- Voice and data service usage percentages by duration: this is obtained from cell statistics (KPIs), may be obtained on hourly basis or averaged over a certain period;
- For data service, distribution of used applications: this is evaluated, in percentage, by analyzing data from probes in the core network. Applications are separated into categories for which the duty factor is measured (Table 34).

Table 34: Distribution of traffic types per time of usage

Traffic type	%time
Browsing	59,39%
Audio streaming	1,65%
Video streaming	11,42%
TV	0,79%
Skype VoIP	4,55%
Skype video	0,10%
File upload	15,71%
File download	6,39%

To summarize, duty factor for GSM voice is statistically combined considering radio conditions, while the duty factor for UMTS voice and data is statistically combined considering, besides radio conditions, the type of service and used application. The process of averaging the duty factor and applying it to the average UE transmit power that was recorded for the cell is graphically represented in Figure 29.

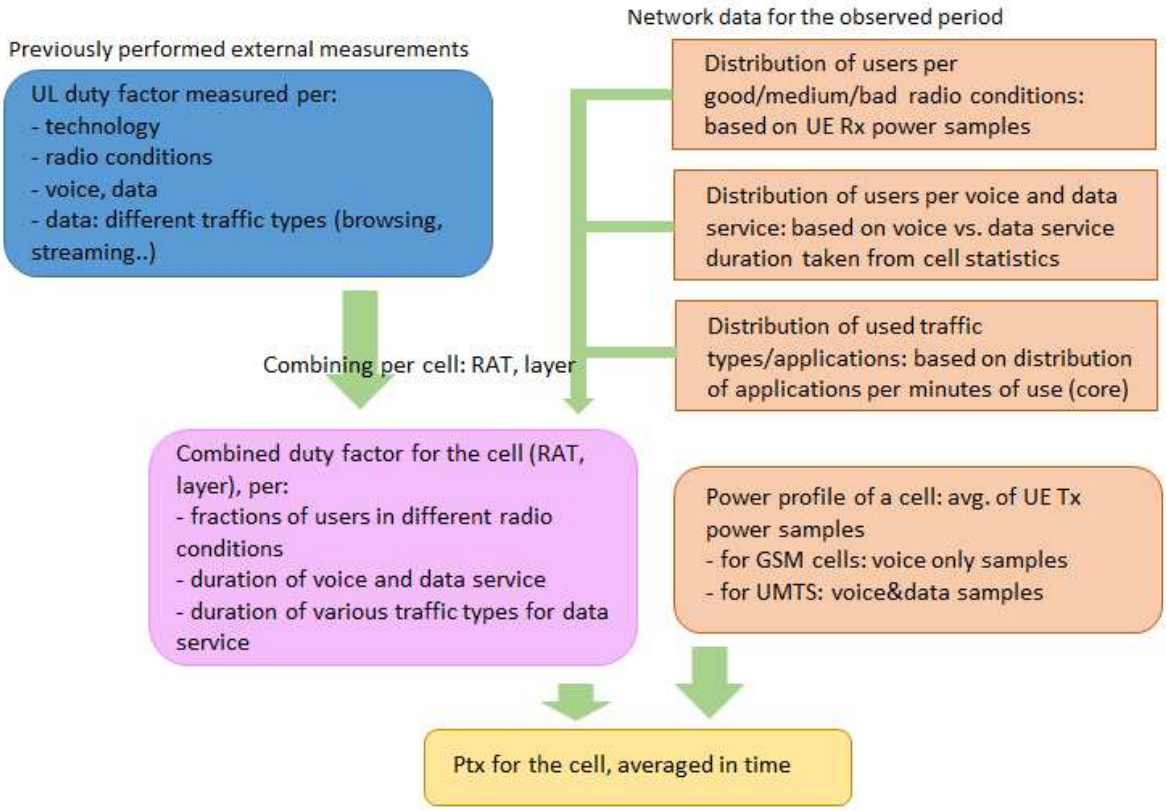

Figure 29: Duty factor averaging per cell and obtaining the P_{tx} factor for the cell.

By applying the right duty factor, the resulting average power value is for the actual usage of the service, while duration of usage will be accounted for in the term d^{UL} of the EI formula.

The other important factor in the EI equation for the UL is the average dose, normalized to 1 W, d^{UL}; it corresponds to the normalized SAR value, multiplied by time of usage, per EI user categories. In order to obtain the average value, statistical combining for different population categories, postures, environments, UE types and times of usage needs to be performed. Data used for this segmentation are as follows:

- Population categories share: taken from the census data [STA], for urban environment, by averaging data for Belgrade municipalities (Table 35); furthermore, based on available SAR values in [D2.8], only two categories are used (children, adults);
- Indoor vs. outdoor per time of usage: taken as an assumption (Table 36); data based on statistical surveys in different countries may be found in [D2.8];
- Phone and laptop users: taken from ADC system (Table 37);
- Posture: there is no statistical data on posture, it is therefore assumed that all users indoors are sitting, while all outdoor users are standing (during usage); furthermore, we also take assumptions about the position of the laptop (lap, desk);

Based on the corresponding percentages, a user segmentation matrix has been created (Table 38). It is assumed that the distribution of users per age and environment categories follows that of the total population.

Table 35: Population categories.

Population (census)	%of population
Children (under 15)	13,50%
Young (15-29)	18,40%
Adults (30-59)	43,60%
Seniors (60 and over)	24,50%

Population (EI calculation)	%of population
Children (under 15)	13,50%
Adults (15 and over)	86,50%

Table 36: Indoor and outdoor users.

Indoor vs. Outdoor	Indoor	Outdoor
Children	80,00%	20%
Young, adults, seniors	70,00%	30%

Table 37: Usage of phone and laptop.

Usage: phone vs. laptop	
Phone	98,56%
Laptop	1,44%

Table 38: User segmentation matrix.

User segmentation matrix									
User	User%	Usage	Usage%	Environment	Env.%	Posture	Position Laptop	Pos.%	Share
Child	13,50%	Phone	98,56%	Indoor	79,71%	Sitting			10,61%
	13,50%		100,00%	Outdoor	20,00%	Standing			2,70%
	13,50%	Laptop	1,44%	Indoor	100,00 %	Sitting	Lap	10%	0,02%
	13,50%					Sitting	Desk	90%	0,17%
Adult	86,50%	Phone	98,56%	Indoor	69,56%	Sitting			59,31%
	86,50%		100,00%	Outdoor	30,00%	Standing			25,95%
	86,50%	Laptop	1,44%	Indoor	100,00 %	Sitting	Lap	30%	0,37%
	86,50%					Sitting	Desk	70%	0,87%

In order to calculate the percentage of users per voice and data service, the data from SAS system is taken for voice-only, data-only and voice and data users (Table 39).

Table 39: Users of voice and data service.

Service used, based on SAS data:	Usage	Share
Data-only users	Laptop	1,44%
Voice-only users	Phone	71,26%
Voice and data users	Phone	27,30%

Assumption:	Children	Adults
Data-only users	1,44%	1,44%
Voice-only users	30,00%	77,70%
Voice and data users	68,56%	20,86%

Combining these data with previous user segmentation, the matrix of usage of voice and data service is made (Table 40), to be further combined with available SAR values presented in [D2.8]. It should be noted that in UMTS, the percentage of users of voice service is 98.56%, while only 28.74% of users are using data services. In GSM, since power measurements are just made for voice usage, the corresponding percentage is 100%.

Table 40: Matrix of usage for combining with SAR values.

Service	Population	Posture	Usage	Position	Share UMTS	Share GSM
Voice	Child	Sitting	Phone		10,61%	10,76%
	Child	Standing	Phone		2,70%	2,74%
	Adult	Sitting	Phone		59,31%	60,17%
	Adult	Standing	Phone		25,95%	26,33%
Data	Child	Sitting	Phone		7,38%	
	Child	Standing	Phone		1,88%	
	Child	Sitting	Laptop	Lap	0,02%	
	Child	Sitting	Laptop	Desk	0,17%	
	Adult	Sitting	Phone		12,55%	
	Adult	Standing	Phone		5,49%	
	Adult	Sitting	Laptop	Lap	0,37%	
	Adult	Sitting	Laptop	Desk	0,87%	

The shares presented in Table 40 are combined respectively with SAR values for the population, posture, usage and position in order to get average normalized (per 1 W of power) SAR values for voice and data usage.

The next aspect in the EI calculation, part of the d^{UL} term, is the usage time duration. It is established based on user profiles, considering previous analysis of user data from SAS and cell statistics, as presented in Table 13 and Table 16 in [D2.8]. Data for urban environment is taken, and only for day time, since the measurements were made during day time (i.e. only part of EI pertaining to high load hours is calculated). The distribution of users per user profile (heavy/moderate/light) is taken from Table 23 of [D2.8], also based on previous analysis of user and cell data for Telekom Srbija 2G and 3G networks; for the EI calculation, values are proportionally reduced to categories “children” and “adult” (Table 41).

Table 41: Repartition of user profiles used in EI calculation.

Repartition used in EI calculation		Heavy	Moderate	Light
Children	Voice	25,00%	50,00%	25,00%
	Data	60,00%	20,00%	20,00%
Adults	Voice	47,00%	25,00%	28,00%
	Data	47,05%	19,28%	33,67%

Based on user profiles and their distribution, average voice call durations are calculated for GSM and UMTS. Average data call duration (for the UL transmission) is calculated based on user profiles and cell statistics data. User profiles for the UL transmission are defined per kB of transferred data, and, in order to transform this to average data usage time, cell statistics on data volume in the UL and UL throughputs is used. These average durations are related to 1h, and could be extracted on a per-hour basis, using cell statistics, to the duration of the observed period. Here, for brevity, average values for the observed period are used (“high-load” part of the day is taken, according to cell statistics, 9-21 h).

The UL component of the EI, per cell, is obtained by simply combining average normalized SAR values for voice and data services with average voice and data call durations, and multiplying afterwards with the previously calculated P_{tx}. This value is only related to users of the observed network.

To get the UL component of the EI originated from Telekom Srbija network (excluding exposure from close users), values of $d^{UL} * \bar{P}_{TX}$ for different RATs and layers (micro, macro) are statistically combined, based on the percentage of users using each technology and layer (Table 33), and then divided by the observed period duration (12h - 43,200 s).

For the EI downlink component, the target value is the mean power density over the whole population. The duty factor for the DL transmission is 100%. Two types of measurements may be used, each of them having its advantages and drawbacks:

- Measured samples of electric field strength in a number of particular points within the area;
- UE Rx samples from network reports.

First, electric field strength measurements are performed with precise equipment (isotropic antenna), so as to consider the whole E-vector. These measurements are made per operators' bands, so the impact of all surrounding base stations, other sectors of the same base station and different carriers in the band is taken into account. In case of the indoor micro (DAS system) with overlaid macro, scenario described in [D5.2], the DL measurements were taken for the micro area, inside the building, on different floors, so they can be considered valid for averaging over the population. For the scenarios presented in section 3.4, the measurements were taken outdoors, and this is the drawback for EI assessment. For the averaging purposes they may be scaled down according to the percentage of population that is indoor and with indoor attenuation factors from the literature. Since more than 70% of population is assumed to be indoors, these assumptions might lead to a rather high uncertainty.

Second, UE Rx samples take into account users in bad, medium and good radio conditions; they are based on a sample of users (measurement methodologies differ per RAT, refer to [POP2][D5.1] for more details). In UMTS, the whole carrier is measured, meaning that the measurement of target cells of different carriers contain power levels received from surrounding base stations/sectors as well. The drawback is that the Rx power measured by the UE cannot be directly linked to power density, since the link depends on the type of antenna and its relative position to the incident wave vector. In other words, the Rx samples do not capture the whole field.

For the DL calculation of scenarios described in section 3.4, the measured average field intensity is scaled, considering percentages of population indoor and outdoor, according to the following formula, where AttFactor is equal to 0.126 (18 dB). The distribution of population indoor and outdoor, according to Table 35 and Table 36, is 71.35% indoor and 28.65% outdoor.

$$\bar{E} = \sqrt{\bar{E}_{outdoor}^2 * Outdoor + (\bar{E}_{outdoor} * AttFactor)^2 * Indoor}$$

For the DL calculation, it is assumed that the distribution of postures per population categories follows the one used for the UL calculation. Postures linked to voice and data usage are statistically combined based on voice vs. data usage time on cell level, in percentages, taken from cell statistics. Both UL and DL data usage are taken into account, since "data duration" is in this case related to the duration of a specific posture and not to the service itself. Normalized SAR values for the DL, presented in [D2.8], are then combined, following a procedure similar to the one discussed for the UL component, based on population categories, environments, usages, postures and voice/data usage; we can then obtain the average normalized SAR value for the downlink. This value is multiplied by the average power density, yielding the DL component of the EI. This DL is related both to users and to the overall population, since the distribution of postures for users and non-users is assumed alike.

The combination of UL and DL components of the per-cell EI needs to be further discussed. UL component is only calculated for users of the network, according to their usage times, while the DL component is established for both users and the whole population, assuming the same distribution of postures.

However, we should estimate the EI for the whole population, including non-users of Telekom Srbija network. In this sense, the UL component needs to be scaled down, by using the ratio of Telekom Srbija users in the overall population. This ratio is obtained from the percentage of usage of mobile phones in the population (91.4% based on ICT usage data survey [STA]) and Telekom Srbija market share by the number of active users (44.56% [RAT]), leading to a value of 40.73%. Hence, by summing the calculated DL component with the 40.73% of the calculated UL component, the EI for the whole population in the area related to exposure from Telekom Srbija network can be obtained.

6.3.3.1 Combining EI components per cells: macro and micro area

For the assessment of EI pertaining to one operator's equipment and connected users, EI components obtained for different cells need to be combined.

The scenarios related to topology changes with the aim of decreasing exposure of the population, presented in section 3.4, involve two network layers: macro and micro. The coverage area of micro base stations is usually like an island with overlaid macro coverage. Thus, the variation of the EI may be observed over the micro and over the macro area, i.e. within the coverage area of the micro base station and within the whole coverage area of the observed macro cells.

Since each layer consists of several cells, pertaining to different technologies and layers, and even the same layer in the macro area might consist of multiple cells, EI components can be assessed on a per-layer basis (multiple cells of the same technology and layer), to be afterwards combined. In this way, all the inputs concerning cell measurements and statistics are taken as an average for all cells of the corresponding layer. The way we combine data from different layers depends on whether we're looking into the micro or the macro area.

If we consider the micro area, we assume that all users are connected to the micro base station. Hence, the UL component of the EI is just related to the micro layer (GSM and UMTS), while the downlink component is related to both macro and micro layers. The UL components are combined, considering the percentages of users per technologies and layers (Table 33) relative to micro layer only, while the downlink component corresponds to the average field intensity measured within the micro area.

If we consider the macro area, we still assume that all users within the coverage are of the micro base station are connected to it, while those outside are connected to the macro layer. Hence, the UL components of the micro and macro cells need to be combined considering the percentage of users per each technology and layer (Table 33). The DL component is related to the average field intensity over the whole macro area.

It is expected that the addition of the micro layer would reduce exposure for the population in the micro area, which will be strongly reflected in the reduction of EI over the micro area, and less reflected in the EI over the macro area. The

corresponding reductions will depend on the network topology and characteristics of the area.

6.3.3.2 Combining EI from multiple operators

The final goal would be to have an EI value per operator in the area, that could be reported to the regulator and combined into the overall EI.

Each operator is aware of its own UL component (own users) that can be scaled over the whole population as well as of the DL component, which is calculated with some assumptions and can be said to be rather accurate for its own users. We can say that non-users per each operator are those who belong to other operators together with the people who do not use mobile telephony. While the UL component can be scaled by considering the operator's market share, the procedure entailing the DL is more complicated.

DL component directly (by applied normalized SAR values) depends on postural behaviour of both users and non-users. Hence, all the operators should exchange network data, or agree on some common assumptions in order to appropriately calculate the corresponding DL components. The DL contribution also depends on overall non-users' habits, but this might be neglected, since the percentage people not using cellular communications is very small. The DL component needs to also consider times when users are not using any service.

Neglecting the uncertainties of the DL component, each operator could derive an EI value scaled over the population. These values could be combined together, leading to the overall EI for an area, consisting of UL components scaled by market share and penetration and DL components per operator bands..

6.3.4 Results

This section gives an illustration for the EI assessment method, based on measurements presented in [D5.2]. A micro area is studied, inside the building Lola, covered with a DAS system, distributed in different floors, and with overlaid macro coverage.

The characteristics of the macro and the micro layers are presented in Table 42.

Table 42: Characteristics of the macro and micro layer.

Site type	Technologies	UMTS carriers / GSM TRXs	Transmit power
Macro site	GSM	4	42 dBm per TRX
	UMTS	2	43 dBm per carrier
Micro site	GSM	2	32 dBm per TRX
	UMTS	2	30 dBm per carrier

The input data are summarized in Table 43. Downlink field measurements were performed on different floors of the building with antennas installed, so the samples are scaled for the floors without antennas.

Table 43: Input data for Lola building micro and macro layer.

Data	UMTS macro layer			UMTS micro layer		
Avg. UE Tx power [dBm]	-9,4			-19,25		
Fractions of UE Rx power samples for good, medium and bad radio conditions [%]	Good	Medium	Bad	Good	Medium	Bad
	42,59%	43,40%	14,01%	78,55%	18,49%	2,96%
Average voice usage in time (per 1h), all users, high load hours [Erl]	25,48			0,99		
Average data usage UL in time (per 1h), all users, high load hours [Erl]	64,88			1,07		
Average data (UL and DL) usage in time (per 1h), all users, high load hours [Erl]	172,87			4,26		
Average data volume UL (per 1h), all users, high load hours [Gbits]	3,19			0,06		
Recorded average field intensity [V/m] in the micro area	-			0,2882		
Data	**GSM macro layer**			**GSM micro layer**		
Avg. UE Tx power for voice service, high load hour [dBm]	31,19			19,83		
Fractions of UE Rx power samples for good, medium and bad radio conditions [%]	Good	Medium	Bad	Good	Medium	Bad
	24,41%	45,57%	30,02%	69,08%	26,37%	4,55%
Average voice usage in time (per 1h), all users, high load hours [Erl]	21,45			2,7		
Recorded average field intensity [V/m] in the micro area	-			0,8954		

Additional information used for the calculation is the one described in Section 6.3.3. The percentage of users per technology and layer given in Table 33 are established from SAS system for the particular cells of this scenario. The micro area is within a business building, so we can assume there are no children, but to be more generic, the EI values are calculated according to the full user segmentation. Excluding children, the obtained values would be smaller, since SAR values for children are higher than for adults. The results are presented in Table 44.

Table 44: EI for the Lola building with micro layer and overlaid macro layer.

EI components	Value [W/kg]
UL component, GSM, users	4,54217E-06
UL component, UMTS, users	1,55237E-09
UL component, for the population	1,85056E-06
DL component for micro area, GSM	3,53951E-06
DL component for micro area, UMTS	1,94449E-08
DL component, for the population	3,55895E-06
Total EI, for the population	**5,40951E-06**

The EI over the whole population is studied with respect to technology and layer. The contributions are shown in Table 45.

Table 45: Contributions to the EI per technology and layer.

EI per population, shares	GSM macro	GSM micro	UMTS macro	UMTS micro
UL	0,00%	34,20%	0,00%	0,01%
DL	65,43%		0,36%	

The contribution of GSM is much higher than the contribution of UMTS, as expected. On the other hand, in the micro area the DL component is higher than the UL component, especially for the UMTS. This could have been somewhat expected, since the DAS system deals with lower powers than the macro, but these are still high, and the antennas are placed close to users. For the UMTS, as an interference limited system, UL component is very low, compared to GSM, and any increase in DL exposure is quite visible, due to the small UL value. DL measurements were performed on floors with antennas, and even considering (with appropriate scaling factors) floors without antennas, average values are high as the macro site is not far (DAS system was deployed with a capacity goal, rather than for coverage reasons), UMTS sectors use two or three carriers, and the higher floors show the most relevant influence of the macro cells DL (compared to the ground floor).

The subject building is a business building, and the EI should only consider 8 hours of occupation for most of the population within the micro area. The calculated EI applies a 12-hour averaged cell statistics on measurements performed during peak hours, and could be considered as the worst case scenario.

6.4 Cellular network simulations

The simulation-based EI assessment in cellular networks relies on the methodology and tools described in [D3.3, section 3.3.1]. The EI simulation methodology, which is demonstrated in this section, is also used for evaluation of new topologies and WiFi offloading later in this document.

6.4.1 EI assessment method

This evaluation puts the focus on two crucial components for operational EI implementation: the availability and accuracy of simulation inputs (network parameters, geographical map data); and the calibration of the prediction models.

The simulation scenario is based on Santander downtown, where network performance and exposure have been measured in April 2015.

The geographical map data has been produced by SIRADEL, based on an industrial and high-resolution process, where stereoscopic images taken from a plane that flies above the city are converted into 3D raster data (terrain elevation) and 3D vectors (description of the clutter). The data has been generated in October 2014, specifically for the project. The size of the Santander geographical map data is 2.5x1.4km²; it covers the part of Santander downtown where the measurement campaign has been conducted plus a 500 m margin that allows the simulation to take all relevant

neighbour base-stations into account. The vertical accuracy of the raster data is 1m, while the horizontal resolution is 5m. The vector accuracy in both horizontal and vertical dimensions is better than 1m.

Figure 30: High-resolution 3D geographical map data of Santander downtown.

The Santander scenario must be fed as much as possible with precise information from the real network. Unfortunately, we were not able to get all required data. As summarized in Table 46, some information suffers from uncertainties; some other is missing. The situation is not ideal; but this can be viewed as a realistic use case when EI would be assessed by public authorities.

Table 46: Network information inputs for Santander simulation.

Simulation input	Source	Level of uncertainty
Radio network infrastructure for Movistar, Vodafone and Yoigo	Public data on site locations given per frequency band (900 MHz, 1.8 GHz and 2.1 GHz) and per operator.	**High** No information on base station antennas (height, orientation, power, # active carriers per cell, etc.). Also, such database generally suffers from large errors on the site locations (few tens of meters).
Radio network infrastructure for Orange	Database from the operator.	**Low to Medium** The comparison between measurements and simulations has shown inconsistency in some of the frequency bands.
User traffic / Cell load	Estimation of the per-operator traffic load from the number of national subscribers, and the cell density in Santander.	**High** But can be corrected by the calibration process.

As not available in public databases, the antenna properties of Movistar, Vodafone and Yoigo operator networks are set to default parameters in the simulation:

- Transmit power: 48 dBm.
- Antenna beamwidth: 65° in horizontal plane; 12° in vertical plane.
- Antenna gain: 14 dBi.
- Downtilt: 6°.
- Height: 3 m above rooftop.

The initial cell loads have been estimated from the user traffic numbers at the national level and from the cell density in the Santander downtown. We were not able to derive absolute values, but only relative cell loads, i.e. *CL* for Movistar, 1.05 x *CL* for Vodafone, 0.75 x *CL* for Orange and 0.36 x *CL* for Yoigo. The absolute values have been fixed after calibration with measurements, as described here below.

Two different exposure simulation scenarios have been evaluated:

1. <u>For 2G 900MHz, 2G 1800MHz and 3G 2100MHz:</u>
   Only DL simulations are available.
   The RSSI SCAN measurements allows for a calibration based on cell loads adjustment. As the uncertainties on transmit powers, antenna gains, etc, are strong, the calibrated cell loads are obviously not exactly representative of the average cell loads in the real network, but integrate a global correction for various sources of error.
   As pointed out in Figure 31, the calibration is performed from outdoor measurements, but the final DL exposure maps and DL EI calculation includes both outdoor and indoor environments.

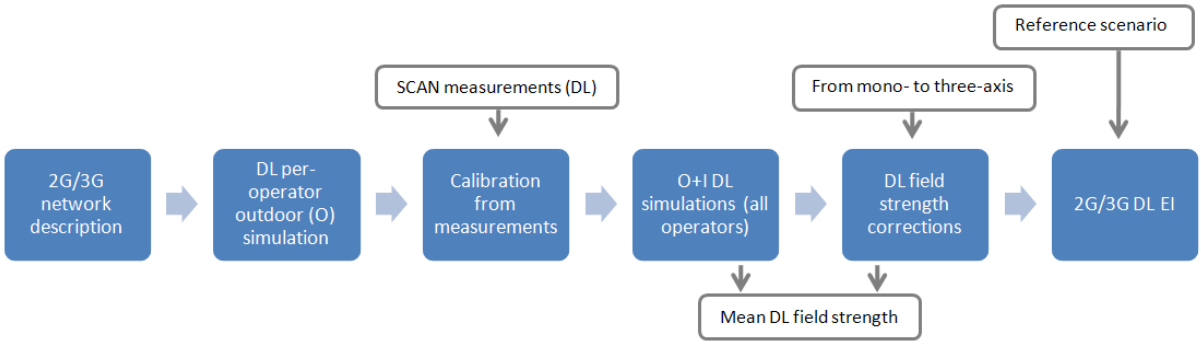

Figure 31: Calibration and simulation methodology for 2G/3G DL EI evaluation.

2. <u>For 4G 1800MHz:</u>
   Both DL and UL simulations are possible.
   The calibration and simulation are performed only for the Orange network, in order to benefit from the more accurate information that is available.
   The RRSI SCAN measurements allows for the calibration of cell loads, while the TRACE mobile data are used as a reference to adjust the predicted UL transmit power and DL/UL throughputs.
   The calibration is performed from outdoor measurements, but the final exposure maps and EI calculation includes both outdoor and indoor environments, as illustrated in Figure 32.

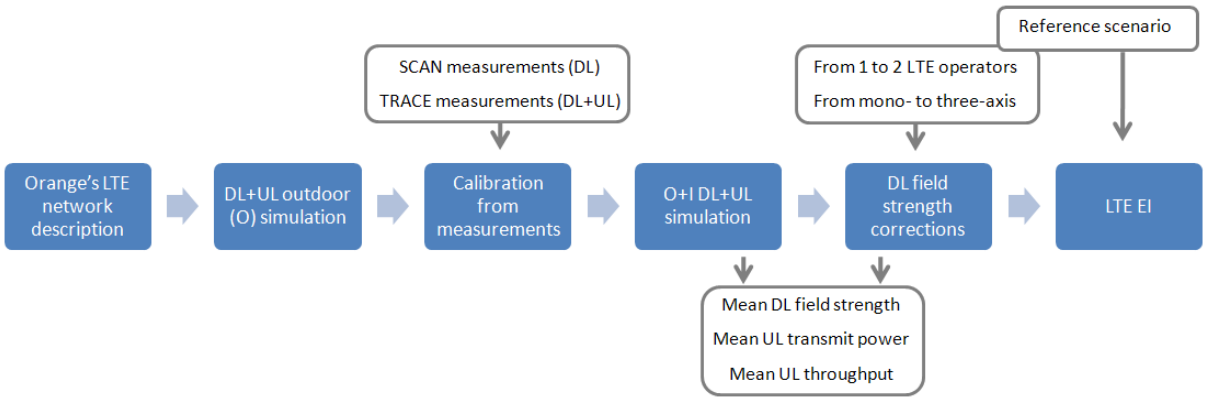

Figure 32: Calibration and simulation methodology for LTE EI evaluation.

In both evaluation scenarios, the EI is computed based on the population life distribution and user traffic defined in the LEXNET reference scenario (section 3.3).
The "mono- to three-axis" operation is required in order to convert the DL field strength that is captured by the mobile user equipment (i.e. with a single-polarization antenna) towards a total field strength estimate. A 2 dB correction factor was found from an experiment based on dosimeter measurements (Appendix A2.2).

In case of the LTE simulation, the conversion of the DL field strength predicted from the single Orange network to a total LTE field strength (with 2 operators) is done based on the measurements; by considering the average ratio between the measured Orange and Vodafone RSSI levels.

6.4.2 Results

As explained in the previous section, the calibration of the simulation tool for 2G and 3G technologies relies on an adjustment of DL traffic loads. This is done for each operator and frequency band, with the objective to reduce the difference between the measured and simulated DL field strengths (reducing the distance between the corresponding CDFs). The result for 3G network is globally good, since the value of calibrated traffic loads are sensible (below 70%), and the measured and simulated CDF match with a RMSE below 3.9 dB (see Figure 32). The comparison for one 3G operator is illustrated using a map in Figure 34.
Some local differences between measurements and simulations have been observed in the Orange's network, which can only be explained by the presence of additional antennas. Nevertheless, the impact on the global statistics is small.

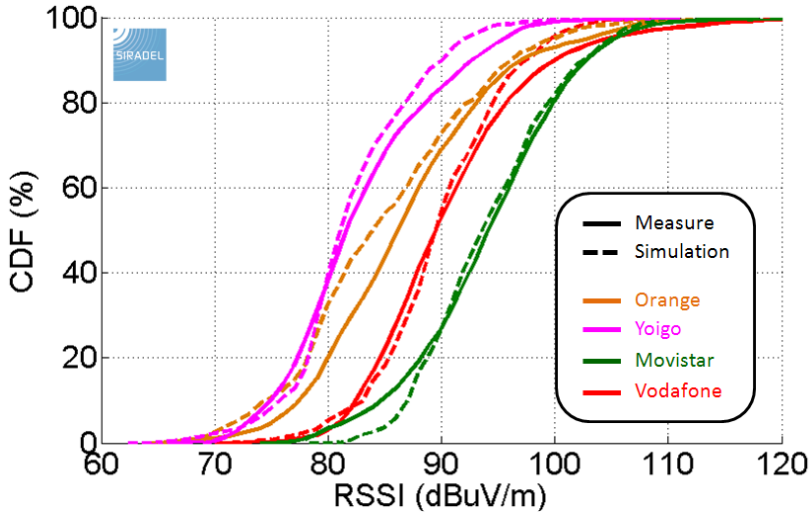

Figure 33: Measured and calibrated RSSI for 3G networks.

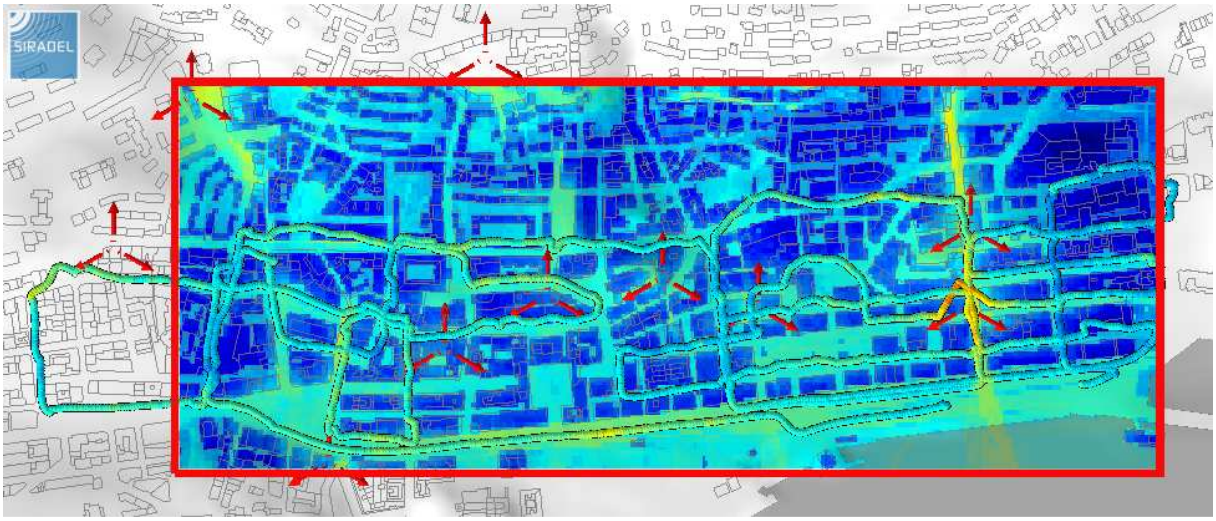

Figure 34: Comparison between measurements and the calibrated RSSI simulation from one 3G network.

The calibrated 3G simulation provides the map shown in Figure 35, with the total field strength in frequency band 2100 MHz.

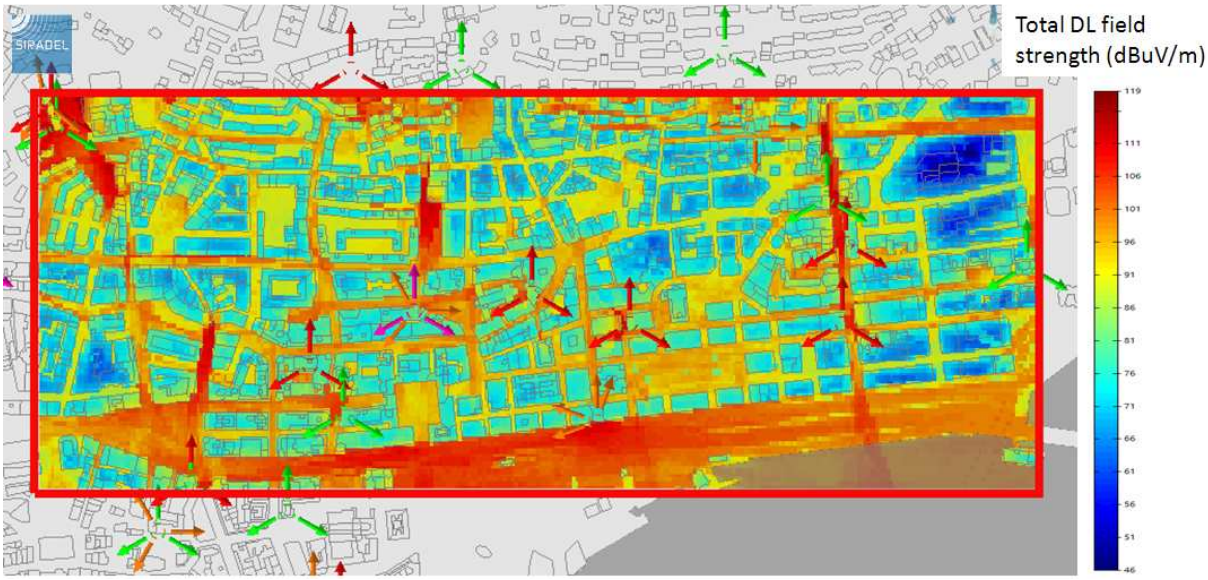

(a) Ground-floor.

(b) 6th floor (height = 19.5 m).

Figure 35: Map of DL total field strength in 3G frequency band, at different floors.

The DL contribution to EI is computed from those maps, and reported in Table 36. In order to assess one possible source of uncertainty in the simulation, we compare in the table the mean indoor field strength computed only at the ground-floor and the one computed from all floors. The conclusion is that the mean ground-floor level is 17 times lower than the mean multi-floor field strength. As a consequence, the DL-EI that is calculated with only an estimate of the mean field strength at the ground-floor strongly underestimates (by a factor of 2.9) the exact DL-EI considering exposure in all floors.

Table 47: EI simulated in Santander 3G network.

Santander 3G	Outdoor	Indoor Grd floor	Indoor All floors
Mean DL power density (W/m²)	2.87E-05	4.14E-07	7.14E-06
EI - DL contribution (W/kg) Outdoor + Grd floor	3.55E-08		
EI - DL contribution (W/kg) Outdoor + All floors	1.02E-07		

We also take benefit from this study to provide examples of outdoor-to-indoor offsets:

- At ground-floor only:
  - Mean offset calculated from field strengths in dB: -18.2 dB.
  - Mean offset calculated from power densities in W/m²: ÷69.
- From all floors:
  - Mean offset calculated from field strengths in dB: -11.8 dB.
  - **Mean offset calculated from power densities in W/m²: ÷4.**

The latter value is the one that should be used in outdoor-to-indoor conversion, when the DL-EI from field strength measurements is collected only in the streets. Remark those offsets depend on the network topology, frequency and environment (building density and height) and thus they cannot be generalized for any scenario.

The comparison between 2G measured and simulated RSSI was more complicated. It is obvious that large differences are due to errors and inaccuracies in the available network parameters. The largest difference is observed for one 2G operator in frequency band 900 MHz, as shown in Figure 36. The field strength predicted in the East part is far below the one captured by the measurements. This is actually an illustration of how crucial the accuracy of input data is for simulation. This is a typical symptom when using public or out-of-date information.

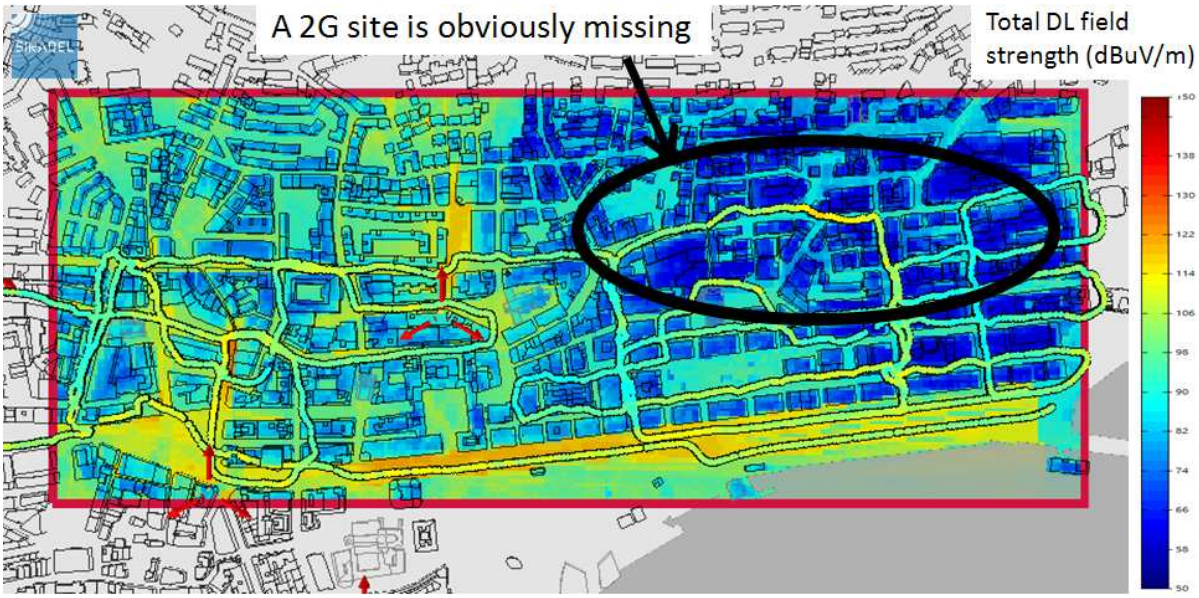

Figure 36: Example of comparison between a 2G 900 MHz measure and simulation.

The exposure analysis in the Orange's LTE network relies on a more precise antenna description, and the use of a complete DL+UL simulation platform. The DL field strength prediction has been calibrated from the SCAN RSSI data, as for 2G and 3G technologies, i.e. based on the DL traffic load, while the prediction of DL/UL throughputs and UL transmit powers have been adjusted by slight modifications in the SNR-throughput mapping tables and the predicted UL interference level. Figure 37 gives the result for all metrics of interest.

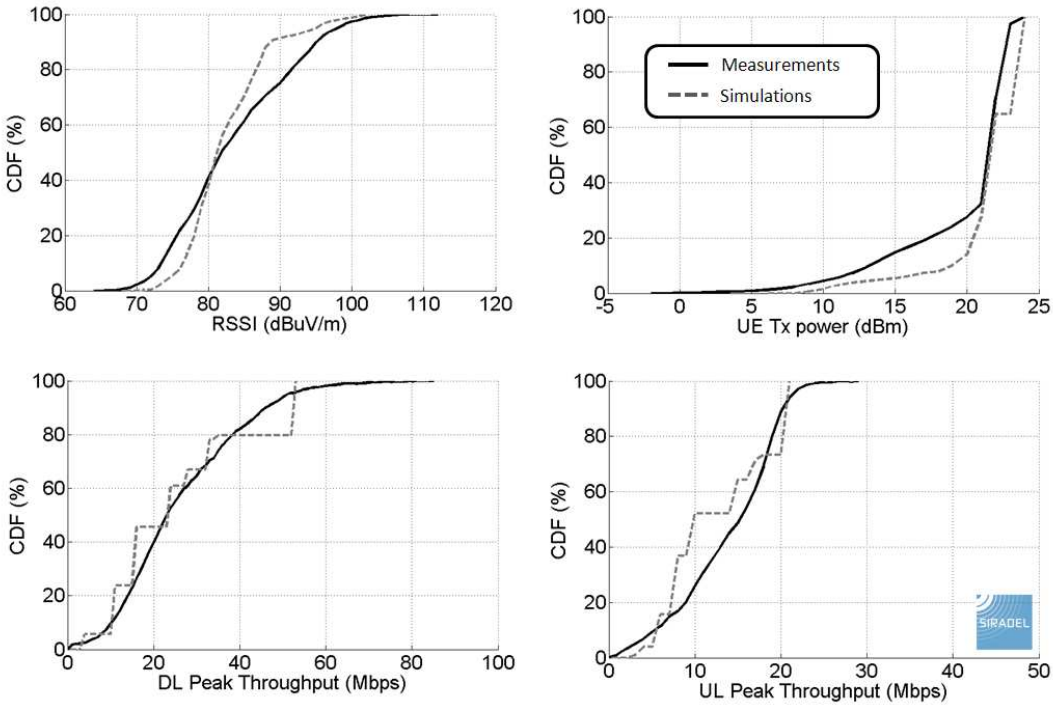

Figure 37: Calibration results on 4G metrics.

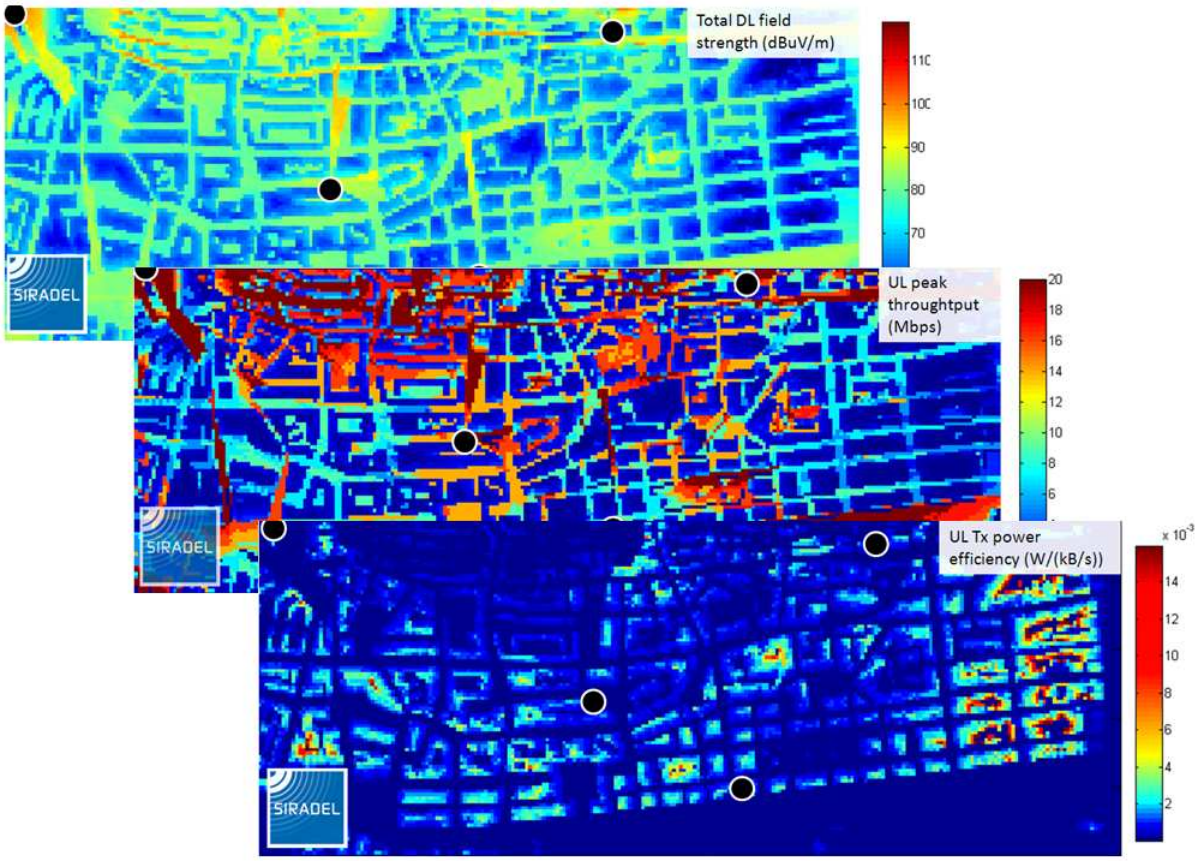

Figure 38: Santander 4G exposure maps.

The EI from Santander 4G cellular networks is computed after the mean DL field strength, UL transmit power and UL throughput have been extracted from the maps shown in Figure 38, distinguishing between outdoor and indoor environments. The EI is calculated following the procedure given in Figure 32.
The results are reported in Table 48. One important conclusion is that the UL contribution is 22 times higher than DL contribution.

Table 48: EI simulated in Santander 4G network.

Santander 4G	Outdoor	Indoor
Mean DL power density (W/m²)	2.75E-06	7.64E-08
Mean UL active transmit power (W)	0.144	0.151
Mean UL peak throughput (kB/s)	1588	214

EI - DL contribution (W/kg)	1.86E-09
EI - UL contribution (W/kg)	4.06E-08
EI (W/kg)	4.25E-08

6.5 In-building simulations

This section discusses the EI calculation module as implemented in the WHIPP tool [D6.1] which focuses on indoor environments. The EI module allows calculating the EI based on the whole-body SAR.

6.5.1 EI assessment method

The EI calculation consists of either entering or reading the input parameters from a database, defining the considered scenario, and calculating the EI.

To illustrate these steps, the following UMTS phone call scenario is used: a standing adult population of which 60% is connected to an outdoor macrocell UMTS base station (MC BS) (black double arrow) and 40% is connected to an UMTS Femtocell base station (FBS) (green double arrow), see Figure 39. The whole-body EI is calculated for usage with the phone to the ear.

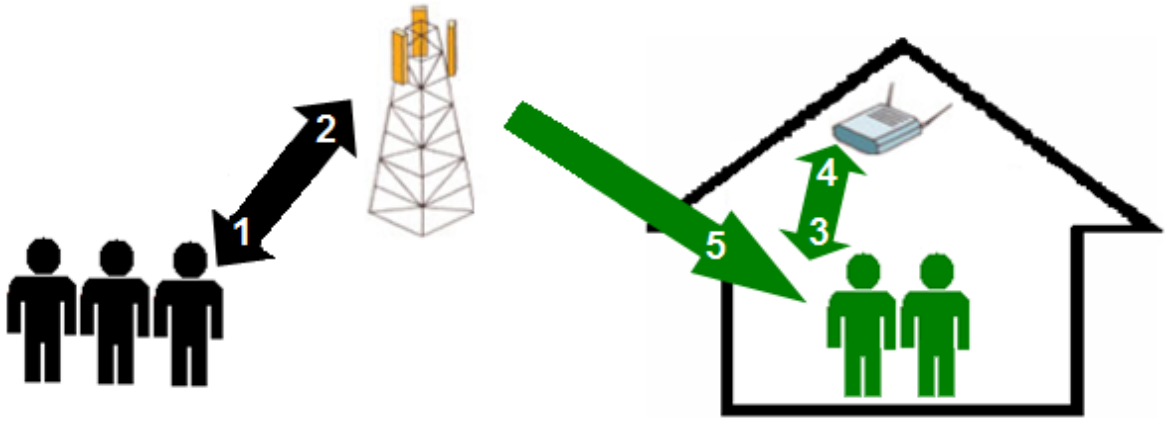

Figure 39: UMTS phone call scenario

The EI evaluation procedure is described below.

1. Entering or reading input (reference SAR values, and powers).

- First, **reference SAR values** are entered, both for transmitted and incident power density. These values depend on the network Radio Access Technology (RAT), the posture, the population and (for the transmitted power) also the usage (orientation of the device relative to the body). Finally, also a differentiation between whole-body and localized values is made. As more reference SAR values become available, a better approach would be to keep these values in a separate database.
  For the considered scenario, reference SAR values for transmitted and received power (density) are required for the UMTS technology, posture standing, type of person adult. For the reference SAR for 1W of transmitted power, also the fact that the phone is held against the ear is required to obtain the correct value:
  - reference SAR for received power: 0.0046 W/kg per W/m².
  - reference SAR for transmitted power: 0.0052 per W.

- Secondly, **average transmitted power** and **incident power density** values are entered or read from the database. For the transmitted power, this value depends on the RAT and cell type, the environment, and the usage (data/voice/… differentiation and orientation of the device relative to the body). For the incident power density, this depends on RAT and cell type, environment, and time of day. It can be chosen to enter these average values as such, but for indoor environments, they can also be simulated by the tool.

In that case, a specific ground plan is required with indication of the relevant parameters (indoor base station location and transmit powers, duty cycles, receiver type,…):

Scenario:
Average transmitted power from indoor to MC BS: 2.7 x 10^{-3} W [VAR].
Average transmitted power from indoor to FBS: 2.9 x 10^{-7} W [VAR].
Average transmitted power from outdoor to MC BS: 1 x 10^{-5} W.

Average received power density indoor from MC BS: 8.2 x 10^{-10} W/m² [VAR].
Average received power density indoor from FBS: 5.2 x 10^{-6} W/m² [VAR].
Average received power density outdoor from MC BS: 6.8 x 10^{-9} W/m².

The outdoor macro-cell powers densities are derived from the indoor macro-cell power densities, based on a building penetration loss of 10 dB.

2. Define scenario: **population distribution** and **uplink and downlink exposure times**.

- Firstly, the exposure time durations are entered. Time durations are entered for specific combinations of RAT (with or without cell type differentiation), time of day, usage (data/voice/… differentiation and orientation of the device relative to the body), posture, and for each of the defined user load profiles.

  Scenario:
  Heavy, moderate, light users call for 30s, 10s, 3s per hour respectively, irrespective of being indoor or outdoor.

- Secondly, the population distribution is characterized. For each of the combinations defined in the exposure time duration characterization, it needs to be known what percentage of the population is exposed to it.

  Scenario:
  A population fraction of 60% is defined as outdoor macro. The 60% are further divided into 6% heavy users, 30% moderate users, 15% light users, and 9% non-users (UL usage). There is a DL contribution (from MC BS to outdoor population, arrow 1), and an UL contribution (from outdoor population to MC BS, arrow 2).
  Another fraction of 40% is defined as indoor femto, again composed of the different user load profiles: 4% heavy users, 20% moderate users, 10% light users, and 6% non-users. There is a DL contribution (FBS to indoor population, arrow 3) and an UL contribution (indoor population to FBS, arrow 4).
  Finally, another fraction of 40% is defined as indoor macro, since there is also a DL contribution of the macro-cell BS to the indoor population (arrow 5). However, the entire 40% is defined as ‘non using’, because all people of the 40% indoor population connect to the femtocell BS, and are thus not using the macro-cell BS. It is clear that this input is also required, since the indoor exposure from the macro-cell BS (arrow 5) should be accounted for.

3. Calculate EI.

   After input validity checks (input values available, checks on sum of time durations and population fractions), the EI formula as proposed in [D2.8] is applied and the different EI contributions are shown, with a separation between UL and DL contributions.

6.5.2 Results

For the considered scenario, the EI (based on the whole-body SAR) equals 1.196E-8 W/kg over a period of one hour in the afternoon. The different contributions are listed in Table 49 and are calculated as follows:

UL: 1/T x fraction x UL_time x SAR_TX x P_TX
DL: 1/T x fraction x DL_time x SAR_RX x S_RX

Table 49: EI contributions over one hour in the afternoon for a standing adult population. Mobile phone users hold their mobile phones at the ear and communicate via UMTS.

Cell	Environment	User load profiles	EI [W/kg]	EI_{UL} [W/kg]	EI_{DL} [W/kg]
Macro	Indoor	No usage	1.50E-10	0.0	1.50E-10
	Outdoor	Heavy	2.32E-10	6.92E-12	2.25E-10
		Moderate	1.14E-9	1.15E-11	1.12E-9
		Light	5.64E-10	1.73E-12	5.62E-10
		No usage	3.37E-10	0.0	3.37E-10
Femto	Indoor	Heavy	9.54E-10	4.94E-13	9.54E-10
		Moderate	4.77E-9	8.23E-13	4.77E-9
		Light	2.39E-9	1.24E-13	2.38E-9
		No usage	1.43E-9	0.0	1.43E-9

From Table 49, we observe that in an indoor environment the uplink contribution of EI can be significantly reduced as compared to the outdoor uplink contribution by employing femto cells at the cost of an increased downlink EI contribution. Although the femto cells will radiate much less than macro cells, people can come closer to the femto cell base station resulting in an increased downlink exposure. Thus, a femto cell will be beneficial in indoor environments where there is a high UL usage.

6.6 LEXNET EI Validation Platform (LEI-VP)

A platform to assess the overall exposure index on multiple datasets is described in this section. The aim for designing the LEI-VP is to show the impact of various categories and technologies on the exposure index over a specified period, typically during the course of the day. Having such a platform helps to demonstrate the EI as a concept to those who are less familiar with the LEXNET project. The design principle of the LEI-VP is based on a data driven approach. This enables separation of the generation of data including real-time measurements from the network element and the various analysis functions that assess the impact of the data on the EI.

6.6.1 EI assessment method

Figure 40 provides an overview of the overall architecture of the LEI-VP developed by FLE. The architecture is centred on a data model needed to calculate the EI over a specified time period (nominally 1 day). The initial data are a combination of reference values from [D2.8] and from measurements and experiments obtained in other LEXNET tasks. Filtered by different criteria, the resulting graphs of the EI values over time provide a method of evaluating and comparing the impact of various network techniques on the overall exposure index.

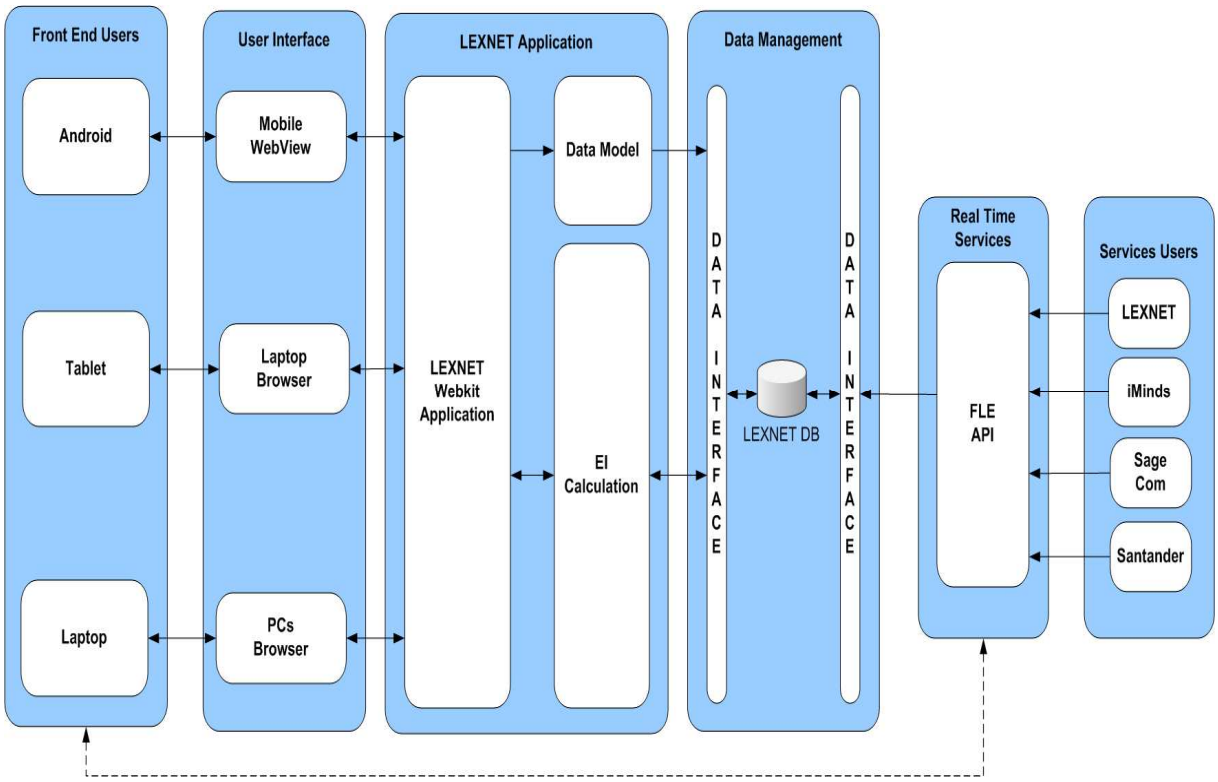

Figure 40: Overall EI validation platform model.

The LEI-VP data model is stored in a relational database and is interrogated using standard SQL queries. The model is populated with data using a semi-automated workflow, but new input modules that directly connect the LEI-VP to the data source can be developed in the future for real-time analysis of the EI. The visualization aspect of the platform is handled using standard HTML, JavaScript and CSS, so it can be used with any compatible browser. Finally, a backend based on Java is responsible of querying the database and computing the EI based on requests received from the users.

The data model reflects the structure of the EI formula and consists of 4 sub-models necessary to calculate the EI:

- *f* – the fraction of the population affected in the given scenario,
- *td* – the time duration of the exposure in that scenario,
- *SAR* – the SAR value that applies to the scenario and
- *power* – the value of the mean transmitted power or received power density in the scenario.

Specific values for each factor in the EI formula corresponds to a scenario. The scenarios are defined by the combinations of the EI input variables defined in [D2.8],

plus: the direction (i.e. uplink or downlink) and the frequency band (to distinguish RATs that operate in multiple bands). As *power* is a constantly measured quantity each value also has a timestamp associated with itwhich enabled the LEI-VP to plot graphs of the EI over time.

For the initial analysis of EI composition, the LEI-VP implements four views, summarized in Table 50. The direction view shows the distribution of EI between downlink and uplink and its variation over time. The RAT view shows how the total EI is split between the different technologies. These two views are generated by partitioning the EI formula into the required parts. The last two views are user centric and show the EI a given individual would have if he/she would be part of that category: child, young, adult or senior for the population view, and heavy, medium, light or the non-users for the user profile view.

Table 50: EI analysis categories and views in the platform GUI.

Direction	Technology	Population	User Profile
Downlink	2G	Children	Heavy
Uplink	3G	Young People	Medium
	4G (LTE)	Adults	Light
	WiFi	Seniors	Non User
	WSN		

6.6.2 Results

Figure 41 is a screenshot of the current LEI-VP demonstrator. The bar at the top of the display enables the user to select a view based on the EI categories outlines in table 50.
The left hand side of the screen enables the user to determine: which components are being plotted and the period of time, while the right hand side offers a description of the dataset used to plot the graph and the assumptions that are made in such specific scenario.

The screenshot shows a comparison between exposure from UL transmission (red line) and exposure from DL transmission (blue line) providing a snapshot of the EI index (vertical axis) over a 4 month period (horizontal axis) for an 3G based Urban scenario.

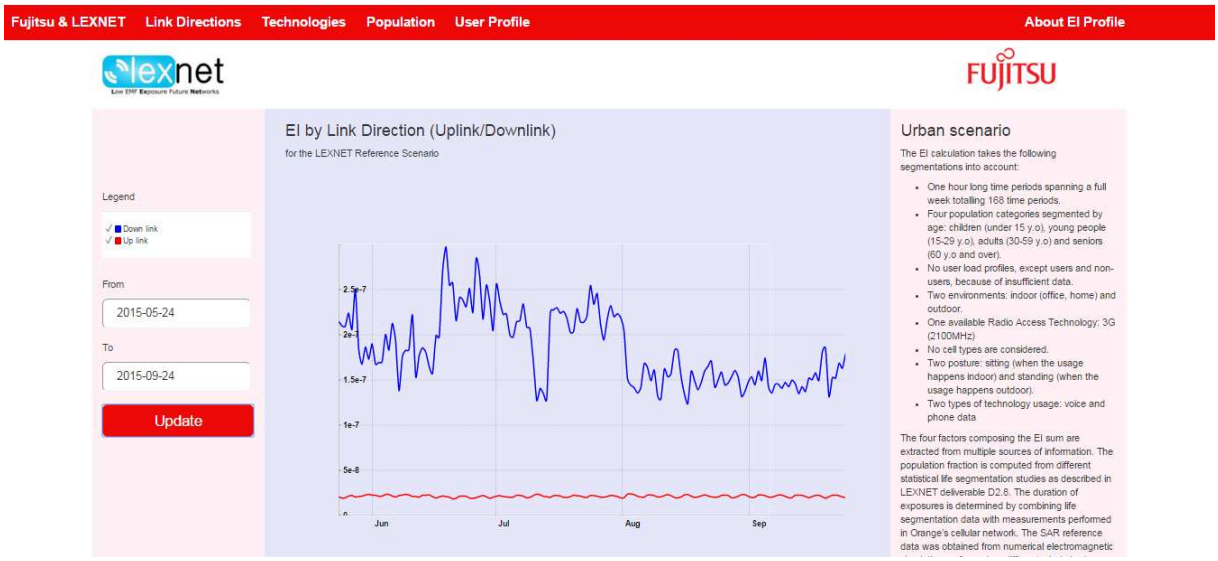

Figure 41: Overview of the LEI-VP user interface

The LEI-VP has been developed as a means to demonstrate the EI concept and enable the assessment of different techniques and behaviours on the overall EI.

7 CONCLUSIONS

Part-A of deliverable D6.2 reports on the EI practical implementation in real testbeds and radio-planning like simulations, relying on existing or new measurement tools, EI calculators and reference inputs (from [D2.8]). The document also discussed the stakeholders that might benefit from the EI, and how the proposed EI assessment methodologies could be used.

At the end, the presented results are expected to fulfill three objectives:

1. Demonstrate the practical feasibility of EI measurement or simulation protocols.
2. Highlight the technical challenges, advantages and drawbacks from each implemented solution.
3. Serve as reference demonstrations in the perspective of EI standardization and industrial implementation.

The assessed EI values are summarized in section 4.

The evaluation of the EI uncertainties is a critical investigation topic that is partly addressed in this document, but still requires further work to be completed. Some results are available, e.g. by measuring the exposure variations from one day to another, or by applying different protocols on the same network. These are only preliminary studies that would need to be completed in further investigations, in particular to support the standardization of new EMF exposure methods.

Finally, we have summarized in Table 51 the main learnings that can be extracted from the evaluations reported in this document.

Table 51: Main evaluation learnings.

Evaluated methodologies	Learnings
Drive test with wearable dosimeters	• The wearable EME Spy 200 dosimeter, with three-axis antenna, proved to be a simple and relevant tool for evaluating the EI-DL component in a large outdoor area. All frequency bands can be measured in parallel; therefore, all required data is collected with only one drive test (at least for one time period). • The measurement with the LEXNET dosimeter enables a more precise analysis of the DL exposure sources, along with a per-operator discrimination. The adaptative filter also facilitates its usage in different world regions (with different allocated frequency bands). • The wearable dosimeter can be associated with a Trace mobile equipment in order to capture both DL and UL metrics. The advantage is obviously (compared to a Trace mobile only protocol) a gain in accuracy.
Drive test with Trace mobile equipment	• The measurement campaign in Santander demonstrated the feasibility of EI assessment from a Trace mobile drive test, but has also illustrated the cost of such an assessment: few day measurements (as the same route is repeated for each RAT and service) and processing. • The cost could certainly be reduced by identifying a limiting number of representative services that would be sufficient to extrapolate the whole EI (e.g. one single data service for each 3G and 4G technology). • We met difficulties to get representative indoor measurements, as the access to various indoor environments in a target large-scale area

	is complicated and the collection of indoor measurements in each location is a long process. Actually, simulations or average extrapolation factors could be of a great help to compensate this. • The DL measurements that were repeated for each service (but should have been independent of the service) as well as the DL/UL measurements repeated with two different equipments have demonstrated significant measurement uncertainty. This needs to be managed, e.g. with precise protocol; fine measurement equipment characterization; and tests on measurement reproducibility. • Trace mobile phone are today professional equipments devoted to network operators. They are associated with advanced software and are quite expensive. But the use of a prototype Tx/Rx platform in the Santander measurement campaign has demonstrated the feasibility for simplified equipment. • The wearable dosimeter might be an interesting complement in order to get accurate DL measurements; then the Trace mobile is used only for UL characterization.
Fixed dosimeter network	• The integration of fixed dosimeters in the SmartSantander platform has clearly demonstrated the feasibility of a large-scale and continuous EI-DL assessment, accompanied with a distant web access to all collected data. • The main difficulties reside in the conversion from the simplified fixed dosimeter equipment to a representative field strength value. Some extrapolation factors have been elaborated in frame of LEXNET, using a wearable dosimeter as a reference. Nevertheless the variability of those extrapolation factors versus RAT is not perfectly understood; and would need further confirmation. • Besides, the continuous dosimeter measurements have shown quite limited exposure variations over a day, a week or a month, and only little correlation from one day (or one week) to another. This result that could be further refined by on a longer-term analysis may be of a great help to adjust the EI assessment protocols.
Cellular network monitoring	• EI assessment from Network monitoring is a promising and highly relevant approach for network operators, in particular in the mid-term perspective of automatic network diagnostic and management. • An implementation based on existing monitoring tools has been realized and has succeeded in providing EI values. Nevertheless the protocol is complex (many sources to cross) and cannot catch precisely all expected measures (existing monitoring metrics are originally devoted to other applications). • The integration of geolocation tools and EMF-specific metrics into the monitoring system would be of a great help to reduce the protocol complexity and increase the accuracy.
Cellular network simulation	• Calibration and simulation of EI have been successfully demonstrated on Santander. This simulation can be of a great help to complement drive test or smart city measurements with UL extrapolation (when measurement only collects DL) or indoor extrapolation. • The importance of considering the 3D indoor environment instead of the ground-floor only has been demonstrated by simulations. • The interest of simulation is further demonstrated in Part-B of the deliverable, where it is employed to evaluate the impact of topology or technology changes on both QoS and EMF metrics. • The Santander experimentation has shown a strong dependency on the input accuracy, specifically in the description of the base station locations and properties. Both situations have been met in the

	Santander testbed: acceptable input accuracy (then possible calibration) in 3G/4G network; strong inaccuracies in 2G networks. Standardization of a simulation-based EI assessment might surely pay a great attention on the necessary inputs and their required precision.

8 REFERENCES

[3GPP] 3GPP, TS 25.331, "Technical Specification Group Radio Access Network; Physical layer; Measurements (FDD) (Release 11)", 2011.

[AER1] S. Aerts, D. Deschrijver, W. Joseph, L. Verloock, F. Goeminne, L. Martens, T. Dhaene, "Exposure assessment of mobile phone base station radiation in an outdoor environment using sequential surrogate modeling", *Bioelectromagnetics* n°34, pp. 300–311, 2013.

[AER2] S. Aerts, D. Deschrijver, L. Verloock, T. Dhaene, L. Martens, W. Joseph, "Assessment of outdoor radiofrequency electromagnetic field exposure through hotspot localization using kriging-based sequential sampling", *Environ. Res.* n°126, pp.184–191, 2013.

[AZP] M.A. Azpurua, K. Dos Ramos, "A comparison of spatial interpolation methods for estimation of average electromagnetic field magnitude", PIER M 14(7), pp. 135-145, 2010.

[CIS] CISCO, Cisco Visual Networking Index: Global Mobile Data Traffic Forecast Update 2014–2019, White paper, 2015, available online at: http://www.cisco.com/c/en/us/solutions/collateral/service-provider/visual-networking-index-vni/white_paper_c11-520862.html.

[COU] I. Couckuyt, J. Aernouts, D. Deschrijver, F. Turck, T. Dhaene, "Identification of quasi-optimal regions in the design space using surrogate modeling", Eng. Comput. Springer-Verlag London Limited, 2012.

[COR] Y. Corre, J. Stéphan and Y. Lostanlen, "Indoor-to-outdoor path-loss models for Femtocell predictions", 22nd IEEE PIMRC, Toronto, 2011.

[CRO] K. Crombecq, D. Gorissen, D. Deschrijver, T. Dhaene, "A novel hybrid sequential design strategy for global surrogate modeling of computer experiments", SIAM J. Sci. Comput., pp. 1948–1974, 2011.

[D2.8] LEXNET Deliverable D2.8: *Global wireless exposure metric definition*, 2015.

[D3.2] LEXNET Deliverable D3.2: *Wideband dosimeter design study & performances characterization*, 2014.

[D3.3] LEXNET Deliverable D3.3: *Exposure Index assessment v2*, 2014.

[D6.1] LEXNET deliverable D6.1: *Validation platform framework and initial assessment*, 2014.

All LEXNET deliverables are available at http://www.lexnet.fr/scientificoutputs/publicdeliverables.html.

[DES] D. Deschrijver, K. Crombecq, H.M. Nguyen, T. Dhaene, « Adaptive Sampling Algorithm for Macromodeling of Parameterized S-Parameter Responses", *IEEE Trans. Microw. Theory. Techn.*, pp. 39–45, 2011.

[DES] D. Deschrijver, F. Vanhee, D. Pissoort, T. Dhaene, "Automated near-field scanning algorithm for the EMC analysis of electronic devices", *IEEE Trans. Electromagn. Compat.* vol.54, pp. 502–510, 2012.

[DIE] L. Diez, L. Rodriguez de Lope, R. Aguero, Y. Corre, J. Stephan, M. Brau, S. Aerts, G. Vermeeren, L. Martens, W. Joseph, "Optimal dosimeter deployment into a smart city IoT platform for wideband EMF exposure assessment", European Conference on Networks and Communications (EuCNC), 2015.

[EME] Information on EME SPY 200 by SATIMO available online at http://www.satimo.com/content/products/eme-spy-200.

[GAT] A. Gati, E. Conil, Man-Fai Wong, J. Wiart, "Duality Between Uplink Local and Downlink Whole-Body Exposures in Operating Networks", *IEEE Transactions on Electromagnetic Compatibility*, vol.52, no.4, pp.829-836, 2010.

[JOS] W. Joseph, L. Verloock, F. Goeminne, G. Vermeeren, L. Martens, "In situ LTE exposure of the general public: characterization and extrapolation", *Bioelectromagnetics* vol. 33, no. 6, pp. 466-475, 2012.

[PAN] J.M. Paniagua, M. Rufo, A. Jimenez, A. Antolin, "The spatial statistics formalism applied to mapping electromagnetic radiation in urban areas", *Environ. Monit. Assess.*, 2013.

[POP1] M. Popović, M. Tešanović, B. Radier, "Strategies for reducing the global EMF exposure: cellular operators perspective", ISWCS, Spain, 2014.

[POP2] M. Popović, M. Koprivica, S. Nikšić, J. Milinković, A. Nešković, "Methodology for the comparison of cellular technologies and services with respect to EMF exposure", TELFOR 2014, Serbia, 2014.

[RAT] RATEL, "An Overview of the Telecom and Postal Services Market in the Republic of Serbia in 2014", available online at: http://www.ratel.rs/market/overviews_of_telecom_market.129.html.

[SMA] Information on SmartSantander, EU FP7 Project Smart Santander (ID 257992), available online at http://www.smartsantander.eu.

[STA] Statistical office of the Republic of Serbia, "Upotreba informaciono-komunikacionih tehnologija u Republici Srbiji", 2015, available online at: http://webrzs.stat.gov.rs/WebSite/Public/PageView.aspx?pKey= 206.

[VAR] N. Varsier, D. Plets, Y. Corre, G. Vermeeren, W. Joseph, S. Aerts, L. Martens and J. Wiart, "A novel method to assess human population exposure induced by a wireless cellular network", *Bioelectromagnetics*, vol. 36, Issue 6, pp 451–463, 2015.

.

APPENDIX A1: INTERNAL REVIEW

	Reviewer 1: Nadège Varsier			Reviewer 2: Ramon Agüero		
	Answer	**Comments**	**Type***	**Answer**	**Comments**	**Type***
1. Is the deliverable in accordance with						
(i) the Description of Work?	☒ Yes ☐ No		☐ M ☐ m ☐ a	☒ Yes ☐ No		☐ M ☐ m ☐ a
(ii) the international State of the Art?	☒ Yes ☐ No		☐ M ☐ m ☐ a	☒ Yes ☐ No		☐ M ☐ m ☐ a
2. Is the quality of the deliverable in a status						
(i) that allows to send it to EC?	☒ Yes ☐ No		☐ M ☐ m ☐ a	☒ Yes ☐ No		☐ M ☐ m ☐ a
(ii) that needs improvement of the writing by the editor of the deliverable?	☒ Yes ☐ No	See my comments	☐ M ☐ m ☐ a	☒ Yes ☐ No	Comments were made in the deliverable to be considered before submitting to the EC	☐ M ☒ m ☐ a
(iii) that needs further work by the partners responsible for the deliverable?	☒ Yes ☐ No	See my comments and recommendations	☐ M ☐ m ☐ a	☐ Yes ☒ No	Most of my comments were editorial and related to presentation; there was anything requiring additional work	☐ M ☒ m ☐ a

* Type of comments: M = Major comment; m = minor comment; a = advice

APPENDIX A2: SANTANDER MEASUREMENTS

Different EI assessment methodologies have been demonstrated in the Santander testbed. Main results are presented in section 6.1, while more details are given in this Appendix.

A2.1. Methodology and environment of the measurement campaign

The Santander exposure characterization is addressed thanks to a wide range of measurement:

- Outdoor drive-test and indoor pedestrian
- Passive and active measurements
  - Passive: dosimeter and scanner based measurement
  - Active: trace mobile and dongle based measurement

All measurement types are complementary for EMF and Quality-of-Service (QoS) characterization. Outdoor drive-test measurements are the basis for the characterization of a large area. Pedestrian measurements usually aim at complementing drive-test measurements in some specific smaller areas: park, pedestrian areas, buildings, etc. They are specifically used here to characterize the EMF exposure and QoS in some buildings.
Passive measurements consist in collecting measurements with dosimeter and scanner based solutions. The former aims at measuring the real-time UL/DL electromagnetic fields on predefined RAT or frequency bands. The scanner-based solution is used to characterize some specific cellular networks at a time by measuring both EMF exposure related metrics and coverage metrics. The active measurements are collected with trace mobile and dongle based solutions. Both allow characterizing the QoS (real-time throughputs in particular) offered for one specific service by one specific cellular network at a time.

Therefore, each of these solutions collects a broad variety of parameters. Table 52 lists for each solution the main metrics usable for EMF and QoS characterization.

Table 52: Main measured metrics by solution.

Solution	Characterization level (at a time)	Coverage/QoS metrics	EMF metrics
Wearable dosimeter	Some predefined RAT or frequency bands	N/A	UL/DL E-field
Fixed dosimeter	Some predefined RAT or frequency bands	N/A	DL E-field
Scanner	Some predefined cellular networks	DL Rx power, SINR/SNR by base station	DL RSSI
Trace mobile / Dongle	One cellular network	DL/UL throughputs DL Rx power, SINR/SNR for main base stations only	DL RSSI UL Tx power

By using several items of each solution at a time and/or an iterative measurement process with different configurations of a single item of each solution, these metrics may be collected for:

- Multi-Radio Access Technology (RAT): 2G (GSM), 3G (HSPA) and 4G (LTE)

- Multi-time periods: Standard Working Time (SWT) and Rest Period (RP)
  - SWT is assumed to be in the range 9hr00–13hr00 and 16hr00–19hr00 in Spain
  - RP is assumed to be in the range 14hr30–16hr00 and 19hr00 – 22hr00 in Spain
- Multi-services (for active measurements only): DL&UL FTP transfer, Voice, Web browsing, Video streaming
- Multi-operator networks.

All the measurements are collected in a common environment: the Santander downtown shown in section 3.1.

Measurements are precisely collected in a specific study area of 0.98 Km^2 in the Santander downtown, in which a reference itinerary was defined for outdoor drive-test measurements and two specific buildings were selected for indoor pedestrian measurements (see Figure 42).

Figure 42: Drive-test path in Santander downtown.

The study area includes a high density of buildings delimited by many small streets and one large avenue (in the extreme south). Buildings are a mix of shops, corporate and residential buildings composed of large concrete or stone walls and standard-size windows. The mean building height is roughly 20 m (7 floors).

Both buildings selected for indoor are markets, respectively "*Mercado del Este*" (building at the East side) and "*Mercado la Esperanza*" (building at the West side). They are both composed of a single floor. The former building is an open area composed of concrete external walls and few wooden and glazed internal partitions. There are windows at the basis of the rooftop almost all along the building (see Figure 43). The latter has a quite comparable configuration than the former one. It is also an open space with concrete external walls but with more internal partitions, which are mainly composed of glass and metal (typical market stall). There also windows all around the boundary of the second building.

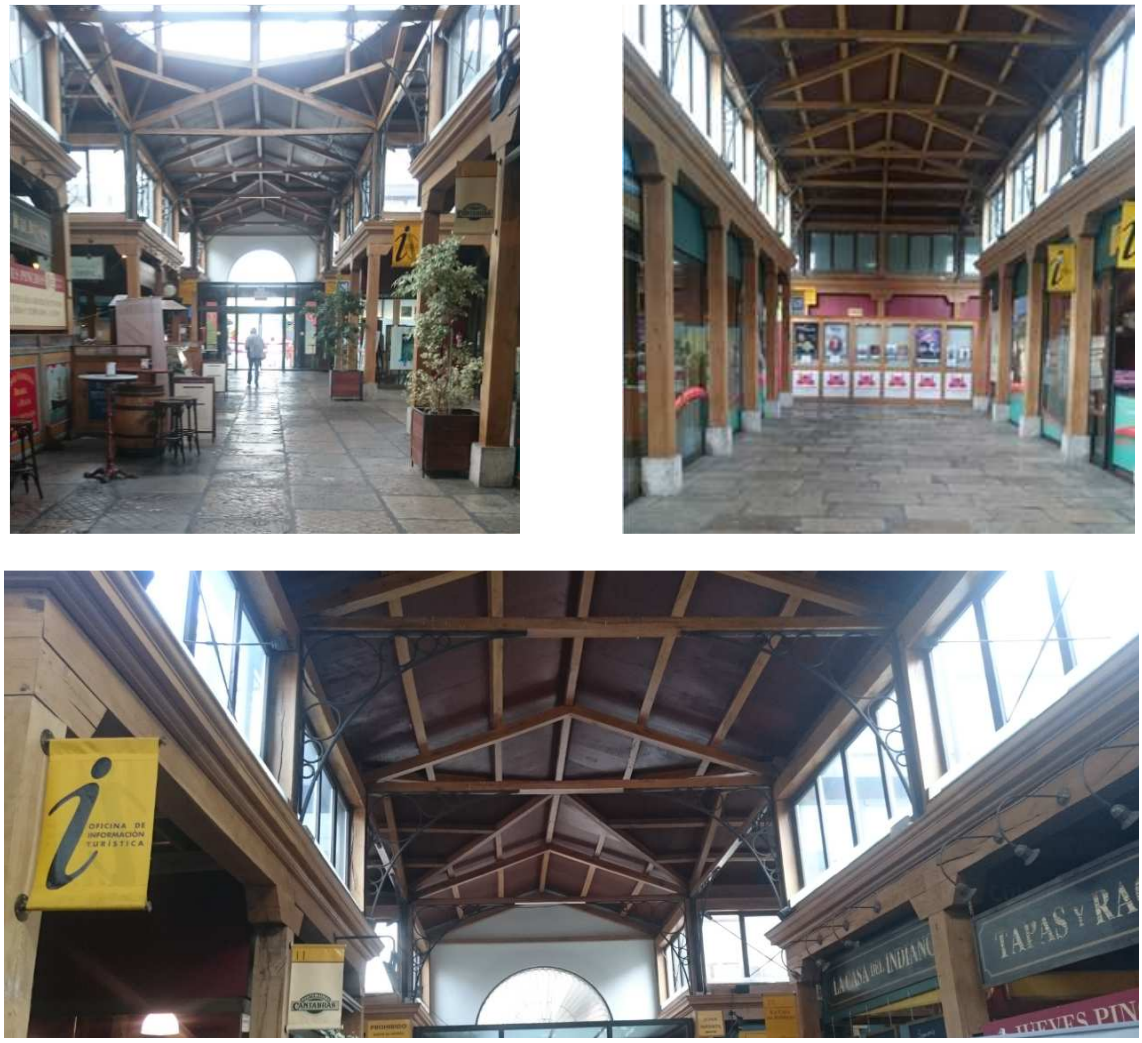

Figure 43: Typical pictures of the building "Mercado del Este".

Indoor measurements are collected at specific static locations as well as along an itinerary that run through the entire buildings. The measurement itinerary for indoor dosimeter measurements, for the two locations described above, is shown in Figure 44 below. The measurements inside the buildings are market by red, light blue, and violet colors. For the "Mercado del Este", both indoor and outdoor measurements were carried out (marked by the red and green lines respectively). The objective was to estimate an extrapolation factor between indoor and outdoor DL E-field.

(a)

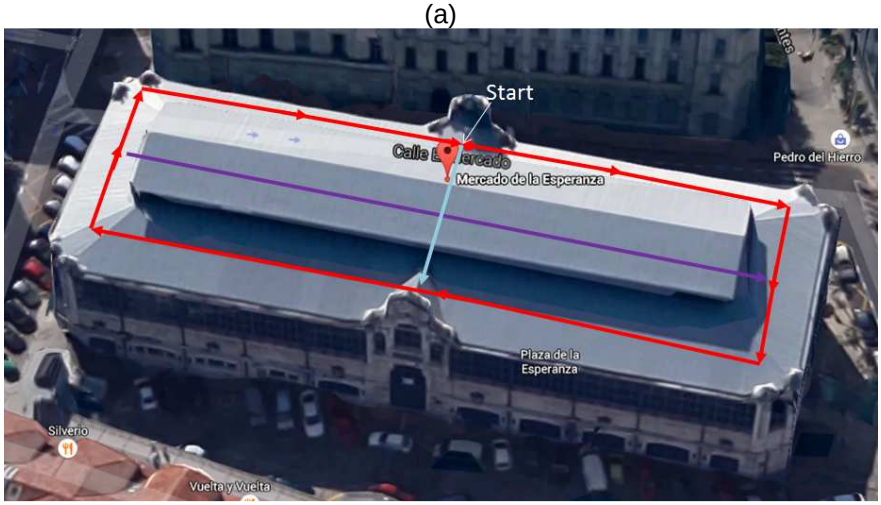

(b)

Figure 44: Indoor / pedestrian measurement itinerary for (a) "Mercado del Este" 60m x 40m, and (b) "Mercado la Esperanza" 70m x 30m. Red, blue and violet lines mark the itinerary inside the market. Green line marks the measurement itinerary outside the market.

Measurements have been collected during a limited timeframe of four (4) full days in April 2015. In this timeframe, a large subset but not the exhaustive list of scenarios resulting from the combination of all targeted RATs, time periods, services, and operators has been measured. Table 53 summarizes all measured scenarios.

Table 53: List of measured scenarios.

Environment	Type	Equipment	Operator	RAT	Service	Period
Outdoor drive-test	Active	Trace mobile	Orange	LTE	DL FTP transfer	SWT
						RP
					UL FTP transfer	SWT
						RP
					Video streaming	SWT
						RP
					Web browsing	SWT
						RP
				HSPA	DL FTP transfer	SWT
						RP
					UL FTP transfer	SWT
						RP
					Voice	SWT
						RP
				GSM	Voice	SWT
						RP
			Movistar	HSPA	UL FTP transfer	RP
		Dongle (Tx/Rx platform)	Orange	LTE	UL FTP transfer	SWT
					Video streaming	SWT*
					Web browsing	SWT
						RP
	Passive	Wearable dosimeter	All	All	N/A	SWT*
						RP*
		Fixed dosimeter **	All	All	N/A	SWT*
						RP*
		Scanner	Movistar + Orange	LTE	N/A	SWT
						RP
			All	HSPA + GSM	N/A	SWT
						RP
Indoor pedestrian in Building 1	Active	Trace mobile	Orange	LTE	DL FTP transfer	SWT
					UL FTP transfer	
					Video streaming	
				HSPA	DL FTP transfer	
					UL FTP transfer	
					Video streaming	
					Voice	
				GSM	Voice	
	Passive	Wearable dosimeter	All	All	N/A	SWT
						RP
Indoor pedestrian in Building 2	Passive	Wearable dosimeter	All	All	N/A	SWT
						RP

**Measurements reproduced several times.*
***The fixed dosimeter only measures DL e-field*

A2.2. DL E-field measurements from the mobile dosimeter

This Appendix reports details on the wearable dosimeter measurements collected in Santander downtown, and used in section 6.1.1 for EI assessment.

1- Outdoor measurements

The distribution for the four main frequency bands (i.e. GSM 900 DL, GSM 1800 and LTE B3 DL, UMTS 2100 DL, and Wi-Fi 2GHz) over the five different time periods is summarized in Figure 45: Statistical distribution of the mobile dosimeter measurements for (a) GSM 900 DL, (b) GSM 1800 and LTE B3 DL, (c) UMTS 2100 DL, and (d) Wi-Fi 2GHz frequency bands.

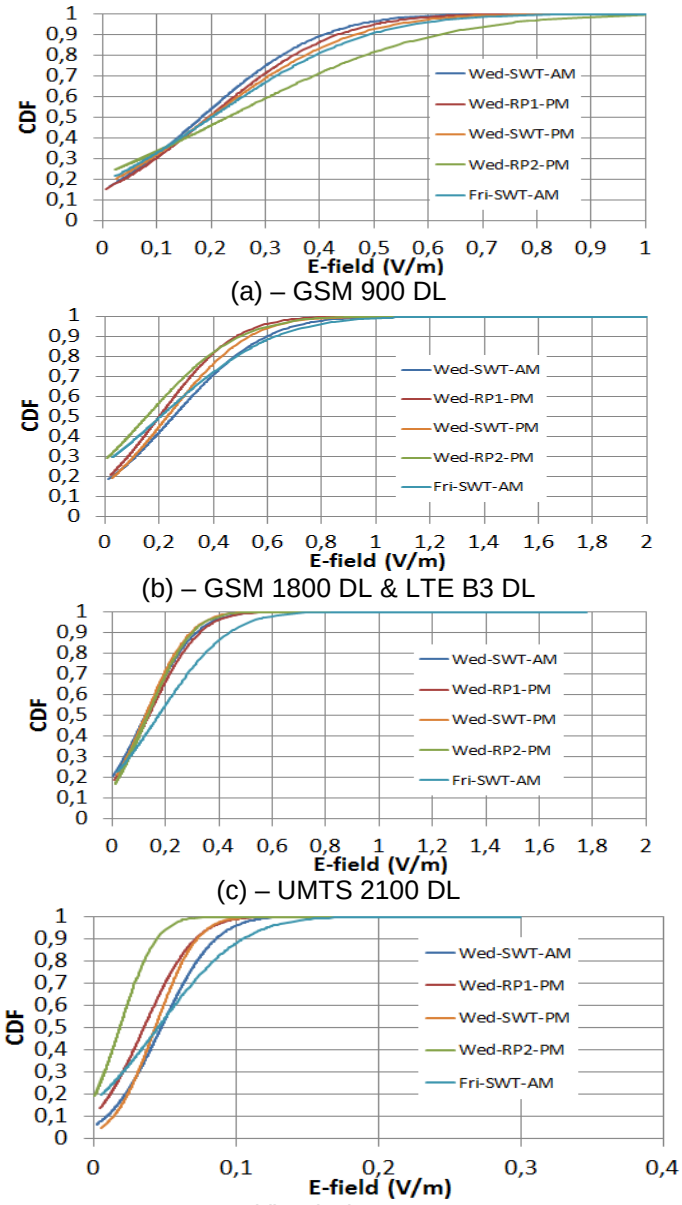

(a) – GSM 900 DL

(b) – GSM 1800 DL & LTE B3 DL

(c) – UMTS 2100 DL

(d) Wi-Fi 2GHz

Figure 45: Statistical distribution of the mobile dosimeter measurements for (a) GSM 900 DL, (b) GSM 1800 and LTE B3 DL, (c) UMTS 2100 DL, and (d) Wi-Fi 2GHz frequency bands.

2- ***Indoor measurement results***

The distributions for different frequency bands are shown in Figure 46 for indoor measurements inside the two market places.

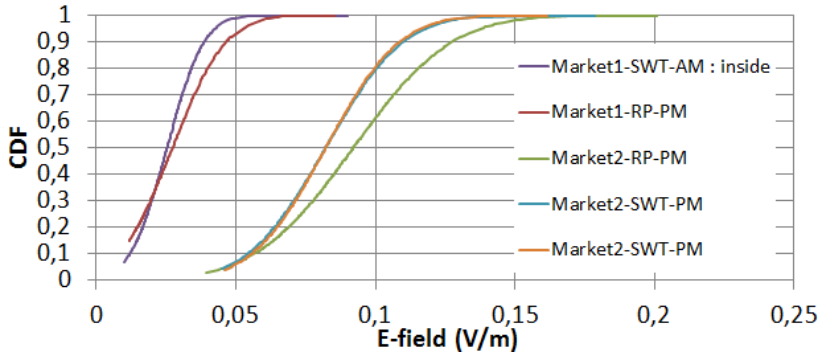

(a) – GSM 900 DL

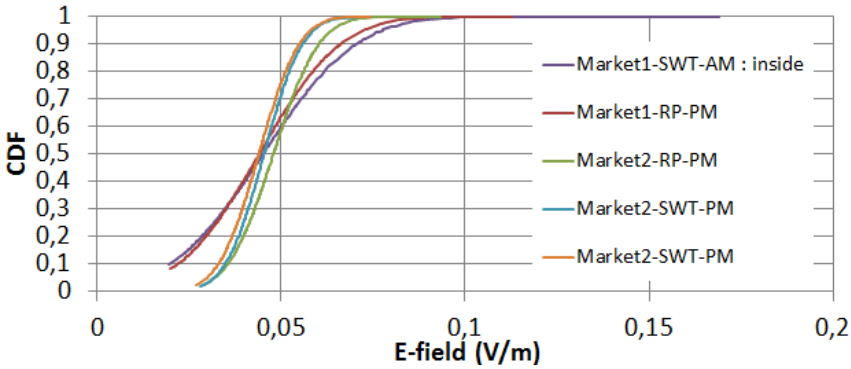

(b) – GSM 1800 DL & LTE B3 DL

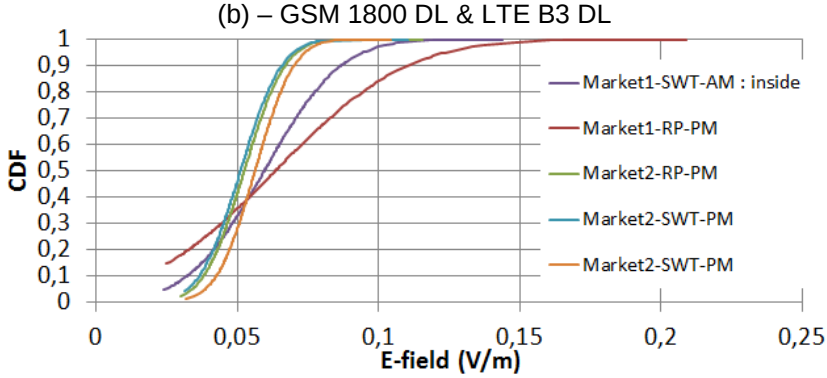

(c) – UMTS 2100 DL

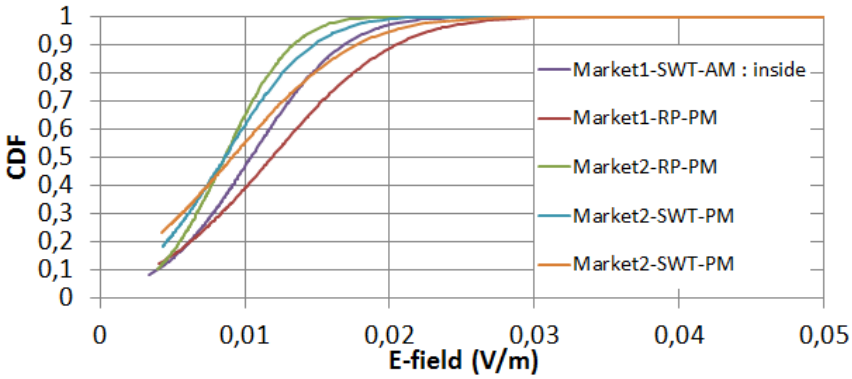

(d) Wi-Fi 2GHz

Figure 46: Statistical distribution of the mobile dosimeter measurements for (a) GSM 900 DL, (b) GSM1800 and LTE B3 DL, (c) UMTS 2100 DL, and (d) Wi-Fi 2GHz frequency bands and for different time periods inside the market buildings.

3- ***Extrapolation from outdoor to indoor E-field through measurements***

E-field measurements were carried out in outdoor and indoor environments as shown in Figure 44a. The distribution comparison for each of the four frequency bands are shown in Figure 47.

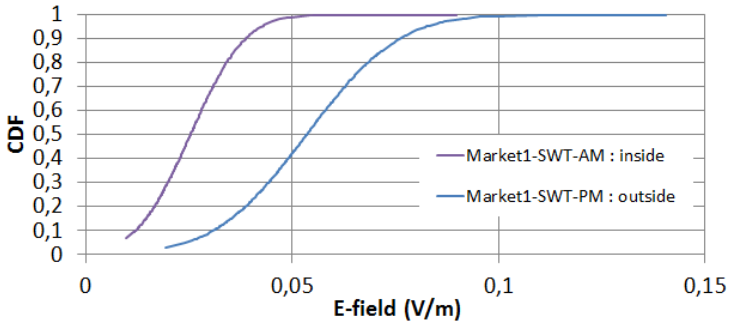

(a) – GSM 900 DL

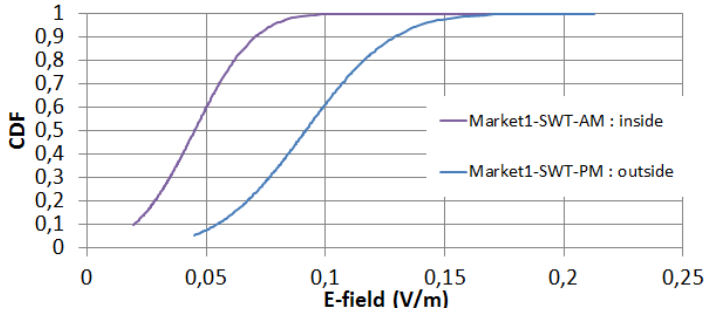

(b) – GSM 1800 DL & LTE B3 DL

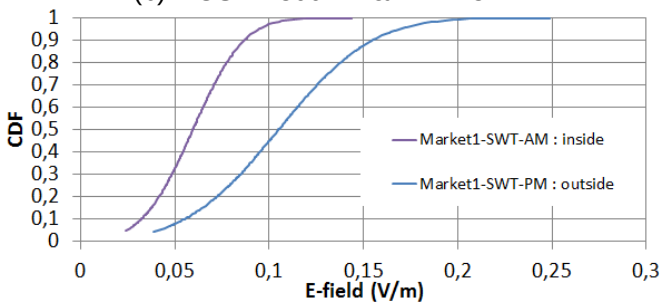

(c) – UMTS 2100 DL

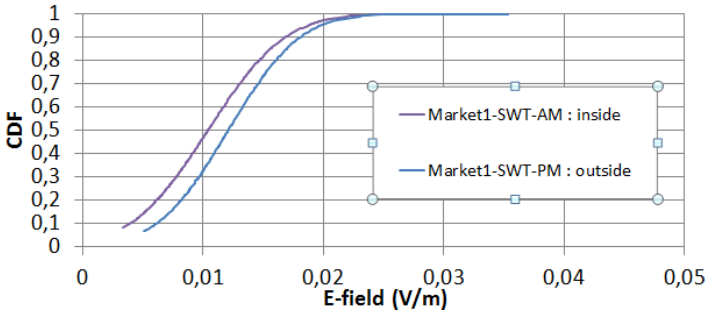

(d) Wi-Fi 2GHz

Figure 47: Statistical distribution of the mobile dosimeter measurements for (a) GSM 900 DL, (b) GSM1800 and LTE B3 DL, (c) UMTS 2100 DL, and (d) Wi-Fi 2GHz frequency bands, inside and outside the market building.

A2.3. Extrapolation from mono-axial measurements to isotropic E-field

The objective of this study was to extract an extrapolation factor for the fixed dosimeters deployed in Santander to monitor the DL E-field exposure. The fixed dosimeters have a mono-axial probe in the vertical position and hence are not capable to measure the isotropic E-field. For this the mobile dosimeter (EMESPY 200) was used to carry out measurements with its isotropic probe and data from the measurements was used to compute a mean extrapolation (or correction) factor for the fixed dosimeters.

1- Extrapolation principles

To estimate an extrapolation factor between mono-axial measurements and isotropic E-field measurements, the extrapolation factors for each of the three probes of the dosimeter are defined as:

$$\eta_x = \frac{E_{tot}}{E_x} \tag{1}$$

$$\eta_y = \frac{E_{tot}}{E_y} \tag{2}$$

$$\eta_z = \frac{E_{tot}}{E_z} \tag{3}$$

Where, η_i represents the extrapolation factor of axis "*i*", Etot represents the total E-field = $\sqrt{(E_x^2 + E_y^2 + E_z^2)}$. The E_x and E_y represents the E-field with horizontal polarization and E_z the vertical polarization.

The mean values of η_x, η_y , and η_z (calculated over the measurement period), the standard deviation and uncertainty are calculated using the following formulas.

$$Mean = \frac{1}{N}\sum_{i=1}^{N}\eta_i \tag{4}$$

$$\sigma = \sqrt{\frac{1}{N}\sum_{i=1}^{N}(\eta_i - mean)^2} \tag{5}$$

$$Uncertainty = \frac{\sigma}{mean} \tag{6}$$

Where, *N* represents the total number of samples and *i* is the index. The value "η" is calculated as the mean value of the three mono-axial values calculated above.

2- Extrapolation factor from mobile dosimeter measurements

An exhaustive one week measurement campaign was carried out in Santander, Spain in the month of April, 2015 (Appendix A2.1). The data from the EMESPY dosimeter was used to extract the extrapolation factor between mono-axial measurements and isotropic measurements. An example of the time domain variation of the total E-field, mono-axial E-field, and the extrapolation coefficients is given in Figure 48.

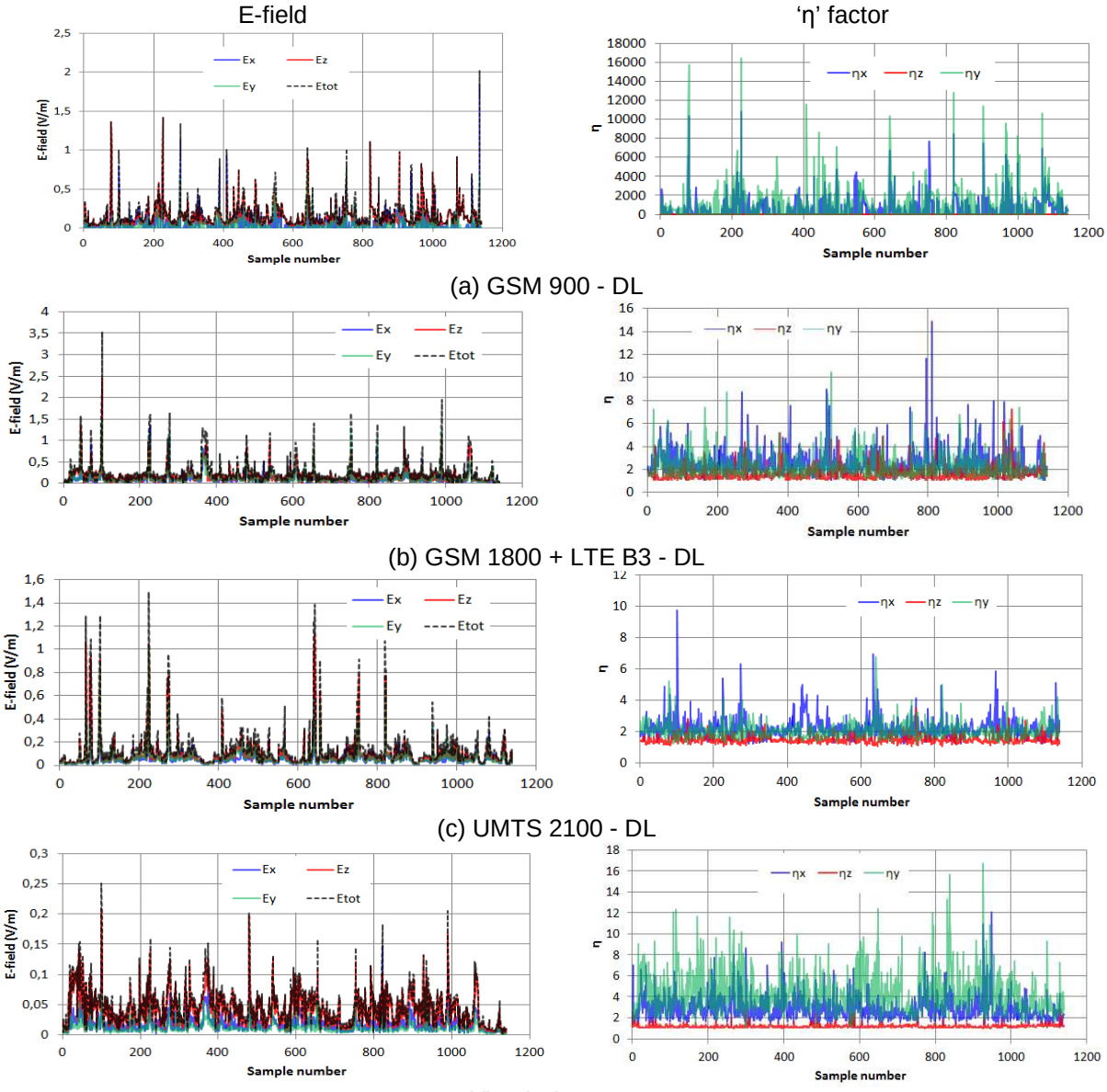

Figure 48: Time domain variation of total E-field, mono-axial E-field, and the extrapolation factors for (a) GSM 900 DL, (b) GSM1800 and LTE B3 DL, (c) UMTS 2100 DL, and (d) Wi-Fi 2GHz frequency bands Wednesday STW – AM slot.

Here,

- SWT (Standard Working Time period) is assumed to be in the range 9hr00–13hr00 and 16hr00–19hr00 in Spain, and
- RP (Rest Period) is assumed to be in the range 14hr30–16hr00 and 19hr00 – 22hr00 in Spain.

From the above results, the GSM 900 DL results provide very high extrapolation factors for E_x and E_y (horizontal Fields). This is due to the internal post-processing of the dosimeter which is applied to frequencies lower than 1 GHz. Thus the results at these frequencies for horizontal mono-axial E-field are not exploitable for this study. However they are provided here for comparison.

All the extrapolation factors, with their standard deviation and the calculated uncertainty, for each frequency band and is summarized in Table 54.

Table 54: Summary of extrapolation factors from mono-axial to isotropic E-field from outdoor mobile measurements.

		Ex			Ez			Ey		
	Measurement cycle	η_x	σ_x	U_x (%)	η_z	σ_z	U_z (%)	η_y	σ_y	U_y (%)
GSM 900 DL	Wed-SWT-AM	595.95	1130.37	189.67	1.46	0.64	43.81	941.71	1730.90	183,80
	Wed-RP1-PM	932.09	1234.50	132.45	1.30	0.52	39.89	1126.12	1832.75	162,75
	Wed-SWT-PM	994.15	1473.01	148.17	1.31	1.19	90.96	1274.55	2148.44	168,56
	Wed-RP2-PM	867.41	1205.31	138.96	1.34	0.77	0.58	1278.37	1984.51	155,24
	Fri-SWT-AM	803.15	1311.64	163.31	1.26	0.59	46.63	1558.29	2599.92	166,84
	Average	**838.55**	**1270.97**	**154.51**	**1.33**	**0.74**	**44.38**	**1235.81**	**2059.30**	**167,44**
GSM 1800 + LTE B3 DL	Wed-SWT-AM	2.46	1.12	45.42	1.59	0.57	35.65	2.28	0.98	43,19
	Wed-RP1-PM	2.42	1.48	61.29	1.64	0.57	34.68	2.06	0.80	38,83
	Wed-SWT-PM	2.69	1.55	57.55	1.66	0.74	44.43	2.06	0.85	41,00
	Wed-RP2-PM	2.28	1.16	50.96	1.74	0.45	0.26	1.80	0.48	26,47
	Fri-SWT-AM	2.06	1.00	48.48	1.88	1.00	52.97	2.19	1.02	46,82
	Average	**2.38**	**1.26**	**52.74**	**1.70**	**0.66**	**33.60**	**2.08**	**0.83**	**39,26**
UMTS 2100 DL	Wed-SWT-AM	2.18	0.66	30.24	1.49	0.24	15.79	2.04	0.48	23,48
	Wed-RP1-PM	2.34	0.83	35.30	1.37	0.22	15.96	2.62	1.04	39,87
	Wed-SWT-PM	2.40	0.89	37.18	1.36	0.22	16.55	2.60	1.02	39,36
	Wed-RP2-PM	2.43	0.96	39.32	1.40	0.28	0.20	2.48	0.99	39,73
	Fri-SWT-AM	2.46	0.90	36.54	1.35	0.22	16.35	2.50	0.92	36,63
	Average	**2.36**	**0.85**	**35.72**	**1.39**	**0.24**	**12.97**	**2.45**	**0.89**	**35,82**
Wi-Fi 2GHz DL	Wed-SWT-AM	2.86	1.16	40.53	1.19	0.18	15.08	4.42	1.95	44,05
	Wed-RP1-PM	2.57	1.34	52.09	1.30	0.33	25.75	3.45	1.81	52,60
	Wed-SWT-PM	2.85	1.35	47.27	1.21	0.16	13.48	3.60	1.26	35,08
	Wed-RP2-PM	2.23	0.70	31.37	1.33	0.19	0.14	2.75	0.82	30,00
	Fri-SWT-AM	2.62	2.38	90.96	1.33	0.29	21.46	3.68	1.84	50,03
	Average	**2.63**	**1.38**	**52.44**	**1.27**	**0.23**	**15.18**	**3.58**	**1.54**	**42,35**
Total average (without the GSM 900 data)		**2,46**	**1,16**	**46,97**	**1,46**	**0,38**	**20,58**	**2,70**	**1,08**	**39,14**

From the above table, the best option is to use the Vertical probe measurements (to measure the Ez component) and to extrapolate the results obtained using a mean extrapolation factor of 1.46 to obtain the isotropic E-field. This measurement results however, would have an extra uncertainty of 20.58 % as compared to the measurements carried out using an isotropic probe.

A2.4. Extrapolation factor for fixed dosimeters

Apart from the extrapolation factor applied to the fixed dosimeters to estimate the isotropic E-field from mono-axial measurements (Appendix A3), there is another extrapolation factor to be applied to the raw measurements from the fixed dosimeters. This extrapolation factor is due to the fixed location and the impact of the immediate environment of a given fixed dosimeter. Due to the fixed location, the dosimeter measurements suffer from small scale fading and due to their placement at a certain height (between 2m to 3m) their measurements does not represent the exposure at the user level (about 1.5m height).
Hence to extract this extrapolation factor, the measurements from the mobile (EMESPY 200) dosimeter were used again. The extrapolation factor due to the fixed dosimeter placement was defined as: *the ratio of the mean isotropic E-field value from the mobile dosimeter and the mean extrapolated isotropic E-field value from the fixed dosimeter (from raw measurements and the appendix-3) for a given frequency band*.

The measured data from the mobile dosimeter (EMESPY 200) over a given day and different time periods is presented in Table 55 for the four RATs that are measured by the fixed dosimeter.

Table 55: Average 'μ' and standard deviation 'σ' for the outdoor mobile dosimeter measurements (all values in V/m).

	GSM 900 DL		GSM1800 / LTE B3 DL		UMTS 2100 DL		Wi-Fi 2GHz	
	μ	σ	μ	σ	μ	σ	μ	σ
Wed-SWT-AM	0.182	0.176	0.253	0.267	0.124	0.149	0.047	0.030
Wed-RP1-PM	0.195	0.186	0.2	0.221	0.137	0.148	0.035	0.028
Wed-SWT-PM	0.197	0.208	0.23	0.236	0.125	0.131	0.043	0.023
Wed-RP2-PM	0.229	0.302	0.153	0.267	0.134	0.129	0.018	0.020
Fri-SWT-AM	0.2	0.227	0.205	0.330	0.174	0.206	0.045	0.047

From the above results we see that the mean values do not vary a lot between standard working hours and rest periods. However a variation is observed for the measurements carried out on Friday SWT AM (morning standard working time) period.

Table 56: Average 'μ' and standard deviation 'σ' for the fixed dosimeter with the isotropic correction factor (all values in V/m).

	GSM 900 DL		GSM/LTE 1800 DL		UMTS 2100 DL		WiFi 2GHz	
	μ	σ	μ	σ	μ	σ	μ	σ
Wed-SWT-AM	0,032	0,017	0,068	0,089	0,100	0,132	0,009	0,006
Wed-RP1-PM	0,033	0,016	0,073	0,091	0,132	0,220	0,010	0,007
Wed-SWT-PM	0,032	0,016	0,075	0,105	0,115	0,167	0,008	0,005
Wed-RP2-PM	0,035	0,017	0,082	0,115	0,129	0,195	0,010	0,012
Week-SWT-AM	0,031	0,016	0,066	0,089	0,098	0,140	0,010	0,008
Week-RP1-PM	0,033	0,016	0,078	0,105	0,115	0,172	0,030	0,220
Week-SWT-PM	0,031	0,015	0,068	0,091	0,100	0,140	0,028	0,215
Week-RP2-PM	0,034	0,017	0,076	0,106	0,116	0,171	0,018	0,129

The measurements from the fixed dosimeters for the same time periods (as in Table 55) are shown in Table 56. These values are the extrapolated isotropic values using the raw measurements and applying the mean extrapolation factor for each frequency band from Table 43. The mean and standard deviation values for the weekly measurements are also shown over the same time periods for reference. We observe that there is no significant variation between the daily mean values and the weekly ones for the GSM 900 band. This may be due to the stable voice data used by this band. For other bands the variation shows the usage change in data services. Finally, the correction (or extrapolation factor) due to installation of the fixed dosimeter is calculated from the ratio of the mean E-field values from Table 44 and Table 56.

Table 57: Correction factor of the fixed dosimeters due to installation (height, environment...).

	GSM 900 DL	GSM/LTE 1800 DL	UMTS 2100 DL	WiFi 2GHz
Wed-SWT-AM	5.77	3.73	1.24	5.03
Wed-RP1-PM	5.92	2.75	1.04	3.48
Wed-SWT-PM	6.25	3.05	1.09	5.15
Wed-RP2-PM	6.63	1.86	1.04	1.73
Week-SWT-AM	5.89	3.81	1.26	4.70
Week-RP1-PM	5.99	2.57	1.19	1.17
Week-SWT-PM	6.43	3.40	1.25	1.55
Week-RP2-PM	6.70	2.01	1.15	0.98
Average value	**6.20**	**2.90**	**1.16**	**2.97**

The results are presented in Table 57. The extrapolation factors are the highest for the GSM 900 frequency bands and lowest for the UMTS band. The mean extrapolation factors are then calculated from the above table (last line in the table) and these can be used to apply to the raw-measurements from the fixed dosimeters to have a calibrated and reliable measurement data representing the DL E-field exposure at the user level in outdoor environment.

A2.5. Tx/Rx platform results

This Appendix gives the statistical distribution of Tx/Rx platform measurements, for the several measurement time periods. Those measurements are involved in the EI assessment of section 6.1.2.

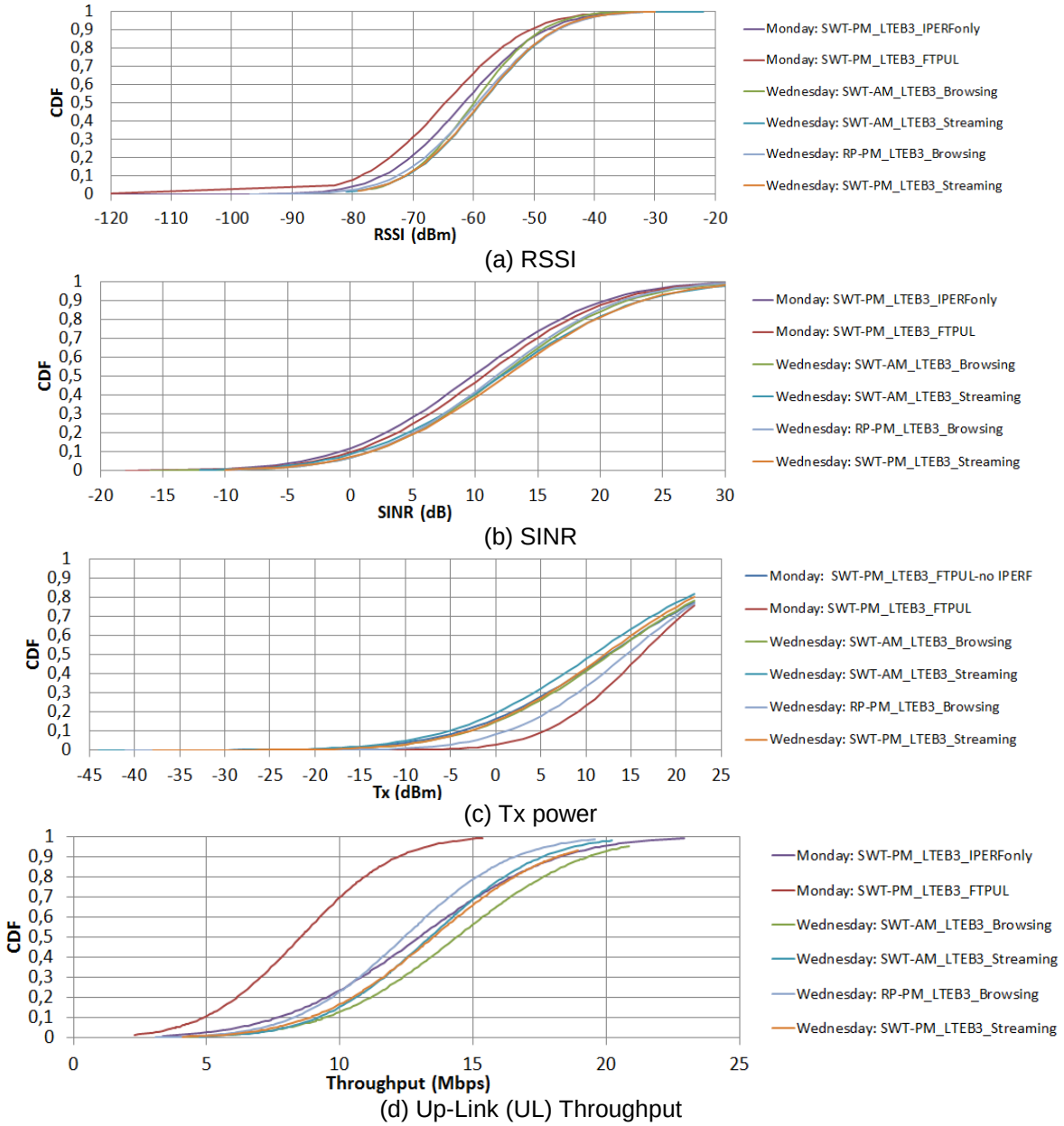

Figure 49: Statistical distribution of the Tx/Rx platform drive-test measurements.

A2.6. Trace mobile measurements

This Appendix reports the detailed statistics extracted from the measurements with the professional Trace mobile equipment.

1. Pedestrian measurements:

Pedestrian measurements have been collected at 4 static points:

- Two indoor positions in a day-light environment (P1/P2);
- One deep indoor position (P3);
- One outdoor position (P4).

All pedestrian measurements have been carried out during SWT-AM. For each service, the test session duration was around two minutes and a half.

The LTE measurement results are presented in Table 58 below. For each service and each measurement point, the average (μ) and standard deviation (σ) of DL signal strengths and UL MAC throughputs are provided.

Table 58: Average 'μ' and standard deviation 'σ' for LTE static measurement points.

P1	RSRP (dBm)		RSSI (dBm)		DL SINR (dB)		PUSCH Tx Power (dBm)		Throughput (Mbps)	
	μ	σ	μ	σ	μ	σ	μ	σ	μ	σ
FTP DL	-95.7	1.8	-65.2	1.6	15.6	3.6	19.9	2.7	0.2	0.05
FTP UL	-96.2	2.0	-68.1	3.4	16.1	3.4	21.8	0.3	19.3	5.6
Video streaming	-98.2	2.3	-70.2	2.3	13.7	3.8	20.3	2.1	0.05	0.01

(a) Static Point 1 (indoor day-light)

P2	RSRP (dBm)		RSSI (dBm)		SINR (dB)		PUSCH Tx Power (dBm)		Throughput (Mbps)	
	μ	σ	μ	σ	μ	σ	μ	σ	μ	σ
FTP DL	-89.6	1.6	-59.3	1.3	17.8	5.5	13.8	3.5	0.18	0.03
FTP UL	-89.0	2.6	-60.5	2.1	16.7	5.1	21.8	0.4	24.6	5.6
Video streaming	-90.0	1.7	-62.4	1.8	20.3	3.3	15.2	4.0	0.07	0.1

(b) Static point 2 (indoor day-light)

P3	RSRP (dBm)		RSSI (dBm)		SINR (dB)		PUSCH Tx Power (dBm)		Throughput (Mbps)	
	μ	σ	μ	σ	μ	σ	μ	σ	μ	σ
FTP DL	-120.9	1.8	-87.6	1.3	-0.6	2.3	23.0	0.5	0.12	0.05
FTP UL	-124.1	2.5	-89.8	1.6	-3.1	3.0	23.0	0.5	0.14	0.05
Video streaming	-120.7	1.9	-87.1	1.8	0.8	2.0	23.0	0.5	0.07	0.05

(c) Static Point 3 (deep indoor)

P4	RSRP (dBm)		RSSI (dBm)		SINR (dB)		PUSCH Tx Power (dBm)		Throughput (Mbps)	
	μ	σ	μ	σ	μ	σ	μ	σ	μ	σ
FTP DL	-82.6	1.8	-51.2	2.2	7.8	6.4	8.4	3.9	0.17	0.02
FTP UL	-83.0	2.4	-53.8	1.9	10.3	3.6	20.3	2.0	29.6	2.7
Video streaming	-83.6	2.1	-55.7	1.8	14.6	4.8	9.9	3.8	0.05	0.09

(d) Static point 4 (outdoor)

In LTE, the transmitted power of PUSCH depends on the path loss. When the UE is in deep indoor conditions, its output power is always at its maximum (+23 dBm). For FTP in uplink, the UE has also to transmit data with strong output power in order to keep the data rate as high as possible.

The 3G measurement results are presented in Table 59 below. For each service and each measurement point, the average (μ) and standard deviation (σ) of signal strength and UL MAC throughputs are provided.

Table 59: Average 'μ' and standard deviation 'σ' for 3G static measurement points.

P1	RSCP (dBm)		RSSI (dBm)		Ec/Io (dB)		Tx Power (dBm)		UL MAC Throughput (Mbps)	
	μ	σ	μ	σ	μ	σ	μ	σ	μ	σ
FTP DL	-78.9	4.1	-71.6	2.5	-8.5	1.5	-11.7	1.8	1.6	0.6
FTP UL	-78.2	2.4	-69.8	1.7	-8.5	1.5	4.3	4.0	2.5	0.9
Video streaming	-80.3	4.3	-72.8	2.2	-8.6	1.6	-13.3	1.9	0.45	0.3
Voice	-78.6	3.1	-69.6	2.6	-8.8	1.8	-18.9	3.4	-	-

(a) Static Point 1 (indoor day-light)

P2	RSCP (dBm)		RSSI (dBm)		Ec/Io (dB)		Tx Power (dBm)		Throughput (Mbps)	
	μ	σ	μ	σ	μ	σ	μ	σ	μ	σ
FTP DL	-70.9	4.9	-62.8	3.5	-7.7	1.8	-20.7	3.2	2.3	1.3
FTP UL	-70.2	3.5	-63.0	3.0	-7.9	2.0	-2.5	2.2	2.8	0.5
Video streaming	-72.1	4.3	-63.7	3.0	-8.9	2.2	-21.8	3.6	3.0	1.7
Voice	-70.4	3.6	-62.7	2.9	-7.5	1.6	-28.0	2.6	-	-

(b) Static Point 2 (indoor day-light)

P3	RSCP (dBm)		RSSI (dBm)		Ec/Io (dB)		Tx Power (dBm)		Throughput (Mbps)	
	μ	σ	μ	σ	μ	σ	μ	σ	μ	σ
FTP DL	-103.2	4.6	-92.8	2.5	-10.8	2.2	14.6	4.9	1.2	1.0
FTP UL	-104.6	2.9	-91.6	1.7	-12.5	2.3	22.0	0.7	0.3	0.25
Video streaming	-105.3	3.9	-93.1	2.0	-10.8	2.2	14.6	3.8	0.9	0.6
Voice	-104.3	5.7	-95.1	3.9	-9.3	2.3	5.9	4.9	-	-

(c) Static Point 3 (deep indoor)

P4	RSCP (dBm)		RSSI (dBm)		Ec/Io (dB)		Tx Power (dBm)		Throughput (Mbps)	
	μ	σ	μ	σ	μ	σ	μ	σ	μ	σ
FTP DL	-65.4	4.4	-59.8	3.6	-8.7	1.9	-27.1	4.0	1.9	0.9
FTP UL	-67.7	5.2	-60.4	4.5	-8.5	1.6	-10.1	8.7	2.6	0.8
Video streaming	-67.2	4.8	-59.8	3.6	-9.1	2.1	-25.8	2.8	2.8	1.9
Voice	-64.3	4.3	-56.3	3.4	-7.7	1.5	-31.9	4.9	-	-

(d) Static Point 4 (outdoor)

As for LTE, the output power in 3G depends on the path loss. For these tests, the CPICH received power (RSCP) shows that the UE was in very good radio conditions for static points P1, P2 and P4, leading to a low output power. Of course, FTP Uplink always requires higher RF power than other services.

For 2G measurement results, only RxLev and Tx Power are reported in this document. Table 60 below presents the average and standard deviation of these measurements results.

Table 60: Average 'μ' and standard deviation 'σ' for 2G static measurement points.

P1	RxLev (dBm)		Tx Power (dBm)	
	μ	σ	μ	σ
Voice	-79.7	7.3	22.9	2.3

(a) Static Point 1 (indoor day-light)

P2	RxLev (dBm)		Tx Power (dBm)	
	μ	σ	μ	σ
Voice	-78.7	6.9	17.5	2.9

(b) Static Point 2 (indoor day-light)

P3	RxLev (dBm)		Tx Power (dBm)	
	μ	σ	μ	σ
Voice	-100.1	5.0	30.0	0.0

(c) Static Point 3 (Deep indoor)

P4	RxLev (dBm)		Tx Power (dBm)	
	μ	σ	μ	σ
Voice	-86.9	7.0	24.5	2.6

(d) Static Point 4 (outdoor)

As expected, the output power for 2G is high. In deep indoor conditions, the UE transmits at maximum power (30 dBm).

2. Drive measurements

The drive tests were always performed on the same route, at different time periods. The duration of the drive depended on the traffic jam. Typically, drives last between 45 mn and one hour.

The LTE measurements statistical distributions of RSSI and PUSCH transmitted power have been plotted respectively in Figure 50 and Figure 51, for different time periods and services. It is clear that RSSI are quite similar for FTP and streaming video. The difference observed with the distribution of RSSI during web browsing test session can be explained by the nature of the traffic which is bursty.

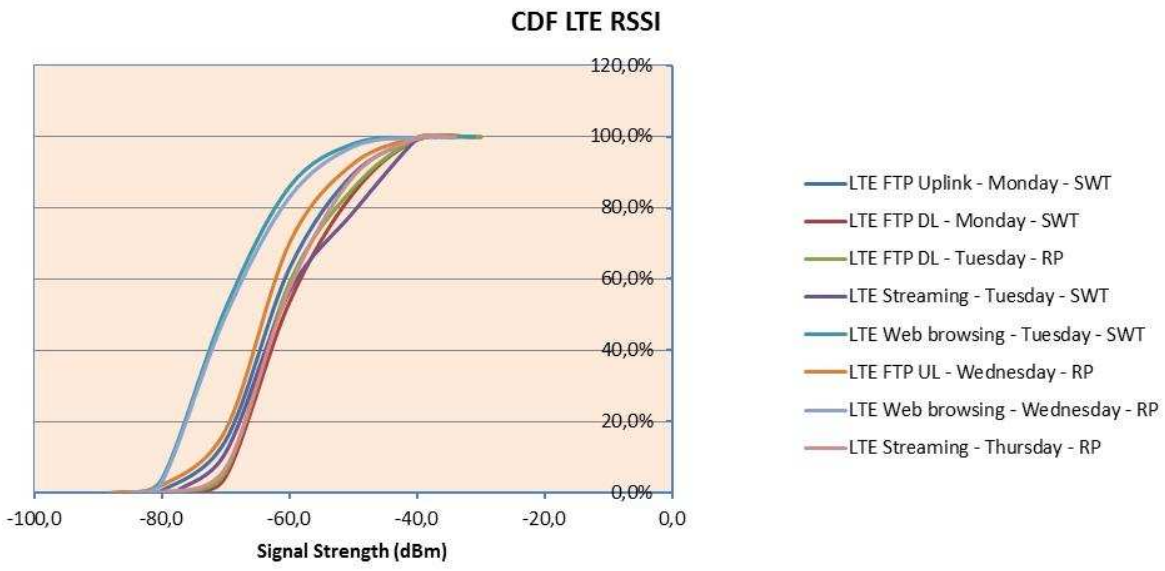

Figure 50: Cumulative distributions of LTE RSSI.

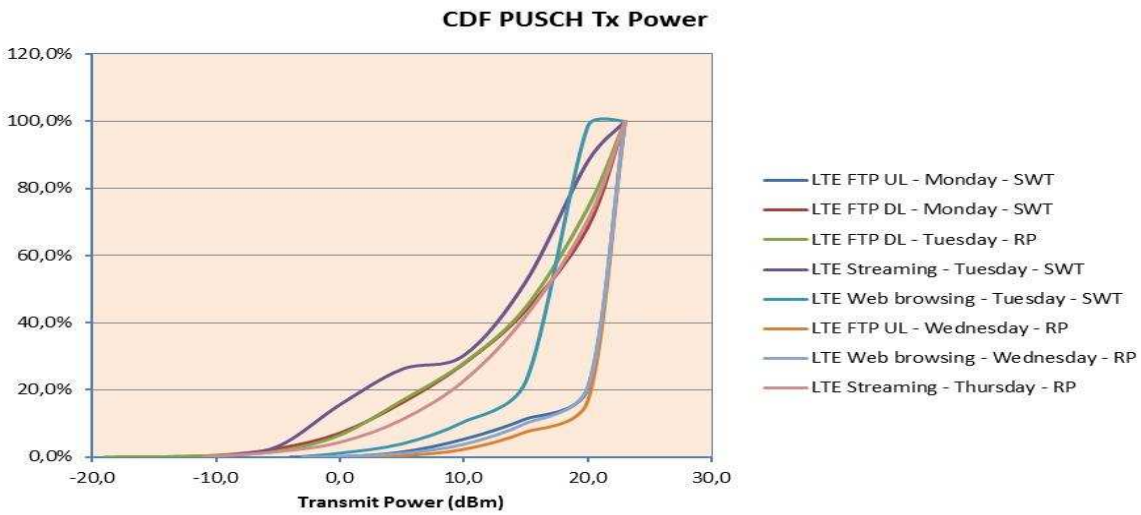

Figure 51: Cumulative distributions of LTE PUSCH Tx Power.

Table 61 summarizes the average and standard deviation values corresponding to these drive tests.

Table 61: Average 'μ' and standard deviation 'σ' for LTE drive tests measurements.

	RSRP (dBm)		RSSI (dBm)		SINR (dB)		PUSCH Tx power (dBm)		PRB number		Throughput (Mbps)	
	μ	σ	μ	σ	μ	σ	μ	σ	μ	σ	μ	σ
FTP-UL (Monday-SWT)	-90.3	9.2	-62.1	8.2	11.0	6.8	20.2	4.2	36.6	9.4	13.6	5.6
FTP-UL (Wednesday-RP)	-92.2	7.9	-63.6	6.1	10.8	5.9	20.8	3.2	35.7	13.2	13.1	5.2
FTP-DL (Monday-SWT)	-89.1	8.8	-59.2	7.9	11.8	6.5	14.1	8.1	64.4	15.8	24.8	13.2
FTP-DL (Tuesday-RP)	-89.7	8.5	-60.1	7.9	13.2	6.3	13.8	7.8	65.9	16.1	25.3	14.0
Streaming (Tuesday-SWT)	-87.3	10.4	-59.5	8.6	14.3	9.7	11.6	8.4	6.4	5.6	1.5	1.4
Streaming (Thursday-RP)	-88.5	8.7	-60.4	7.6	11.6	7.2	14.9	7.0	7.3	15.9	2.4	5.4
Web-browsing (Tuesday-SWT)	-96.4	8.7	-68.9	7.8	12.4	7.2	20.5	4.1	-	-	0.6	1.7
Web-browsing (Wednesday-RP)	-95.6	9.0	-68.3	8.1	12.9	7.1	20.7	4.0	-	-	0.6	1.7

These results show that the averaged signal levels received and transmitted by the UE are quite close for the same service and do not depend on the time the test was performed. However, for web-browsing, there is a difference of about 8 dB on averaged RSSI, compared to FTP and video streaming.

The 3G measurements statistical distributions of RSSI and transmitted power have been plotted respectively in Figure 52 and Figure 53, for different time periods and services.

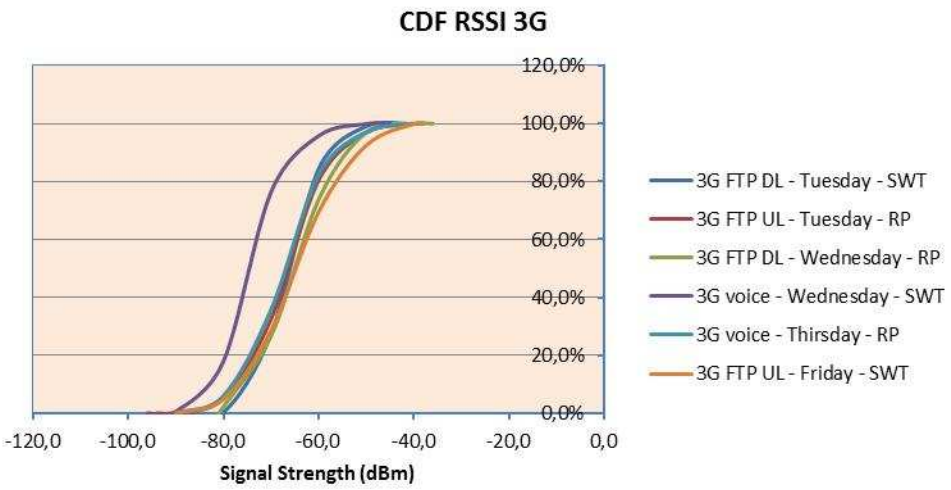

Figure 52: Comparative distributions of 3G RSSI.

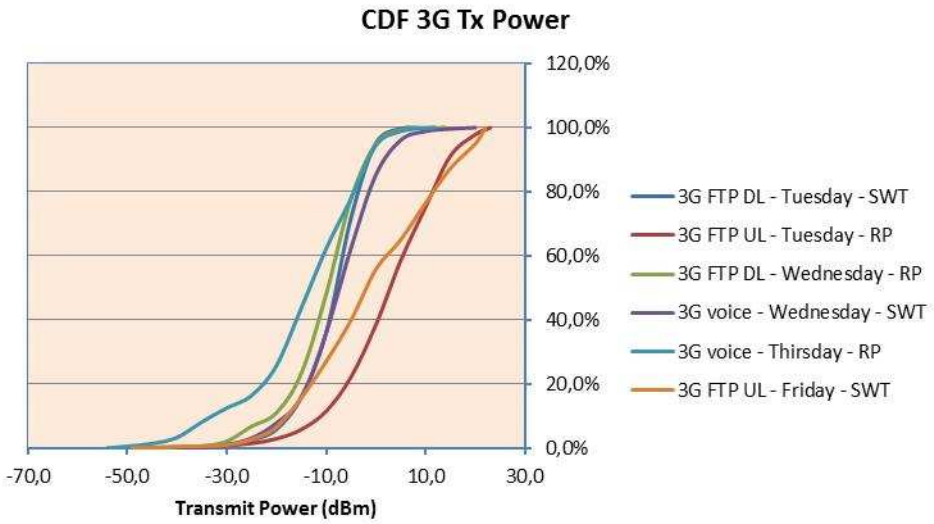

Figure 53: Comparative distributions of 3G Tx Power.

Table 62 summarizes the average and standard deviation values corresponding to these drive tests.

Table 62: Average 'μ' and standard deviation 'σ' for 3G drive tests measurements.

	RSCP (dBm)		RSSI (dBm)		Ec/Io (dB)		Tx power (dBm)		Throughput (Mbps)	
	μ	σ	μ	σ	μ	σ	μ	σ	μ	σ
FTP-UL (Tuesday-RP)	-76.3	9.0	-66.6	8.3	-9.4	2.3	2.1	10.3	1.3	0.9
FTP-UL (Friday-SWT)	-75.9	9.7	-64.7	9.4	-10.4	2.4	-1.2	12.9	1.0	1.0
FTP-DL (Tuesday-SWT)	-77.3	7.2	-66.1	6.0	-10.3	2.0	-8.9	6.4	2.5	1.7
FTP-DL (Wednesday-RP)	-76.0	7.9	-64.8	7.2	-10.7	2.2	-10.7	7.8	3.5	2.7
Voice (Wednesday-SWT)	-82.7	7.4	-74.2	7.1	-8.8	1.7	-7.7	8.0	-	-
Voice (Thursday-RP)	-76.3	9.4	-67.0	8.5	-9.4	2.3	-14.7	11.6	-	-

Like LTE, the received and transmitted signal levels for FTP are quite similar. However, there is a significant difference for voice for which RSCP is about 6 dB higher in RP time period. This difference is therefore about the same for Tx power parameter.

The 2G measurements statistical distributions of RxLev and transmitted power have been plotted respectively in Figure 54 and Figure 55, for different time periods and services.

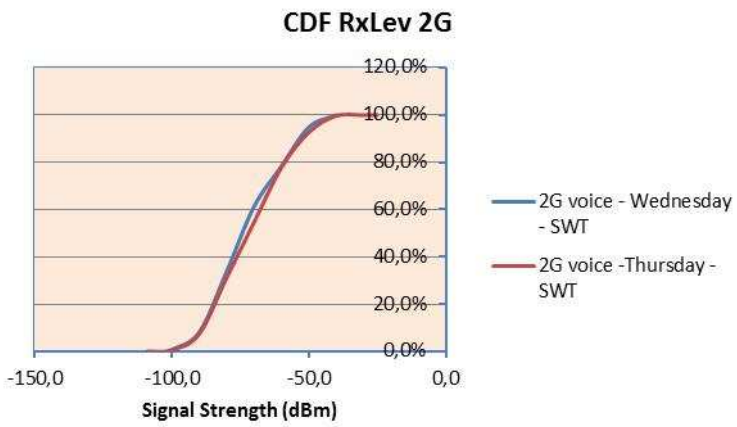

Figure 54: Comparative distributions of 2G RxLev.

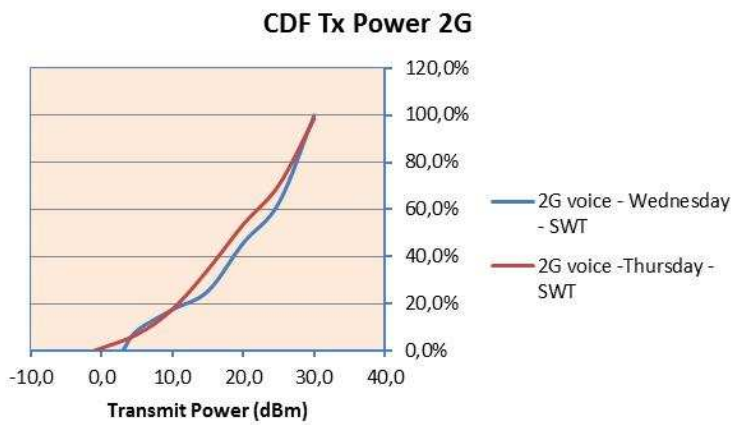

Figure 55: Comparative distributions of 2G Tx Power.

Table 63 summarizes the average and standard deviation values corresponding to these drive tests.

Table 63: Average 'μ' and standard deviation 'σ' for 2G drive tests measurements.

	RxLev (dBm)		Tx Power (dBm)	
	μ	σ	μ	σ
Voice (Wednesday-SWT)	-72.4	13.1	20.4	8.4
Voice (Thursday-SWT)	-71.4	13.5	18.8	8.2

A2.7. Comparison between Tx/Rx platform vs Professional drive-test equipment

During the measurement campaign in Santander, the Tx/Rx platform developed during the project was compared to a professional drive test tool. Both systems are described in detail in [D6.1, section 3.4].
The measurement setup was as follows. The Tx/Rx platform was placed inside a car with the antennas placed closed together as shown in Figure 56a. The drive test was placed inside another separate car Figure 56b. The itinerary followed is shown in Figure 42.

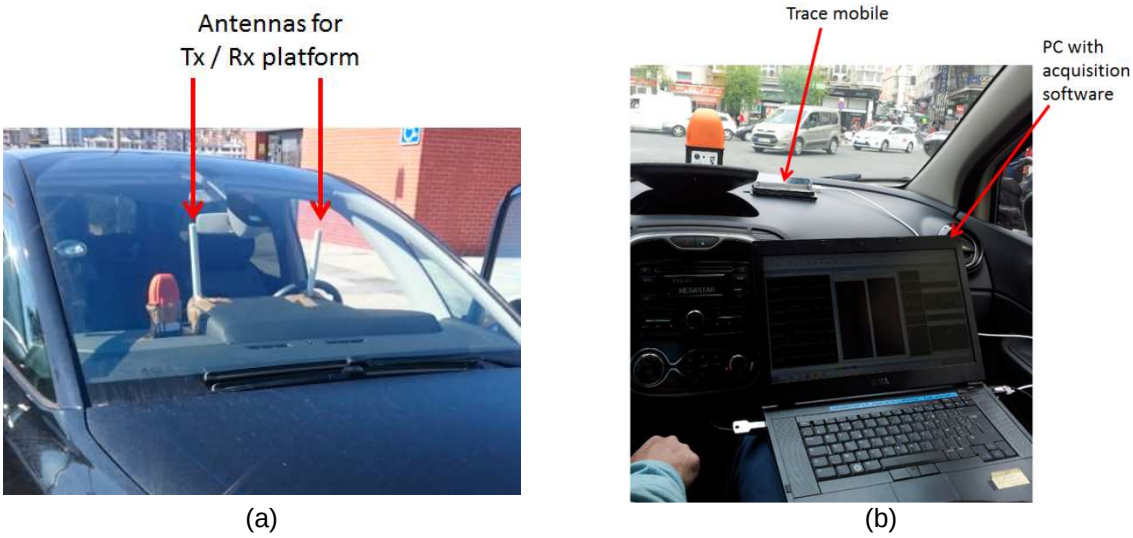

Figure 56: Measurement setup for Tx/Rx platform (a) and professional drive test tool (b) during Santander measurement campaign.

The results from both systems are compared in Figure 57. These results were obtained at the same time (on Monday 20/04/2015 between 18:00 hours and 19:24 hours). During this time period both systems were connected to the Orange network and performing FTP UL operation (i.e. sending a heavy file to a distant server). Remark that the transferred file size and the distant servers used during the measurements by both systems were not the same.

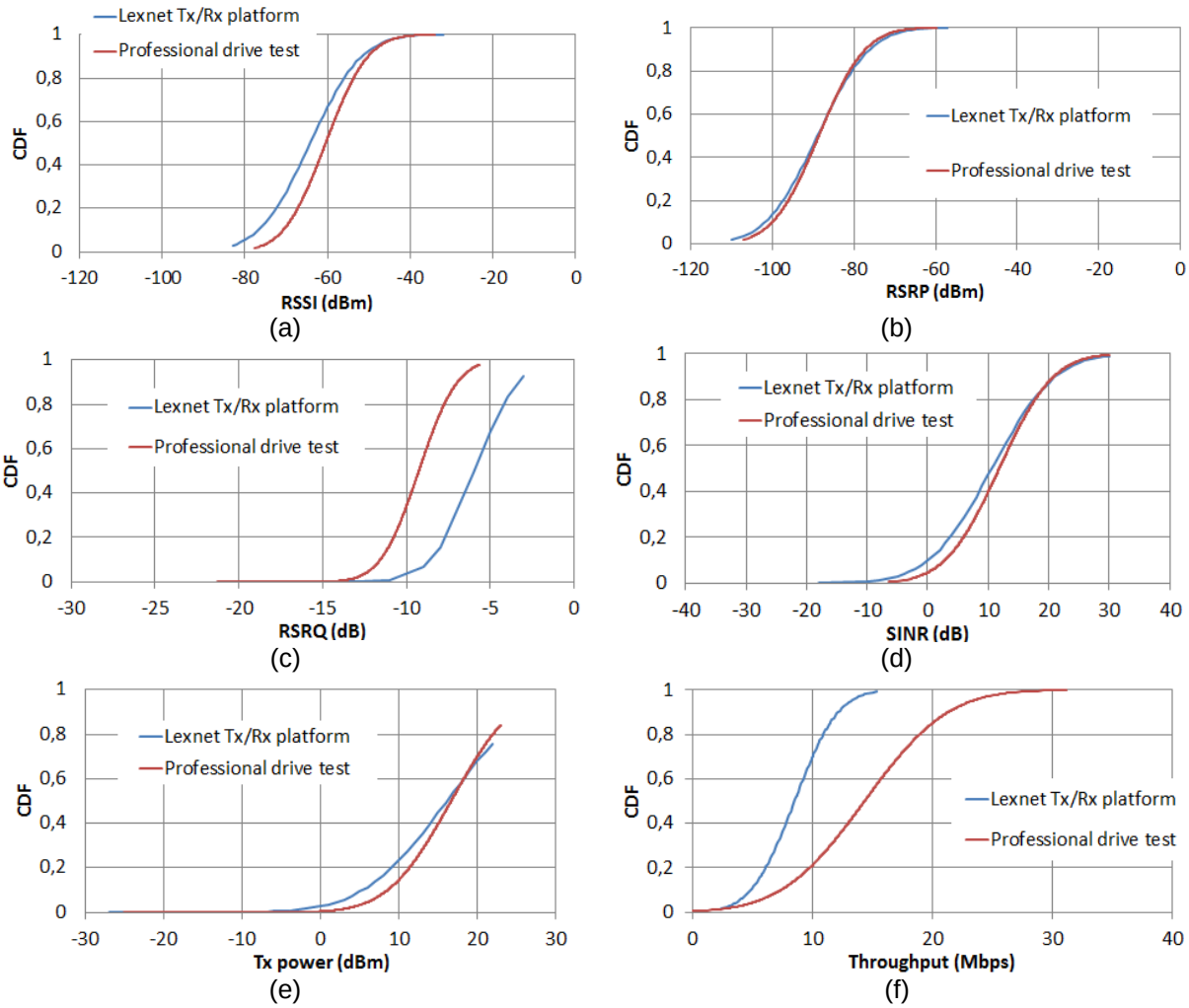

Figure 57: Measurement results comparison between Tx/Rx platform and professional drive test equipment during FTP-UL operation (a) RSRP, (b) RSSI, (c) RSRQ, (d) SINR, (e) Tx power, (f) UL-Throughput in Mbps.

The results for receiving parameters (RSSI and RSRP) and SINR are similar for the two tools. The RSRQ is better for the Tx/Rx platform because of the two external antennas as compared to integrated antennas for the mobile phone in the case of drive test equipment. The total transmit (Tx) power parameter distribution is quite similar for the two tools. The UL throughput parameter is quite different however. The difference might be due to the combined effect of the external antennas and better diversity conditions for the tx/rx platform and the difference of the file type, file size, and FTP server used for the experiment.

To conclude, we can consider the low-cost network monitoring tool to carry out measurements as an alternative solution to the professional drive test equipment. The reception and transmission power parameters are similar from both solutions. The throughput and quality parameters however depend on the usage and antenna diversity.

A2.8. Scanner LTE RSSI measurements

Scanner measurements have been collected for two LTE networks (Orange and Movistar) at both targeted time periods (SWT and RP). Figure 58 shows the raw RSSI collected for each network.

Figure 58: RSSI collected for LTE Orange and Movistar networks with the scanner.

These raw measurements have been post-processed as follows:

1) Filtering measurement bins that are closer each other than 3m in order that the measurements collected when the car is stopped do not bias the computation of global statistics.
2) Filtering the portions where there are not data collected from all drive-test.

The statistical results are given by Figure 59. The differences on collected RSSI between both LTE networks are significant (Orange LTE network is 4 dB higher), while there is only a weak difference between both time periods (~0.4 dB). These results demonstrate we cannot easily extrapolate the exposure level from one LTE network to another, and that daily variations are not as strong as expected. This same observation is shared with the other drive-test and fixed dosimeter measurements.

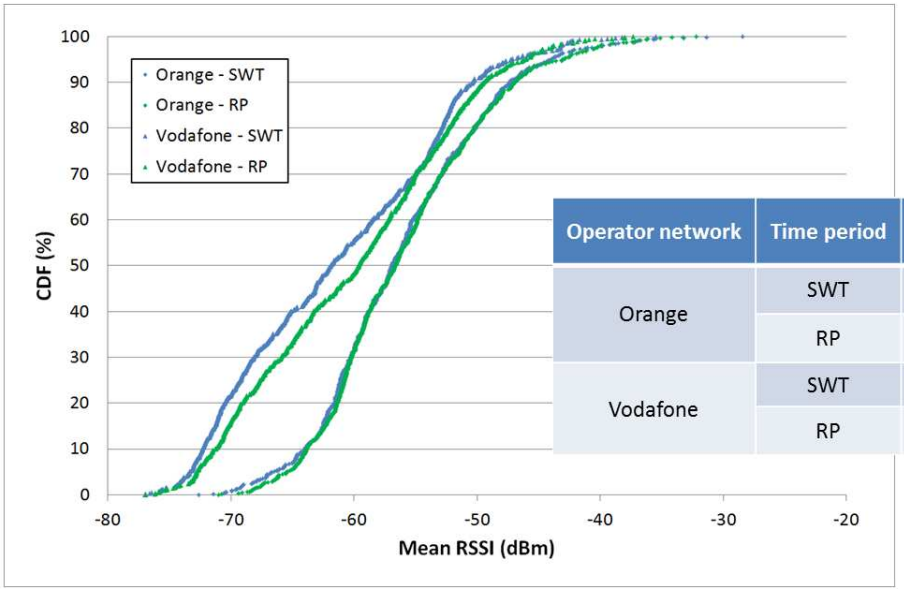

Operator network	Time period	Mean (dBm)	Median (dBm)
Orange	SWT	-49.28	-56.67
	RP	-48.77	-56.92
Vodafone	SWT	-52.66	-59.59
	RP	-52.99	-61.88

Figure 59: Global statistics computed from the LTE SCANNER data.

APPENDIX A3: COMPARISON BETWEEN LEXNET DOSIMETER AND STATE OF THE ART EMESPY200 DOSIMETER

The EMESPY 200 dosimeter is currently commercialized by Satimo industries, France and has the capability to measure 20 frequency bands with the sensitivity level of 5mV/m and a dynamic range of 60dB [EME]. The measured rejection curves for UMTS (UL & DL), Wi-Fi and LTE-B7 (UL & DL) bands for the EMESPY 200 dosimeter and the LEXNET dosimeter are compared in Figure 60.

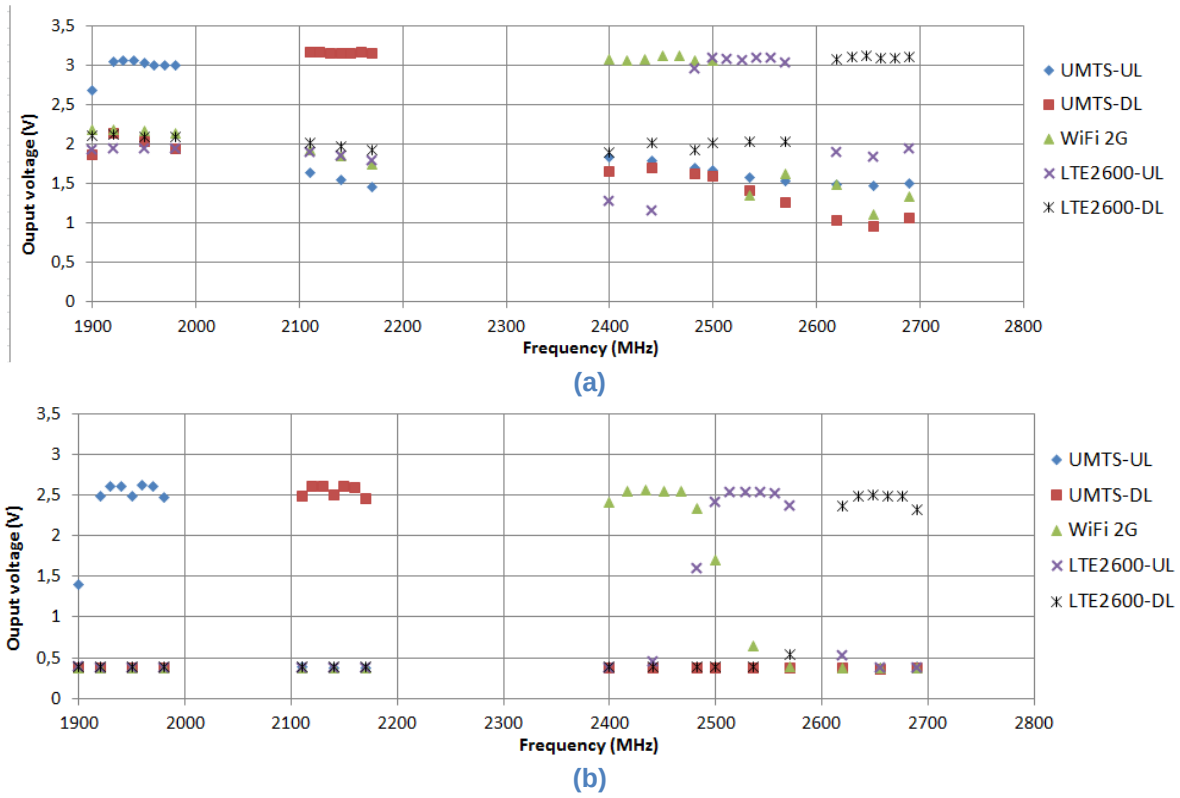

Figure 60: Comparison between (a) EMESPY 200 dosimeter and (b) LEXNET dosimeter rejection curves.

From the EMESPY results, we can observe that the output for each band is polluted significantly by the neighbouring bands. This mediocre rejection is due to the natural rejection curves of the RF frequency filter. To have a clean response of the E-field from a given frequency band and to remove the contribution of all other bands, post-processing is applied to the raw-measurements. Looking at the response of the LEXNET dosimeter for the same frequency bands, excellent rejection is observed. This is mainly due to the high selectivity of the base-band filter used in the LEXNET architecture. The post-processing load for the LEXNET dosimeter is thus significantly reduced and raw-measurements are close to final measurement data.
Apart from the excellent rejection advantage provided by the LEXNET dosimeter, the other major quality is the ability to adapt to any frequency band as required by the client needs, which is not possible with the EMESPY 200 architecture. A quantitative comparison in terms of performance and mechanical design is presented in Table 64 between the two solutions. In addition to the improvement in performance and flexibility, the LEXNET dosimeter also provides a slimmer and lighter design (Figure 18a). In terms of cost comparison, LEXNET dosimeter will be slightly more expensive

due to front end components and expensive battery. But comparing the total development cost in terms of design and prototyping, the EMESPY type dosimeters with fixed bands will be more expensive in the long run, because a new hardware iteration has to be made every time the clients need changes in terms of geographical location and/or evolution in the frequency bands.

Parameter	EMESPY 200	LEXNET dosimeter
Frequency standards covered	Predefined 20 fixed bands 80 MHz – 6 GHz	Programmable any number of bands (400 MHz – 6 GHz)
Frequency band resolution	Fixed by RF filters	From 7 MHz up to 100 MHz
Polarization	Three axes - isotropic	Three axes - isotropic
Dynamic range	Up to 61.6 dB	60 dB
Sensitivity	5 mV/m	5mV/m
Power supply	2 AA battery cells, 1.2V / 2600 mAh	Flat battery 3.7 volts / 3700 mAh
Power supply type	Removable battery cells	Integrated battery
Output type	E-field in real time with dedicated android app, or E-field stored in the memory on-board the device	E-field in real time with dedicated android app, or E-field stored in the memory on-board the device
Dimensions (mm)	168.5 x 79 x 49.7	166 x 70 x 42.5
Weight	440 g	360 g
Certification	IP55 (vertical position)	IP55 (vertical position)

Table 64: Main specifications of the wearable dosimeter.

APPENDIX A4: PLANNING THE LOW-COST DOSIMETER DEPLOYMENT

This Appendix gives additional details on the low-cost dosimeter deployment procedure implemented in SmartSantander. See section 6.2.1 for the overall picture on the procedure.

A4.2 Planning the low-cost dosimeter deployment

Radio-planning-like simulation is a convenient way to evaluate the performance of the dosimeter network and to adjust its design before on-field deployment. The simulations do reproduce measurements, as it would be done with a dosimeter deployment, leading to an evaluation of sensing error statistics.
The basic principles of the simulation study are as follows. First, the downlink E-field strength is predicted over a map (or pixel grid) that covers the whole study area. This map is considered as a realistic EMF realization, which is used afterwards as a reference. Then, the dosimeter measurements are emulated by picking sample values in the reference map, at locations chosen according to the deployment strategy under test. Finally, the E-field strength statistics computed from the whole map are compared to the E-field strength statistics derived from the emulated measurements, in order to evaluate the performance of the sensor network.

This study has to be conducted considering all HSPA base stations from the four operators.

Sub-section 1 gives a description of the simulation setup along with a basic characterization of the prediction EMF map.
Sub-section 2 evaluates the sensor network performance considering an uniform deployment strategy.
Finally, sub-section 3 evaluates the difference between street-level and lamppost field strength levels.

1. *Simulation setup*

The results given below are obtained from the four HSPA networks operating at 2100 MHz: 169 macro-cells in a surface of 0.45 km² composed of Santander downtown plus a margin of 500 meters. The downlink E-field strength from those HSPA networks is predicted in the downtown area.
Some base station parameters (antenna pattern, orientation and height) were unknown for the study. Therefore typical values have been applied to those base stations: directional antenna with 60° horizontal beamwidth, 12° vertical beamwidth and maximum gain of 14 dBi, height of the support (building, pylon) plus two meters.
The downlink EMF exposure, in the sense of LEXNET, depends on the dynamic transmit power, which is below the maximum transmit power usually considered in EMF exposure regulation. This dynamic transmit power is function of the average percentage of resources allocated to serve the network users, the so-called traffic load. For the pre-deployment dosimeter planning, which is reported here, a unique 50% traffic load is assumed for all base stations.
The simulation relies on the 3D representation of the environment, composed of the raster terrain altitude (resolution 5 meters) and 3D vectors to model buildings,

vegetation, bridges and water bodies. The propagation loss is computed by the Volcano deterministic model [COR] that predict physical propagation mechanisms (diffraction in particular) to provide realistic downlink E-field strength maps.
Even with a deterministic model, the shadowing loss suffers from a prediction error (when compared to real measurements) that usually follows a lognormal distribution. Thus a random shadowing is simulated, in several successive realizations, with standard deviation of about 7 dB and a correlation distance of 50 meters.

The dosimeters are installed at a height of few meters above the streets; therefore the measurements must be converted (from statistical rules) to street-level estimates in order to get relevant data for the computation of the people exposure. For simplicity here, the uncertainties that will be produced by those conversions are not considered. The emulated dosimeters are assumed to be installed at the height of 1.5 m. Only the error due to the sampling procedure is used to evaluate the performance of the sensor networks.

Figure 61 shows the outdoor downlink E-field strength maps predicted with a resolution of 5 meters, at one random realization, for respectively one specific network operator (Orange) and the sum of the four operators. The statistics extracted from those maps lead to the reference CDFs shown in Figure 62.

.

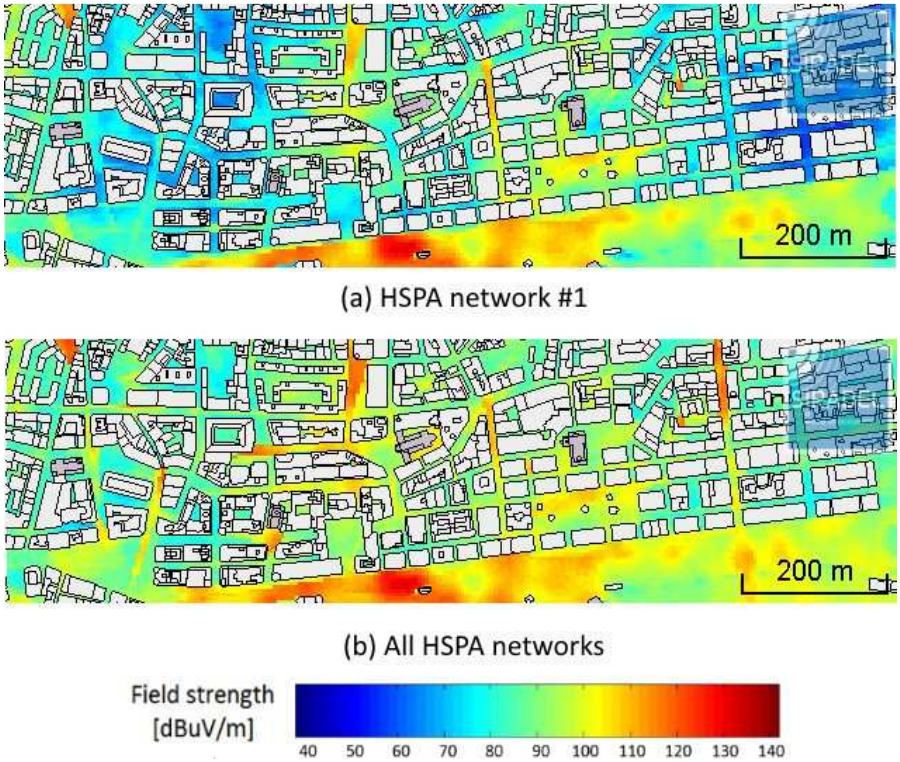

Figure 61: Outdoor downlink E-field strength maps for WSN error emulation.

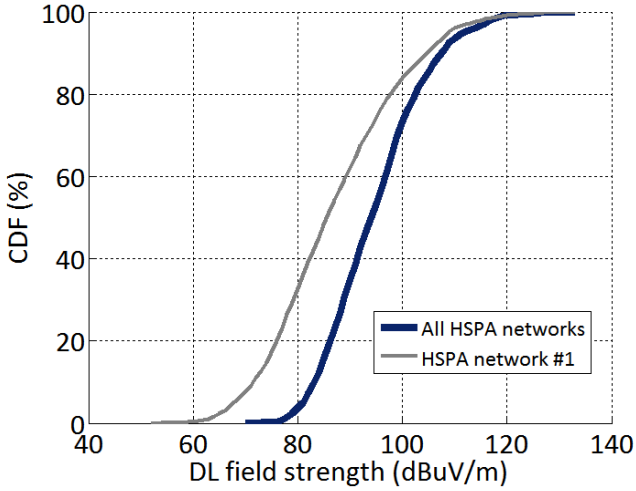

Figure 62: CDF of outdoor downlink E-field strength over the whole study area.

Those figures give two interesting pieces of information regarding the downlink E-field strength distribution in a dense urban area: peaks are observed, as expected in the close vicinity of base stations; but variations over the remaining of the area are quite small, except the strong differences between confined/street areas (lower levels) and large open areas (higher levels).

2. ***Evaluation of different deployment strategies***

Three different deployment densities are evaluated with respectively 10, 25 and 50 sensors. In all cases, the dosimeters are deployed uniformly in the streets of the whole considered area. One example is illustrated in Figure 63.

.

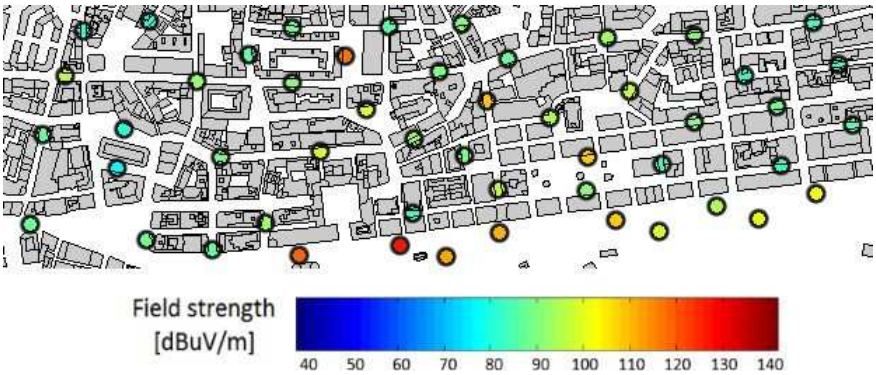

Figure 63: Measured E-field strength levels from the 50-sensor deployment.

Figure 64 gives the sensor measured field levels CDF from the different tested densities, obtained at one random realization. The root mean square error (RMSE) and the bias (or mean error) are calculated for each realization and dosimeter density. The RMSE and absolute bias values are averaged over the several realizations to get the average performance statistics shown in Table 65. We observe first that the RMSE error when measuring the exposure coming from all HSPA networks together is lower than the error related to one single network. This simply results from the fact that spatial exposure variations decrease as the number of contributing networks increase (provided the base stations from different operators are not all collocated). Beside, the most important conclusion from this study is the relationship between the number of dosimeters and the assessment error: the error degradation between 50 and 25 dosimeters is very small (4% on the all-networks

RMSE) while it is much significant when changing from 25 to 10 dosimeters (47%). This study gives obviously valuable indicators to make a trade-off between accuracy and deployment cost. Knowing the maximum number of dosimeters available for the Santander deployment is 50, and that the dosimeters not used in the downtown area will serve for other test areas, it looks like 25 is a reasonable trade-off that will provide an error very close to the optimal.

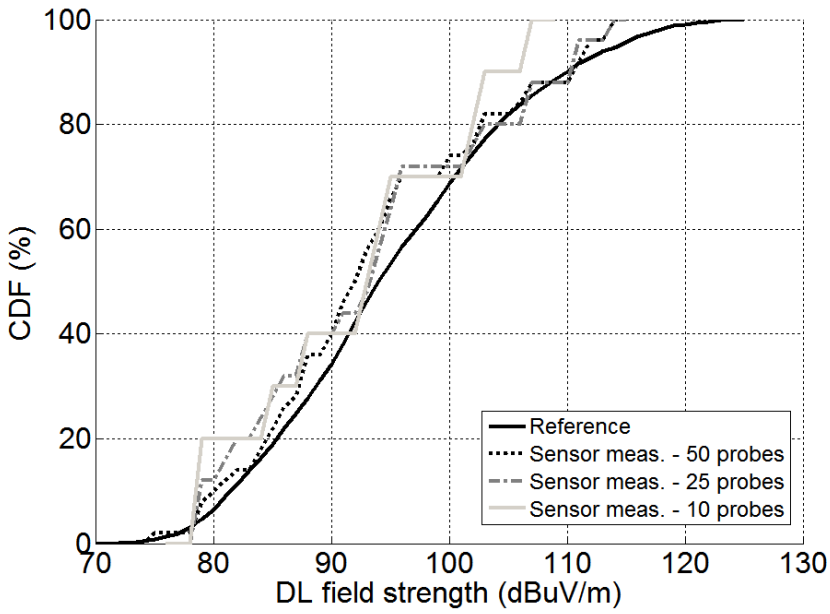

Figure 64: E-field strength CDF from dosimeter measurements.

Table 65: Error statistics from different dosimeter deployments.

Sensor network with	50 probes		25 probes		10 probes	
	Mean |bias| (dB)	RMSE (dB)	Mean |bias| (dB)	RMSE (dB)	Mean |bias| (dB)	RMSE (dB)
Single HSPA network	1.17	3.06	1.03	3.48	2.38	5.19
All HSPA networks	1.38	2.52	1.40	2.63	1.71	3.87

3. ***Impact of sensor height***

Sensors are placed on lamppost, thus not at street level where the DL field strength level must be assessed. It is therefore of great importance to get a transfer function that converts the sensor measurement at lamppost height to an estimate at street level.

For this purpose, the DL field strength maps are predicted at both heights 1.5 m and 6 m above the ground. The difference between both predictions (field strength at height 6 m is the highest one) is calculated at each pixel of the maps before extracting statistics.

As the Santander geographical map data was not yet available at the time of this study, the simulation was carried out from a similar urban HSPA network deployment in Paris. Figure 65 gives the statistical properties of the simulated difference

Difference between outdoor DL field strength at 6m and 1.5m	
Mean (dB)	Std dev (dB)
1.5	1.4

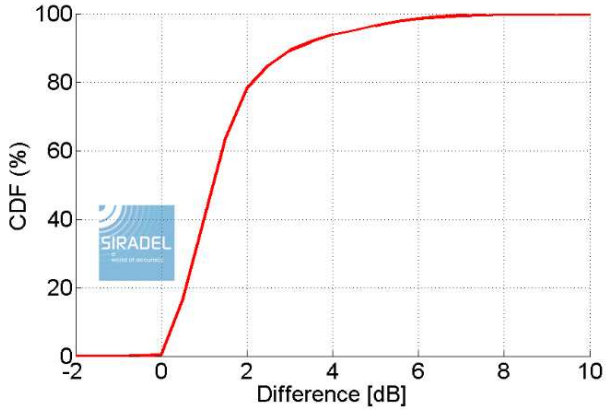

Figure 65: Difference between the DL field strengths at 6m and 1.5m above the ground.

A4.2 Measurement-based sequential EMF sensor network deployment

Assuming we have no previous knowledge about the electric-field strength in the area under study, we can assume it is an unknown function of the location. An exact evaluation of this function is not feasible, although it can be approximated by a so-called surrogate model, defined as “an approximation model for a computationally expensive simulation or a physical experiment, built from generally time-expensive samples at well-chosen locations” [CRO].

The choice of measurement or sample locations is called the design of experiments, and it is critical for the model reliability. In measurement-based RF-EMF modelling studies, the design of experiments is usually a random grid, which is fixed before any measurements are performed (this is also called “one-shot approach”).

However, a design of experiments can also be sequentially built starting from a limited set of measurements (usually distributed along a Latin hypercube configuration). Next a space-filling design is applied, which distributes the initial measurement locations so that the area of interest is covered as fairly as possible and determining the optimal location of additional measurement points in an automated way ([CRO], [STE]). In other words, the algorithm used in the sequential modelling approach "learns" the EMF exposure on the fly, based on the knowledge acquired from the previous measurements, and sequentially proposes optimal locations for future measurements that should be performed. At any moment in time, the gain of these additional measurements – a quantification of how much information is added to the model – can be assessed, and a well-chosen stopping criterion can be defined to detect convergence of the algorithm.

The advantage of sequential sampling consists of both performing relatively more measurements in regions that are potentially interesting – e.g., a highly-varying electric-field strength [AER1], or hotspot regions where the electric-field strength is high [AER2] – and carrying out only as many measurements as needed to obtain the

desired accuracy, thus significantly limiting the time to perform measurements ([DES1], [DES2]).

A sequential design always involves a trade-off between exploration and exploitation, with the former selecting data points in unexplored regions and the latter suggesting points in regions previously identified as interesting, e.g., peaks and/or valleys. This dual strategy (combined using a weighting function) results in a more efficient distribution of measurement locations compared to other traditional designs, such as uniform or random distributions (e.g. [AZZ], [JOS], [PAN]).

The robust and efficient hybrid sequential design algorithm used in [AER1] and developed by Crombecq et al. [CRO] employs Voronoi tessellation for exploration and local linear approximation (LOLA) for exploitation.

A Voronoi tessellation divides the area into multiple polygonal cells, generated by the selected measurements locations. Each cell consists of those points that are closer to one measurement location (i.e., the one that generated the cell) than any other point. The algorithm then distributes more data points in the larger cells, i.e., as far as possible from the previously chosen locations.

LOLA on the other hand, distributes the data points such that the density of the points is proportional to the local nonlinearity of the approximation function (in this case, the interpolation model), as dynamical regions are more difficult to approximate than linear regions.

In [AER1] the exploitation algorithm is presented. It consists of a generalized probability of improvement criterion, defined as "the probability that the electric-field strength at a certain location lies within a certain output range" (e.g., above a certain predetermined value), which ensures that interesting areas (in this case hotspots) are sampled more densely. The exploration consisted on a minimum distance criterion, which, when maximized, ensures the research area is properly searched and samples are widely spread. The mathematical breakdown of the two criteria is given in [COU].